

**The MIT Design Advisor: Simple and Rapid Energy Simulation
of Early-Stage Building Designs**

by

Bryan J. Urban

B.S., Mechanical Engineering
Cornell University, 2004

Submitted to the Department of Mechanical Engineering
in Partial Fulfillment of the Requirements for the Degree of

Master of Science in Mechanical Engineering
at the
Massachusetts Institute of Technology

June 2007

© 2007 Massachusetts Institute of Technology
All rights reserved

Signature of Author: _____
Bryan J. Urban
Department of Mechanical Engineering
21 May, 2007

Certified by: _____
Leon R. Glicksman
Professor of Mechanical Engineering
Thesis Supervisor

Accepted by: _____
Lallit Anand
Professor of Mechanical Engineering
Chairman, Department Committee on Graduate Students

[this page intentionally left blank]

The MIT Design Advisor: Simple and Rapid Energy Simulation of Early-Stage Building Designs

by

Bryan J. Urban

Submitted to the Department of Mechanical Engineering on May 21, 2007
in Partial Fulfillment of the Requirements for the Degree of
Master of Science in Mechanical Engineering

ABSTRACT

Simulation tools, when applied early in the design process, can considerably reduce the energy demand of newly constructed buildings. For a simulation tool to assist with design, it must be easy to use, provide feedback quickly, and allow rapid comparisons. Most existing tools do not meet these needs, usually because they were intended for modeling finalized building designs. Often there is no user interface, and it can take hours or days to prepare, run, and interpret results. Such tools are too sophisticated for design purposes.

In this document the MIT Design Advisor is presented as a simple and rapid building energy simulation tool, developed specifically for architects and building designers. Conceptual building designs can be modeled quickly and without formal training. Results are interpreted graphically and displayed to the user in a simple user interface. Side-by-side comparisons of building designs can be made, allowing users to quickly learn which building components have the biggest impact on energy consumption (heating, cooling, and lighting), indoor daylight levels, and thermal comfort.

User-specified building parameters are used together with local weather data to predict monthly and annual energy use. The heat transfer model used to make the energy predictions is explained in detail in this thesis. Calculation methods are given and validated. Agreement with existing models is quite good. The MIT Design Advisor is available at <http://designadvisor.mit.edu>.

Thesis Supervisor: Leon R. Glicksman
Title: Professor of Mechanical Engineering

[this page intentionally left blank]

ACKNOWLEDGEMENTS

I would like to thank the Permasteelisa Group and the Cambridge MIT Institute for their financial support of this MIT Design Advisor research project. Appreciation is due to Henk DeBleecker and Maaïke Berckmoes of Permasteelisa for their careful attention to detail and many helpful suggestions. The software is better because of them.

A special thanks to Matt Lehar and Jim Gouldstone for their patience in helping me learn the ropes of a new program and programming language. Their guidance and willingness to help have made this project approachable and enjoyable. Additional thanks to Matt and Jim, and all the unnamed contributors who have worked on this project before – without them I wouldn't be writing this. A debt of gratitude is owed to Betsy Ricker for making the comparisons with Energy Plus a successful reality.

Thanks to family and friends, near and far, for their steady and uplifting moral support. Thanks especially to those who have patiently endured my sometimes continued absence while working on this little document.

Thank you, Leon, for your generous support and dedication to both the project and my own academic development. Our many conversations have been and continue to be extremely valuable. Thanks especially for the many rewarding opportunities, travel and otherwise, afforded during my stay at MIT.

It all amounts to a most gratifying experience.

Dedicated with love to Mom and Dad.
Your encouragement keeps me going.

BIOGRAPHIC NOTE

I completed my Bachelors of Science degree in June 2004 at Cornell University. During that time I worked on and published a paper investigating and modeling a new, efficient way to produce hydrogen gas from liquid methanol. Since coming to MIT in the fall of 2004, I have had the opportunity to work on a wide array of fun and rewarding projects. In 2005 I acted with a Sloan E-Lab team consulting for a company in Lyon, France that makes a liquid lens for camera phones. During IAP of 2007 I spent three weeks in Lesotho, Africa with a team of MIT students working on a market study for a solar heat engine that can be built from common car parts. I have had the fortune to present the building-technology research that follows at conferences in Thailand, Germany, Spain, and at MIT. In the future I hope to work for and/or start up a company in the clean energy sector.

Please send questions or comments to the author at:

burban@alum.mit.edu

TABLE OF CONTENTS

1 INTRODUCTION: BUILDINGS, ENERGY, AND SIMULATION.....	11
1.1 Energy Use in Buildings	11
1.2 Building Design	13
1.3 Simulation Design Tools	15
1.4 The MIT Design Advisor.....	18
1.5 Outline of This Thesis	20
2 THE MIT DESIGN ADVISOR INTERFACE.....	23
2.1 Introduction	23
2.2 Overview of the MIT Design Advisor Interface.....	24
2.3 Basic Inputs: Detailed Description of Options.....	29
2.4 Advanced Inputs: Detailed Description of Options.....	33
2.5 Outputs: Overview and Detailed Description	34
2.7 More Information	40
3 RADIANT SOLAR ENERGY	41
3.1 Introduction.....	41
3.2 Radiation Basics.....	42
3.3 Weather Data Overview	43
3.4 Method of Finding the Incident Solar Flux.....	44
3.5 Calculation of the Angle of Incidence.....	44
3.6 Components of Solar Radiation	53
3.7 Validation.....	56
4 WINDOW OPTICS	61
4.1 Introduction.....	61
4.2 Radiation and Optics Background.....	62
4.3 Computing the Angle Dependent Property Variation	64
4.4 Diffuse Hemispherical Values of Optical Properties	68
4.5 Using Pane Properties in Multi-Layered Glazings	69
4.6 Solar Shading Devices	71
4.7 Optical Properties of Window Panes and Blinds.....	73
4.8 Validation.....	74
4.9 Quick Reference: How to Compute Angle Dependence of Optical Properties	77
5 ARTIFICIAL LIGHTING	79
5.1 Introduction.....	79
5.2 Lighting Basics	81
5.3 Modeling Light Requirements of Buildings.....	86
5.4 Lighting Input Options and the User Interface.....	89
5.5 Sample Output	93
6 THERMAL MASS	95
6.1 Introduction.....	95
6.2 A Simple Thermal Mass Model	96
6.3 Energy Balance & Numerical Technique	107
6.4 Validating the Model.....	113
7 ENVELOPE LOADS	119
7.1 Introduction.....	119
7.2 Thermal Exchange through Exterior Walls and Windows.....	120
7.3 Thermal Resistance Calculations.....	125
7.4 Envelope Model Validation.....	136
7.5 A Note on the Wall Construction Approximation	142

8 ENERGY BALANCE	143
8.1 Introduction	143
8.2 Modeling Overview	143
8.3 Room & Building Dimensions	144
8.4 Details of Load Calculations	148
8.5 Energy Balance.....	156
8.6 Weighted Average of Energy Use In Building Space	161
8.7 Validation	163
8.8 Conclusion	168
9 NOMENCLATURE	169
10 REFERENCES	173

LIST OF TABLES AND FIGURES

CHAPTER 1 INTRODUCTION: BUILDINGS, ENERGY, AND SIMULATION

Table 1-1. U.S. Buildings Sector Energy Consumption (DOE 2004).

Table 1-2. Buildings Sector Energy Consumption Breakdown in 1995 (Price).

Figure 1-1. Energy breakdown in the U.S. (EIA 2006).

Figure 1-2. Building costs by category (BOMA 1999).

Figure 1-3. Page 1 of 41 in the eQUEST Schematic Design Wizard.

Figure 1-4. Logic diagram of MIT Design Advisor software.

Figure 1-5. A portion of the single-page MIT Design Advisor interface.

CHAPTER 2 THE MIT DESIGN ADVISOR INTERFACE

Table 2-1. Basic Input Options

Table 2-2. Advanced Input Options

Table 2-3. Model Outputs

Figure 2-1. The MIT Design Advisor interface.

Figure 2-2. Basic MIT Design Advisor Setup page.

Figure 2-3. Advanced setup options for experienced users.

Figure 2-4. Setup-data is saved to the first Scenario Box.

Figure 2-5. Two types of airflow windows.

Figure 2-6. Annual energy use for a building in Boston.

Figure 2-7. Monthly energy use for a building in Boston.

Figure 2-8. A design situated in two different cities: Boston, left and Tokyo, right.

Figure 2-9. Thermal comfort graph of a mechanically-ventilated East-facing room.

Figure 2-10. Thermal comfort graph of a naturally-ventilated room.

Figure 2-11. Lighting distribution on the 2-D workplane surface.

Figure 2-12. Three-dimensional lighting distribution facing the window.

Figure 2-13. Left: lifecycle cost of energy.

CHAPTER 3 RADIANT SOLAR FLUX

Table 3-1. Surface Azimuth for Various Surface Orientations

Figure 3-1. Average solar flux reaching the earth's atmosphere.

Figure 3-2. The angle of incidence.

Figure 3-3. Declination angle varies with season as the earth orbits the sun.

Figure 3-4. Variation of the solar declination with the time of year, 0=January 1st.

- Figure 3-5. Equation of time vs. time of year.
- Figure 3-6. The difference between AST and LST in Boston.
- Figure 3-7. Solar altitude and azimuth angles: QOH and SOH, respectively.
- Figure 3-8. Solar azimuth ϕ , surface azimuth ψ , and surface solar azimuth γ .
- Figure 3-9. Surface tilt angle.
- Figure 3-10. Ratio Y of diffuse-vertical to diffuse-horizontal radiation.
- Figure 3-11. Astronomical parameter C .
- Figure 3-12. Ground reflected fraction of direct radiation using different values of C .
- Figure 3-13. Comparison of two sources of TMY2 weather data for Boston, MA.
- Figure 3-14. Yearly-averaged hourly solar flux data for two very different climates.
- Figure 3-15. Monthly-averaged hourly solar flux in Boston, MA.
- Figure 3-16. Monthly averaged hourly solar flux in Johannesburg, South Africa.
- Figure 3-17. Total incident solar radiation on an East-Facing vertical building surface.

CHAPTER 4 WINDOW OPTICS

- Table 4-1. Bounce-by-bounce accounting of radiation in a single pane.
- Table 4-2. Radiation Interaction Accounting for a Triple-Pane Window.
- Table 4-3. Pane Properties as Defined in the MIT Design Advisor Software.
- Table 4-4. Blind Slat Properties as Defined in the MIT Design Advisor Software.

- Figure 4-1. A simplified radiation diagram for reflectance, transmittance, and absorptance.
- Figure 4-2. Detailed illustration of reflectance, transmittance, and absorptance.
- Figure 4-3. Snell's Law of Refraction.
- Figure 4-4. Reflections between panes occur in multi-layered windows.
- Figure 4-5. Reflections and interaction between a window pane and blinds.
- Figure 4-6. Radiation passing between two adjacent blinds (Arons 2000).
- Figure 4-7. Radiation reflected from the top surface of one blind (Arons 2000).
- Figure 4-8. Fresnel vs. ASHRAE spectral property comparison.

CHAPTER 5 ARTIFICIAL LIGHTING

- Table 5-1. Luminous efficiency of select light sources.
- Table 5-2. Minimum luminous intensity for common environments.

- Figure 5-1. US lighting energy end-use by sector.
- Figure 5-2. A 60-watt incandescent bulb emitting 1000 lumens.
- Figure 5-3. Simple lighting diagram.
- Figure 5-4. Two-dimensional workplane grid.
- Figure 5-5. Top view of workplane daylight levels.
- Figure 5-6. Lighting requirement input field on the MIT Design Advisor interface.
- Figure 5-7. Occupancy schedule input field on the MIT Design Advisor interface.
- Figure 5-8. Lighting control input field on the MIT Design Advisor interface.
- Figure 5-9. Lighting loads: 3 lighting control schemes, for an East-facing window.

CHAPTER 6 THERMAL MASS

- Table 6-1. Heat capacity of materials in a typical room, estimated.
- Table 6-2. Solar Absorption Properties of Selected Surface Materials (Incropera).
- Table 6-3. Three levels of thermal mass, specified by the user.
- Table 6-4. Summary of floor surface heat transfer coefficients.
- Table 6-5. Thermal mass properties used in the MIT Design Advisor calculations.
- Table 6-6. Maximum size of slice thickness and time steps used in simulation.
- Table 6-7. Validation cases: assumptions and results

- Figure 6-1. Heat exchange between thermal mass and air inside room.
- Figure 6-2. Radiation convection coefficient vs. surface temperature & effective emissivity.
- Figure 6-3. Convection driven by ventilation.

- Figure 6-4. Floor-air convection coefficient, ΔT dominated, ac/h term negligible.
- Figure 6-5. Exploded view of thermal mass.
- Figure 6-6. Example of matrix equations for a 5-node system.
- Figure 6-7. The semi-infinite solid.
- Figure 6-8. A semi-infinite solid with two different surface conditions.
- Figure 6-9. Case 1a, constant surface heat flux into thermal mass.
- Figure 6-10. Case 1b, constant surface heat flux out of thermal mass.
- Figure 6-11. Case 2a, surface convection into thermal mass.
- Figure 6-12. Case 2b, surface convection out of thermal mass.

CHAPTER 7 ENVELOPE LOADS

- Table 7-1. Reference Convection Coefficients.
- Table 7-2. Parameters for Window Thermal Performance Comparisons.
- Table 7-3. U-Value comparison.
- Table 7-4. SHGC comparison.
- Table 7-5. Lightweight Case (Plaster Construction)
- Table 7-6. Heavyweight Case (Concrete Construction)

- Figure 7-1. Thermal exchange through the building envelope includes the combined heat transfer through the exterior wall and the window.
- Figure 7-2. Heat transfer through the wall – a simple resistive circuit.
- Figure 7-3. Cross section of a room showing the envelope heat exchange.
- Figure 7-4. Center of glass U-Values for 3 types of gas vs. cavity width (ASHRAE).
- Figure 7-5. Two types of airflow windows.
- Figure 7-6. A representation of the energy balance in an airflow window (Lehar).
- Figure 7-7. U-Value illustration.
- Figure 7-8. Solar Heat Gain Coefficient illustration.
- Figure 7-9. Center-of-glass U-Value comparison with LBNL WINDOW5 Software.
- Figure 7-10. SHGC comparison with LBNL WINDOW5 Software.

CHAPTER 8 ENERGY BALANCE

- Table 8-2. Summary of variables used for the energy balance.
 - Table 8-2. Parameters for Stability Analysis.
 - Table 8-3. Common Parameters for Detailed Simulation Comparison.
 - Table 8-4. Specific Details of Case Comparisons.
 - Table 8-5. Data for Low Thermal Mass Case Comparisons.
 - Table 8-6. Data for High Thermal Mass Case Comparisons.
-
- Figure 8-1. Multi-storied rectangular building, 50% glazed façade.
 - Figure 8-2. Plan view of building divided into 5 subsections.
 - Figure 8-3. An example south-facing zone divided into 6 representative rooms.
 - Figure 8-4. Representative exterior room dimensions.
 - Figure 8-5. Heat exchange with the air in a room.
 - Figure 8-6. Air density variation with temperature, according to the ideal gas law.
 - Figure 8-7. Thermal circuit for heat exchange through a window.
 - Figure 8-8. Thermal mass.
 - Figure 8-9. Air temperature predictions with varying timestep size.
 - Figure 8-10. Hourly software logic for room load calculations.
 - Figure 8-11. Annual load comparison, low and high thermal mass.
 - Figure 8-12. Case 6 monthly comparison, low thermal mass.

CHAPTER 1

INTRODUCTION: BUILDINGS, ENERGY, AND SIMULATION

1.1 ENERGY USE IN BUILDINGS

Global Energy Consumption & the Role of Buildings

Energy consumption in the buildings sector represents 25 to 30% of the world's carbon dioxide emissions (DOE 2004). This includes energy required to operate building equipment, and maintain comfortable living conditions in the space. It does not include the energy required to construct the buildings. Table 1-1 shows the contribution of the buildings sector to the U.S. primary energy consumption.

As a percentage of total energy consumption, the buildings sector is predicted to remain relatively constant, while global energy consumption is growing at about 5-6% per year (Price 1999). In the U.S., the rate of carbon emissions due to buildings is growing at about 2% per year. Regardless of exactly how fast energy consumption will change in the future, it is clear that buildings are and will continue to represent a large component of the growing energy sector.

Table 1-3. U.S. Buildings Sector Energy Consumption (DOE 2004).

Buildings Share of U.S. Primary Energy Consumption (percent) (1)								Total Consumption
	Residential	Commercial	Total Buildings	Industry	Transportation	TOTAL		(quads)
1980 (2)	20%	14%	34%	41%	25%	100%		78.5
1990	20%	15%	35%	38%	27%	100%		84.1
2000	19%	15%	34%	39%	27%	100%		98.2
2002	21%	18%	39%	33%	28%	100%		97.8
2005	21%	18%	39%	33%	28%	100%		102.8
2010	21%	18%	39%	32%	29%	100%		111.8
2020	20%	19%	38%	32%	30%	100%		128.0
2025	19%	19%	38%	32%	30%	100%		136.6

Note(s): 1) Buildings-related energy consumption in the industrial sector in 1991 was 1.96 of 31.76 quads; for comparison, 2002 industrial sector energy use was 32.47 quads. 2) Renewables are not included in the 1980 data.

Source(s): EIA, State Energy Data 2000, April 2003, Tables 8-12, p. 18-22 for 1980, 1990 and 2000; and EIA, AEO 2004, Jan. 2004, Table A2, p. 134-136 for 2002-2025 data and Table A18, p. 157 for non-marketed renewable energy.

Renewable Energy Generation vs. Demand Reduction

Global concerns of depleting resources, pollution, and the greenhouse effect are associated with the traditional fossil-based means of energy production. Much attention is given to alternative energy technologies – solar, wind, geothermal, etc. – which all have reduced environmental impact as compared with traditional fossil-

based generation. While these technologies are promising, many are not yet cost effective on the large scale. Reducing energy demand, in many cases, is less costly than producing clean energy with advanced generation technology.

In the buildings sector there is a large opportunity for reducing demand by promoting more energy efficient building design. Buildings tend to have a long lifetime, often 40 years or more. Consequently, if poor design choices are made and implemented, the building will perform poorly for a very long time, adding to the environmental impact. If, instead, a building is designed in an energy-conscious manner, it may for a long time perform very well.

Building Energy Breakdown

Because buildings have varied energy needs and services, it is important to examine in which ways energy is consumed to better understand opportunities for improvement. The buildings sector can be subdivided into two main categories: commercial and residential buildings. A breakdown of energy consumption is illustrated in Table 1-2. Values are similar for both worldwide and industrialized countries. While residential energy consumption is higher, it is not overwhelmingly so. Both commercial and residential buildings have opportunity for improvement.

Table 1-2. Buildings Sector Energy Consumption Breakdown in 1995 (Price).

	Primary Energy		Electricity	
	Industrialized Countries	Worldwide	Industrialized Countries	Worldwide
Commercial	40%	37%	46%	42%
Residential	60%	63%	54%	58%

It is useful to understand how energy is consumed in buildings. Figure 1-1 shows the breakdown of energy consumption by percentage in U.S. commercial and residential buildings. Space heating is generally the largest energy requirement, followed by lighting energy. Combined, these comprise roughly 50-75% of a

building's energy needs. Accordingly, a useful simulation tool should consider these main uses of energy.

Actual building energy needs deviate substantially from these average values. Owing to the wide variety of climates on this planet, some locations require almost no heat, others no cooling. Buildings situated near the equator, for example, may have very large cooling loads. From the aggregate percentage data, this is not obvious. Climate variation, in fact, is a strong motivation for use of simulation tools for designing buildings. If climate were not a variable, it is conceivable that an optimized building design strategy would exist and have been discovered, eliminating the need for the work that follows. Since this is not the case, we shall proceed.

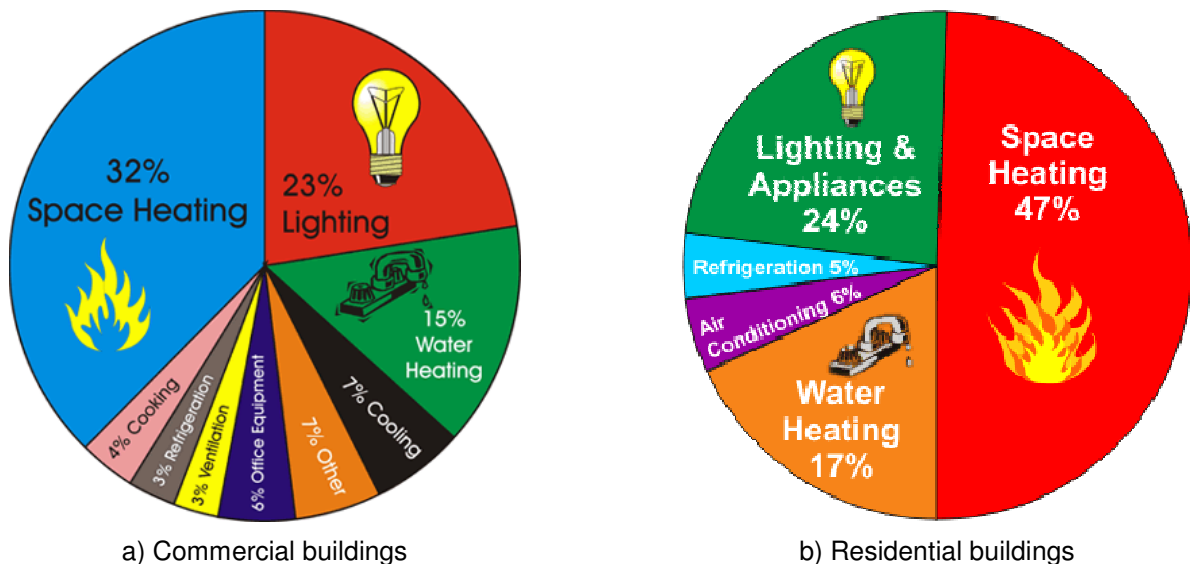


Figure 1-1. Energy breakdown in the U.S. (EIA 2006).

1.2 BUILDING DESIGN

Incentives for Improved Design

Apart from environmental concerns, the efficiency-conscious building designer has a monetary incentive to perform, since artificial lighting, heating, and cooling all come at a cost to the building owner or occupant. Effective presentation of daylight and indoor air quality is believed to improve employee productivity. According to the Building Owners and Managers Association (BOMA), per unit floor

area, the office workers' salaries represent the largest expense (1999), Fig. 1-2. Increasing worker productivity, therefore, by better building design and operation can have a substantial monetary benefit.

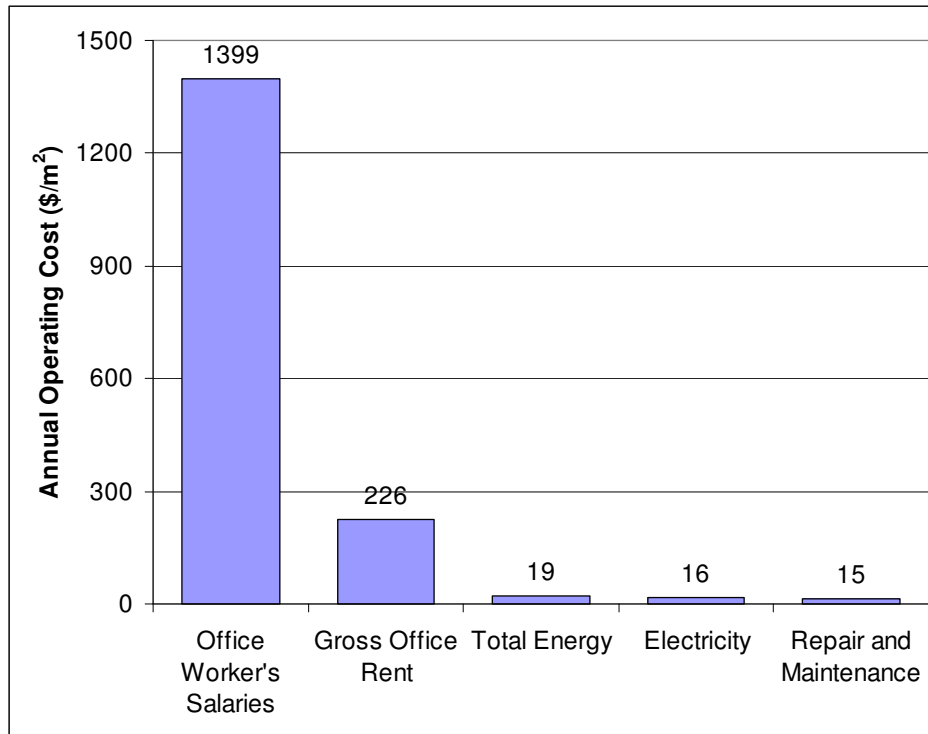


Figure 1-2. Building costs by category (BOMA 1999).

The authors of a sustainability taskforce report indicate that “traditional building development processes do not encourage lifecycle assessment” (Pederson). Instead, developers tend to focus on meeting short-term market demands. To effect change in this area, design tools must address not only environmental concerns, but also demonstrate economic returns on investment. Clear demonstration of benefit is especially important in convincing a designer to consider and use an unfamiliar system or technology. To facilitate this process and to encourage the production of more efficient building designs, an array of simulation tools have been developed that can evaluate the performance of a building design.

Early Stage Design

By considering energy efficiency at an early stage of the design process, the architect has the most control and the greatest ability to implement a good solution. Parameters such as building orientation, type and size of ventilation systems, and room dimensions are typically decided upon early in the design process. Once these decisions have been finalized, it can be very difficult or impossible to make alterations to improve efficiency. By incorporating efficient design from the start, the building designer is in a much better position to create a more sustainable product.

In the conceptual stages of design, building designers are often forced to make decisions based on prior knowledge or experience. When (if) consultants are called upon to improve energy efficiency, it usually happens after conceptual decisions have been finalized and potential for big energy savings is lost. By providing architects with an early-stage design tool, the designer can be empowered to make educated decisions, and at the time when such decisions can have the greatest impact.

1.3 SIMULATION DESIGN TOOLS¹

The use of software tools to aid in the design process is becoming increasingly popular with building designers. An abundance of tools have been developed (DOE 2006) though many existing tools are not well suited to the needs of architects.

We shall now examine a few design tools that address energy concerns in buildings. To review the full spectrum of building energy simulation tools would be a task for a different thesis; and in fact this has been done several years ago (Hong 1999). Instead, we will note the features and potential drawbacks of some popular tools as they pertain to early stage design. Two distinct categories of design software will be discussed: computational simulation engines, and user-interface based programs.

¹ Portions of this subsection are taken from a manuscript the author has submitted to the Oak Ridge National Labs (ORNL) Buildings Conference, 2007. It is currently under peer-review and expected to be published December of 2007.

Computational Simulation Engines

The category of simulation engines refers to software tools that are built with high level sophistication to lend users the greatest modeling flexibility. Examples include two programs developed by the U.S. Department of Energy (DOE), Energy Plus and DOE-2. These types of tools are intended for a highly experienced, technical user base. Usability is typically compromised in favor of increased ability to model complex building scenarios. Many underlying assumptions are made without being explicitly evident to the casual user. Users must have a detailed understanding of the simulation process to make useful design comparisons.

Most of these engines lack a pre-packaged simplified user interface. Inputs must be prepared as large text files fraught with technical jargon and programming constructs. Preparing input files can be a daunting task. Finally, simulation engines usually contain no interface for making comparisons of output results. Raw output data must be interpreted independently, which can take significant time for the novice user. Consequently the most powerful simulation tools are used only by experienced consultants and only then to simulate finalized or near-finalized building designs.

User Interface Based Programs

A number of third-party user interfaces have been developed for use with simulation engines. These applications are intended to make the creation of input files and the interpretation of results accessible to more users. Sometimes these packages are add-on software which must be installed independently of the simulation engine. Other third-party software includes the simulation engine. For simplicity, the latter is preferred. More than 18 different user-interface programs have been developed for the Energy Plus simulation engine alone.

Although interfaces may be helpful, many still fail to address the needs of the non-technical user. Typical interfaces often require very fine details before a simulation can be run. Many of the interfaces for Energy Plus, for example, require CAD model inputs of the building. Such a level of sophistication is disastrous for exploring design options due to the large time investment in preparing simulations.

The “Quick Energy Simulation Tool” (eQUEST) for the DOE-2 simulation engine is one example. The schematic design wizard feature of eQUEST, shown in Fig. 1-3, requires some 41 screens of user-input before even a simple building configuration can be modeled.

Figure 1-3. Page 1 of 41 in the eQUEST Schematic Design Wizard. A daunting amount of information is required to prepare a simulation for even the simplest designs.

Most simulation tools require a similarly high level of detailed input to generate results. At the early stage of design, a sophisticated level of detail is not available. Architects tend to have neither the time nor the resources to spend on complex preliminary design models. Regarding the nature of overly powerful tools, a point is well made by Hong,

“Choosing an ‘overpowered’ [building simulation program] is not only unnecessary and expensive but can be costly when mistakes are made due to the complexity of the software.”

In the hands of specialists, complex tools can be very effective at predicting building performance of a well-developed design, or even to help complete late-stage designs. For the architect beginning a project, they are not much help.

1.4 THE MIT DESIGN ADVISOR

To address the needs of the early stage building designer, a tool has been developed. The focus of this tool is to enable building designers to conceptualize, simulate, and analyze building designs rapidly for their energy consumption. By specifying only the most important building parameters, and without needing to know the technical terms associated with building simulation, the untrained user is able to make educated comparisons of competing designs.

A logic diagram, Fig. 1-4, shows how the software works. First, the user selects building options on a simplified user interface, Fig. 1-5. When completed, the data are sent to a simulation engine. Weather data are retrieved for the building's location. A simulation engine models the available daylight, which can be displayed graphically for several times of day. This daylight information is used to predict how much artificial lighting is needed to light the indoor space. Electric lighting loads are then computed hourly for the entire year. An HVAC loads module then uses the weather and building information to predict the monthly and annual heating, cooling, and lighting energy needs. Information about occupant comfort is also produced. These results are then displayed to the user graphically. The entire simulation process and data interpretation takes less than a minute's time.

Once a simulation is completed, the user may revise the design options and repeat the process, comparing results side-by-side. Instant design feedback allows the user to quickly learn which components have large influences on building energy consumption.

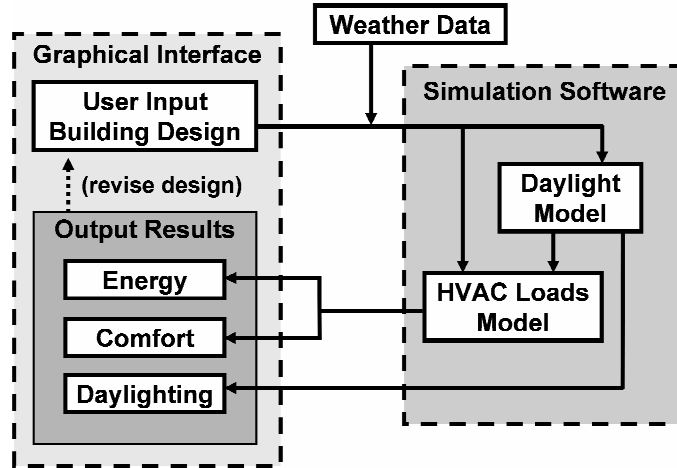


Figure 1-4. Logic diagram of MIT Design Advisor software.

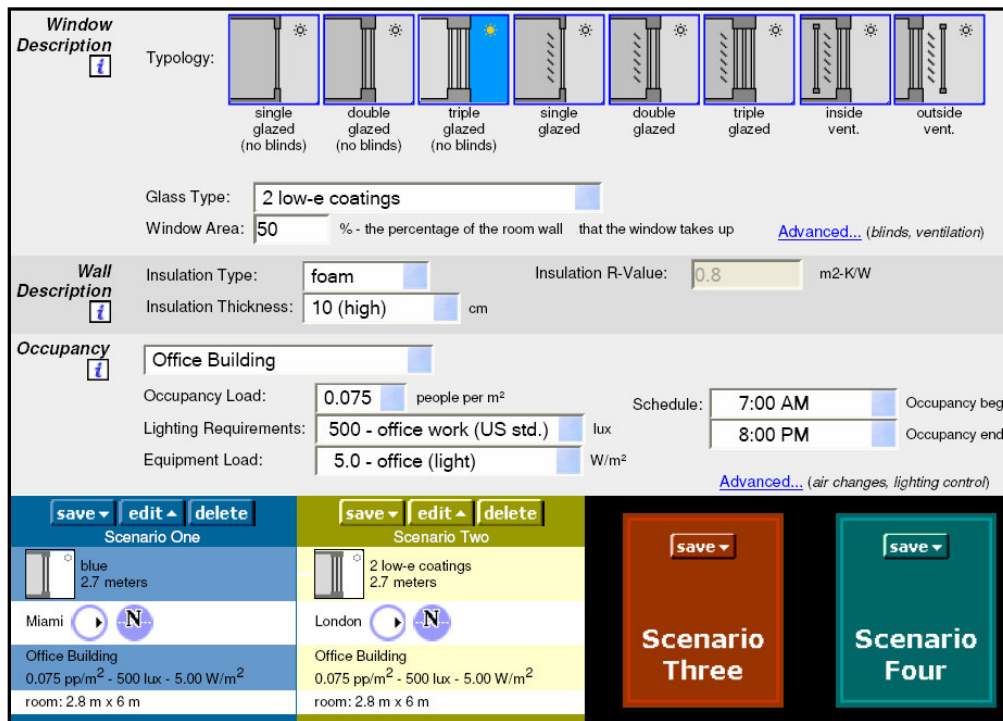


Figure 1-5. A portion of the single-page MIT Design Advisor interface.

1.5 OUTLINE OF THIS THESIS

What follows in the remaining chapters is a summary of the MIT Design Advisor simulation tool. First, in Chapter 2 a detailed overview of the tool is given, including a discussion and examples of features, user input, and program output. The remaining Chapters 3-8 focus on the methods of simulating the energy use in buildings. These chapters explain the procedures used to calculate hourly, monthly, and yearly building loads. Chapters 3-7 present subroutines used to compute components of building thermal exchange, and Chapter 8 demonstrates how to integrate these components and compute required energy loads.

Chapters 3-6 are focused on radiation and lighting. In Chapter 3 a method is explained to predict the amount of solar gains incident on a building surface based on typical weather data, geometry, building location, and time of day and year. Solar gains can be a significant source of energy in buildings. Chapter 4 discusses the optics of materials, and illustrates a method for determining how much solar radiation enters a building through a window system. Interactions between many surfaces (glass, blinds, etc.) are considered in the analysis. Chapter 5 lends itself to the computation of lighting needs based on several possible lighting strategies. Sunlight can be used to supplement artificial light and reduce electrical demand.

Chapters 6 and 7 are related to thermal gain predictions. Chapter 6 focuses on the thermal mass effect in buildings. Heat can be stored by a building's solid mass and released gradually in time to the indoor air. This effect can reduce heating or cooling loads by providing a time-delay to the internal heat gains and losses. Chapter 7 outlines a method for determining heat flow from exterior building surfaces to the indoor space by convection, conduction, and infrared radiation. Heat flow through windows and poorly insulated walls can be substantial.

Finally, Chapter 8 illustrates how to use the predicted internal gains, solar gains, thermal mass exchanges, lighting energy, envelope conduction, and ventilation requirements to predict the indoor air temperature variation with time. This prediction is used to calculate heating and cooling loads throughout the year.

At the end of each of the Chapters 3-8, a validation section is presented to show that modeling assumptions are reasonable and that calculations are carried

out properly in the MIT Design Advisor software implementation. Accuracy is demonstrated through comparisons with industry-accepted software, closed-form calculations, and tabular data from the literature. Discussions of the results are given, and agreement is quite good.

[this page intentionally left blank]

CHAPTER 2

THE MIT DESIGN ADVISOR INTERFACE

2.1 INTRODUCTION

A suitable user-interface is a primary requirement for a software tool to be useful to a particular audience. At the time of this writing, most building simulation tools have been written for an audience of scientists and engineers. Interfaces tend to focus on maximum flexibility – large numbers of options, variables, and settings – offering the ability to model even the smallest details. Complicated text-based input/output systems are commonly available, as they lend the greatest simulation freedom to the user. Such interfaces are not well suited to the needs of architects and building designers. It is far too time consuming and even unnecessary for this audience to learn specific programming languages and to construct detailed simulations to make useful design comparisons. Instead a specialized user-interface should be developed that lends the power of simulation to users that may not have a background in computer programming or thermal engineering.

Such third-party interfaces are available for many leading simulation tools. Users must first download and install the simulation engine and then purchase and install the interface. This is cumbersome and enough to deter many potential users. One further drawback to add-on software is that it adds an extra layer of complexity. Both the simulation engine and the interface may have many inherent assumptions that are not obvious to the casual user (or expert!) that could make the simulations inaccurate. Finally, while better than text-only interfaces, most of the existing graphical interfaces are still overly detailed for the very earliest stages of design. Speed of iteration is most critical for early design revision.

To meet the specific needs of the building-design audience, the MIT Design Advisor software is intended to be simple to use for a person without technical or programming experience. A new user should be able to understand and master most of the software's functions in less than an hours' time and without formal instruction. Describing a conceptual building design should take only a few minutes. Simulation results should also be available quickly, preferably in less than one

minute, and displayed graphically for easy interpretation. Such a user-interface has been developed to meet these goals.

In this chapter an overview of the MIT Design Advisor modeling software is given. This overview contains the high-level information regarding the simulation procedure, input/output options, and graphical displays. Detailed explanations of the modeling concepts and procedures are discussed in the chapters that follow.

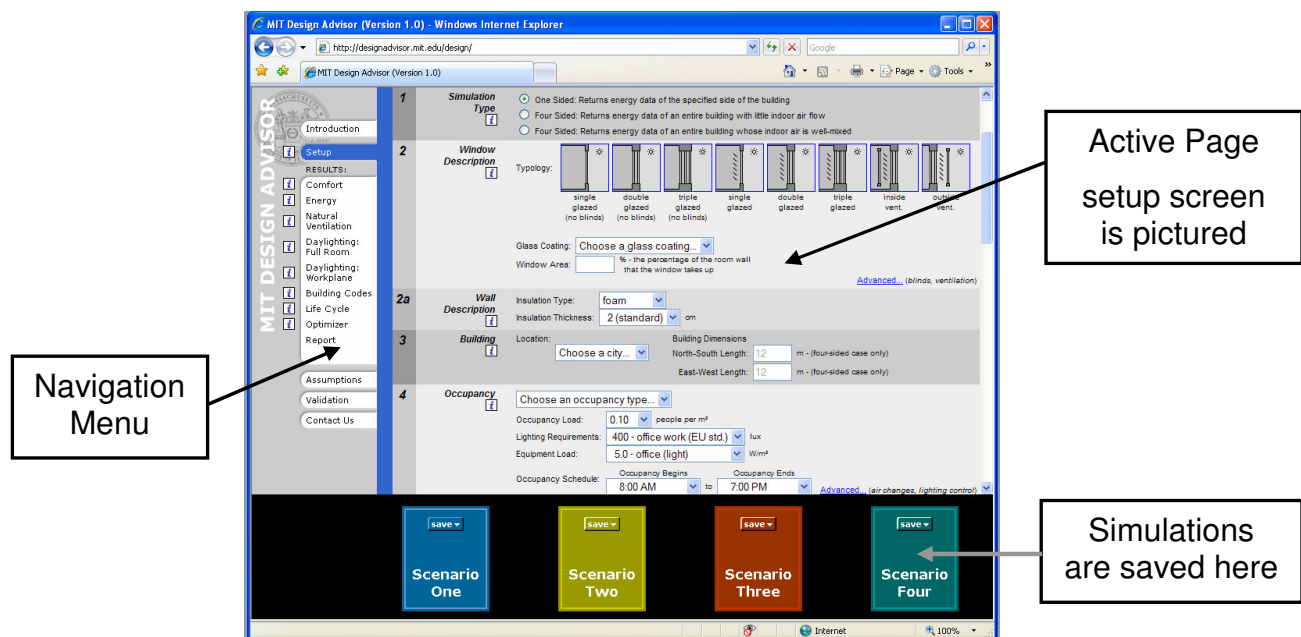


Figure 2-1. The MIT Design Advisor interface.

2.2 OVERVIEW OF THE MIT DESIGN ADVISOR INTERFACE

The MIT Design Advisor software is presently a Web-based utility. One can access and use the program directly on the Internet at <http://designadvisor.mit.edu>. A screenshot of the page as of June 2007 is shown in Fig. 2-1. The site is divided into three sections: the 'Active Page' (top right section), the 'Navigation Menu' (left, vertical bar), and the 'Saved Scenario Boxes' (bottom, four colored boxes). Most user interaction takes place on the active page. The links on the navigation menu switch the content of the active page between the setup page and the results pages. The boxes on the bottom of the page act as placeholders for saving and retrieving the user-specified building configuration data. The scenario boxes are both

numbered and colored for easy identification and referencing when comparing simulation outputs.

To perform a simulation the user must first load the SETUP page by clicking the appropriate link in the navigation menu. This loads the setup-interface in the primary section of the page. A series of basic building parameters, Fig. 2-2, and optional advanced parameters, Fig. 2-3, are then specified by the user. This process is facilitated with drop-down menus which provide informative suggestions of typical values and settings. The user options are detailed later in this chapter. Once the SETUP options have been specified, the user must then save the building configuration in any one of the four color-coded SCENARIO BOXES at the bottom of the page. When this is completed the data is sent to the simulation engine where the climate-based energy simulation takes place. The simulation results are then sent back to the user and displayed graphically for easy interpretation. These graphical results are accessible by NAVIGATING to the desired results pages. In short, the user-experience typically follows these steps:

1. User specifies a building configuration;
2. User saves the building configuration in a scenario box;
3. Building configuration is sent to the MIT Design Advisor simulation engine;
4. A yearly building simulation is performed by the MIT Design Advisor;
5. Results are returned to the user and displayed graphically;
6. User creates another design, or edits an existing design and repeats the steps (1-5) above;
7. By comparing results, the user identifies which building options have the largest impact on energy use, thermal comfort, and available daylight in a given building design. This information is used to improve conceptual design.

User Input & the Setup Page

The user-input space has been restricted to those choices which have the greatest impact on the performance of a building. Excessive complexity makes simulation tools unusable for early design. In an effort to minimize complexity and maximize accuracy, the reduced input space in Table 2-1 has been created. Advanced options, listed in Table 2-2, are hidden from the casual user. Experienced users may access these options if they wish. If these options are not explicitly set by the user, typical default values will be assumed.

Table 2-1. Basic Input Options

Inputs	Description
1. Zone configuration	a) One zone confined to a single-side of the building, b) Four-sided building with well-mixed air, OR c) Four-sided building with air unmixed between zones
2. Building	Location: select the nearest city for climate data Building Dimensions: NS and EW lengths
3. Room	Primary Façade Orientation: N,S,E, or W Room Dimensions: depth, width, and height
4. Window	Type: single-, double-, triple- glazed, or double-skin façade Coating: clear, low-e, etc. Glazed Area: as percentage of wall area
5. Wall	Specify: low, medium, or high insulation
6. Thermal mass	Specify: low, medium, or high thermal mass
7. Occupancy	Occupant Density: # people per floor area Equipment Load: Watts per floor area Min. Lighting Req.: Lux Occupancy Schedule: hours of occupancy
8. Ventilation	a) Mechanical system, b) Natural ventilation only, OR c) Hybrid mechanical & natural ventilation

Table 2-2. Advanced Input Options

9. Thermostat	Set upper and lower bounds on room temperature Set nighttime setback temperatures
10. Ventilation Rate	Specify the volumetric fresh air rate: L/s/person
11. Lighting Controls	a) lights always on b) lights dim together to supplement daylight c) lights dim independently to supplement daylight
12. Blinds	Dimensions: width of blinds and spacing Select color: shiny, painted, etc. Angle of blinds when closed Daytime & Nighttime schedules: always opened or closed, responding actively to temperature or solar intensity
13. Double Skinned Façades & Airflow Windows	Depth of airflow cavity Air flow rates through the façade Location of supply & exhaust vents (interior or exterior)

Simulation Type 	<input checked="" type="radio"/> One Sided: Returns energy data of the specified side of the building <input type="radio"/> Four Sided: Returns energy data of an entire building with little indoor air flow <input type="radio"/> Four Sided: Returns energy data of an entire building whose indoor air is well-mixed																
Window Description 	Typology: <table border="0"> <tr> <td></td> <td></td> <td></td> <td></td> <td></td> <td></td> <td></td> <td></td> </tr> <tr> <td>single glazed (no blinds)</td> <td>double glazed (no blinds)</td> <td>triple glazed (no blinds)</td> <td>single glazed</td> <td>double glazed</td> <td>triple glazed</td> <td>inside vent.</td> <td>outside vent.</td> </tr> </table> Glass Coating: <input type="text" value="low-e"/> Window Area: <input type="text" value="50"/> % - the percentage of the room wall that the window takes up Advanced... (blinds, ventilation)									single glazed (no blinds)	double glazed (no blinds)	triple glazed (no blinds)	single glazed	double glazed	triple glazed	inside vent.	outside vent.
single glazed (no blinds)	double glazed (no blinds)	triple glazed (no blinds)	single glazed	double glazed	triple glazed	inside vent.	outside vent.										
Wall Description 	Insulation Type: <input type="text" value="foam"/> Insulation Thickness: <input type="text" value="5"/> cm																
Building 	Location: <input type="text" value="Boston"/> Building Dimensions North-South Length: <input type="text" value="12"/> m - (four-sided case only) East-West Length: <input type="text" value="12"/> m - (four-sided case only)																
Occupancy 	Office Building <input type="text" value="Office Building"/> Occupancy Load: <input type="text" value="0.075"/> people per m ² Lighting Requirements: <input type="text" value="500 - office work (US std.)"/> lux Equipment Load: <input type="text" value="5.0 - office (light)"/> W/m ² Occupancy Schedule: Occupancy Begins <input type="text" value="7:00 AM"/> to Occupancy Ends <input type="text" value="8:00 PM"/> Advanced... (air changes, lighting control)																
Representative Room 	<table border="0"> <tr> <td rowspan="3"> Window Orientation </td> <td>Room Depth: <input type="text" value="6"/> m - perpendicular to windowed surface</td> </tr> <tr> <td>Room Width: <input type="text" value="5"/> m - parallel to windowed surface</td> </tr> <tr> <td>Room Height: <input type="text" value="3"/> m - vertically parallel to windowed surface</td> </tr> </table>	 Window Orientation	Room Depth: <input type="text" value="6"/> m - perpendicular to windowed surface	Room Width: <input type="text" value="5"/> m - parallel to windowed surface	Room Height: <input type="text" value="3"/> m - vertically parallel to windowed surface												
 Window Orientation	Room Depth: <input type="text" value="6"/> m - perpendicular to windowed surface																
	Room Width: <input type="text" value="5"/> m - parallel to windowed surface																
	Room Height: <input type="text" value="3"/> m - vertically parallel to windowed surface																
Ventilation System 	<input checked="" type="radio"/> Pure Mechanical Energy System <input type="radio"/> Pure Naturally Ventilated System <input type="radio"/> Joint Natural Ventilation and Mechanical Energy System																
Thermal Mass 	<input checked="" type="radio"/> High Thermal Mass: exposed ceiling and floor; concrete slab system <input type="radio"/> Low Thermal Mass: carpeting/ wood, stone systems <input type="radio"/> Zero Thermal Mass																
Overhang 	Overhang Depth: <input type="text" value="0"/> m - (0 indicates no overhang)																

Figure 2-2. Basic MIT Design Advisor Setup page. A single page of inputs can be used to estimate conceptual building design performance.

Window Description: Advanced close x

**Inside
Ventilated
Section**

Ventilation

Cavity Depth: mm (b)

Air Flow Rate*: m³/hr ↑
* per meter of window width

Vent Supply: interior
 exterior

Vent Exhaust: interior
 exterior

Blinds
Click for [Blind Settings...](#)
(color, dimensions, schedule)

Blind Parameters close x

Blinds

Blind Width: mm (c)

Blind Schedule (occupied hours):

Blind Schedule (unoccupied hours):

Blind Angle When Closed:

Blind Color:

Room Ventilation close x

Air Change Rate Per Occupant: liters / sec per person

Total Air Changes: per hour

Lighting Control

Always on (least efficient):
During occupancy hours, all lights are on at full brightness

Lights all dim together (more efficient):
A single light sensor controls all lights together

Lights dim independently (most efficient):
All lights in room dimmed independently to supplement sunlight

Figure 2-3. Advanced setup options for experienced users.

After the building parameters are specified and the user clicks SAVE on one of the four scenario boxes, data is transmitted to the simulation engine. A colored scenario box is then updated to include basic information about the saved simulation, Fig. 2-4. This makes it easy to quickly recognize the differences between saved scenarios when comparing the results.

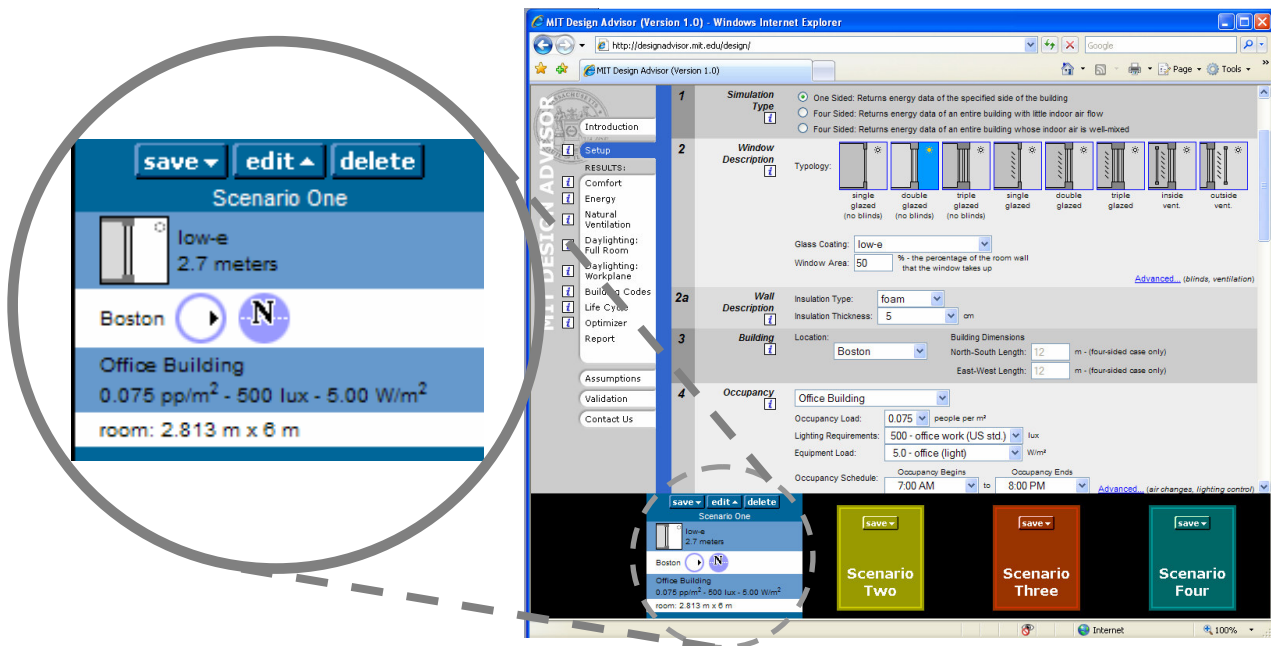


Figure 2-4. Setup-data is saved to the first Scenario Box. A summary of user-input parameters is displayed in the box for reference. Setup-data is quickly retrieved by clicking on the 'edit' button.

2.3 BASIC INPUTS: DETAILED DESCRIPTION OF OPTIONS

Zone Configuration / Simulation Type

The software can simulate an entire four-sided rectangular building, or it can simulate a single side of a building façade. By specifying a single-sided simulation the model assumes that heat transfer occurs only through the selected side of the building's façade (e.g. North, South, East, or West-face) and by ventilation exchanges. If the user selects a whole-building (four-sided) simulation, then heating, cooling, and lighting loads are computed separately for all five zones (four building

faces and one central core). In the case of whole building simulations, the air can be well-mixed or non-mixed between each of the zones of a building. When air is non-mixed, then the heating and cooling loads are simply added up for each building façade and core. When air is well-mixed, then it is assumed that a heating load in one zone of a building can offset a cooling load on another zone. The building core is assumed to receive no solar radiation or natural light. Users may decide if the core has the same occupancy conditions as the rest of the building or not.

Building: Location & Dimensions

A building is specified by its location and its rectangular floor plan dimensions, or footprint. The location, or city, determines the climate data that is used in the simulation. A series of cities in varying climates are presently available for modeling. When four-sided building simulations are being performed, the user must also specify the rectangular dimensions of the building so that the energy loads can be properly weighted between the four sides of a building.

Room: Orientation & Dimensions

Cardinal orientation (North, East, South, or West) and room dimensions – width, depth, and height – must be specified to characterize a typical room. For a single-sided simulation, the selected orientation represents the facing-direction of the exterior wall. For each simulation this representative room is the one that is used to produce the thermal-comfort graphs and the 2-D and 3-D daylighting images.

Window: Type, Area, Overhang

A window is specified by its typology, glass coloring or coating, and its area. Presently eight options are available for window typology. The first six are simple windows: single-, double-, and triple- glazed windows; with and without internal blinds. The last two types are double-skin façade systems, in which air flows through a cavity formed between two panes of glass, Fig. 2-5.

Each of the window typologies has several options for spectral coatings and colored glazings. These options change the window's optical properties and

influence solar heat gains and losses. They also affect the amount of visible light that is transmitted into the room.

Finally, the window area must be specified as a percentage of the exterior-facing wall. Windows are assumed to be strip windows spanning the horizontal width of the room and centered vertically on the wall. The specified window percentage, then, determines the height of the window as a percentage of the room height. A window-frame is automatically assumed to comprise 16% of the specified window area. For instance if a user specified a 50% glazing area, then the window frame would comprise $16\% \times 50\% = 8\%$ of the wall; the window element would comprise $84\% \times 50\% = 42\%$ of the wall; and the wall insulation would comprise the remaining 50% of the wall.

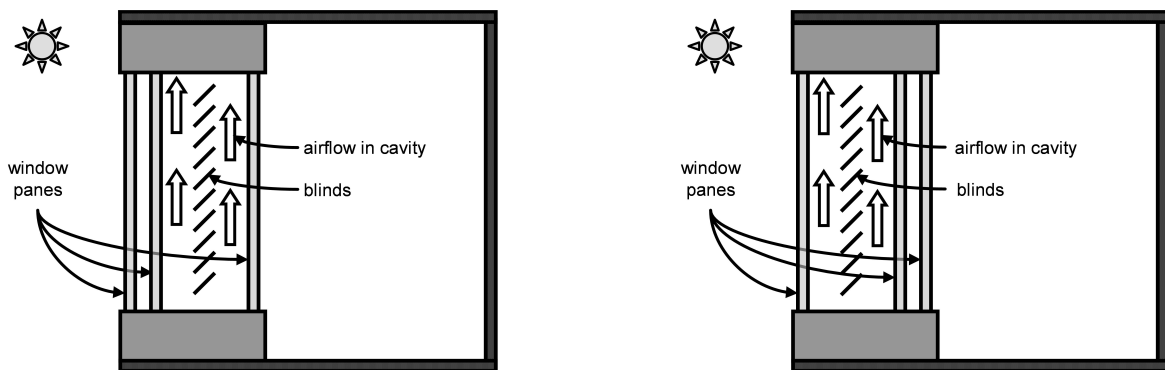


Figure 2-5. Two types of airflow windows. The double-glazing can be positioned closer to the inside or outside of the building.

An optional window overhang can also be specified. An overhang is an external element that extends horizontally outward from the top of the window to provide shading from the sun. The overhang can be specified by the distance it extends beyond the window.

Wall: Insulation Type & Thickness

The exterior-wall is described simply as a material and a thickness. Two common materials are available: foam and fiberglass, each with different insulation properties. Common values for insulation thickness are provided in the option menu.

Simple thermal resistance values are computed and displayed in real-time based on the user selections.

Thermal Mass

The user can select from low, medium, or high thermal mass. These choices affect the transient behavior of the room's energy balance. Much of the transmitted solar radiation is absorbed by the thermal mass. The amount of thermal mass determines how and when heating and cooling loads are required. Buildings that have high thermal mass can have reduced thermal loads in some climates.

Occupancy Conditions

The person-density, minimum lighting requirement, equipment load, and hours of operation must be specified to characterize the building's occupancy conditions. Typical values for each of these options are given in the menus. A quick and easy alternative is available for specifying these parameters: by selecting a building type (school, factory, residence, etc.) common values will automatically populate the input fields.

Ventilation System

The ventilation system can be mechanically ventilated, naturally ventilated, or a hybrid of the two. A mechanical building ventilation system means that windows are not operable, and heating and cooling loads are handled by a mechanical system. A naturally ventilated building is the same as a mechanically ventilated building, but during the hot season, windows can be opened to cool the space with the natural flow of fresh outdoor air. In this case, because there is no mechanical cooling, there may be hours of the year where the room temperature is uncomfortably hot. Graphs are provided to show how many hours per year the room temperature is too great. See Fig. 2-9 for an example. Finally, hybrid ventilation allows the windows to be opened or closed to assist with building temperature modulation. When the room temperature exceeds the comfortable maximum temperature, the windows are shut and mechanical cooling is applied.

2.4 ADVANCED INPUTS: DETAILED DESCRIPTION OF OPTIONS

Thermostat

The thermostat feature allows the user to specify the maximum and minimum temperatures of a building space. Advanced users may wish to use setback temperatures to reduce heating and cooling loads during times when the building is unoccupied.

Ventilation Rate

Fresh air must be introduced into a building to ensure safe and comfortable air quality. The ventilation rate is specified by the number of air changes per hour. For users who ignore this option, the air change rate is automatically linked to the occupancy conditions. Minimum ventilation rates per occupant are given in ASHRAE Standard 62-2001. Typical values are in the vicinity of 10 Liters/sec/person. Users wanting more control over the ventilation rate can specify it directly.

Lighting Control

Three lighting control strategies are available to the user: always on, more-efficient, and most-efficient. The always-on strategy simply keeps the artificial lights on during the hours that the building is occupied. The more-efficient strategy adjusts all of the lights in a room according to a single dimmer switch that is located in the darkest part of the room. In this way, sunlight can reduce the lighting load that is required. The most-efficient strategy assumes that every light fixture has its own light-sensor and can dim independently of all other lights. In this way, even more energy can be saved when sunlight is available.

Window Blinds

Blinds are specified by their material type, angle when closed, width & spacing, and control system. The material type is used to determine the amount of solar energy that is reflected, transmitted through, or absorbed by the blind system. The geometry (angle, width, and spacing) are also required to make these

calculations. The control system options allow users to specify when the blinds are opened or closed, and if the blinds can respond to temperature or glare.

Double Skin Façades & Airflow Windows

The airflow cavity windows require information on the flow rate of air through the cavity, the dimensions of the cavity, and the positions of the intake- and exhaust-vents. Vents can be connected either to the indoor space or the exterior environment.

2.5 OUTPUTS: OVERVIEW AND DETAILED DESCRIPTION

The outputs of the MIT Design Advisor model are listed in Table 2-3. In this section, a brief description of each of the outputs is given with examples.

Table 2-3. Model Outputs

Outputs	Description
Energy Requirements	Monthly & Annual heating, cooling, and lighting loads
Thermal Comfort	Comfort of occupants as a function of distance from the window Room temperature of naturally ventilated buildings to indicate how many hours the building is too hot
Daylighting	2-D and 3-D illustrations of a room's daylight distribution
Building Codes	Comparisons of a user's building with building code energy standards
Life Cycle Analysis	Annual and life-cycle energy cost and CO ₂ emissions
Detailed Report	Report file containing a scenario's inputs, energy-use outputs, and monthly- and hourly- averaged building conditions

Energy Use: Yearly & Monthly

Annual energy use is displayed in an itemized fashion as heating, cooling, and lighting loads per unit floor area. An example annual energy plot is given in Fig 2-6. Results can also be displayed monthly as shown in Fig. 2-7. The taller grey bars on the monthly plots indicate the sum of heating, cooling, and lighting loads, while the darker bars indicate the individual load (heating, cooling, or lighting). This makes it easy to see which energy requirement dominates during each season and to see when the peak loads will occur.

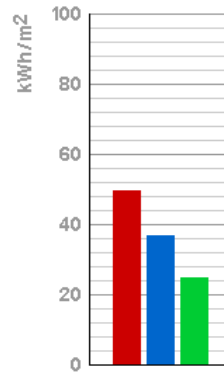


Figure 2-6. Annual energy use for a building in Boston.
 Left to right, the bars indicate heating, cooling, and lighting loads.

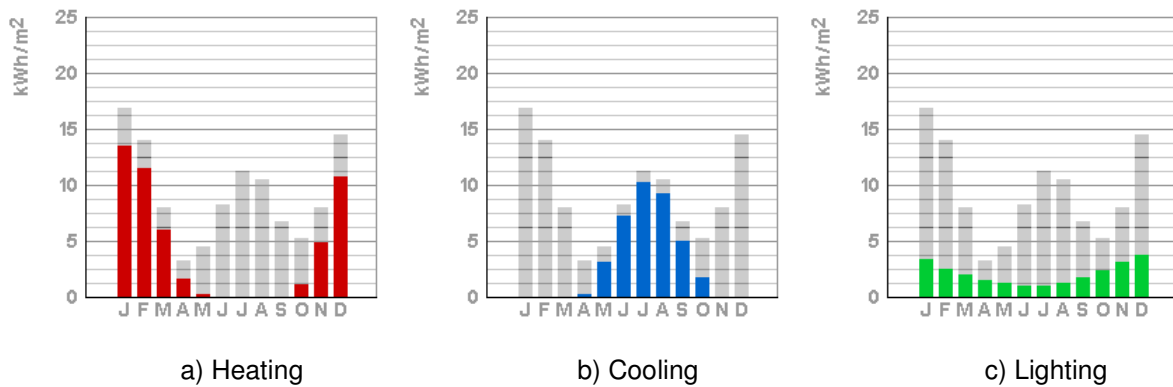


Figure 2-7. Monthly energy use for a building in Boston.
 The tall, light-colored bars indicate total energy consumption.
 The shorter, dark-colored bars indicate heating, cooling, or lighting loads.

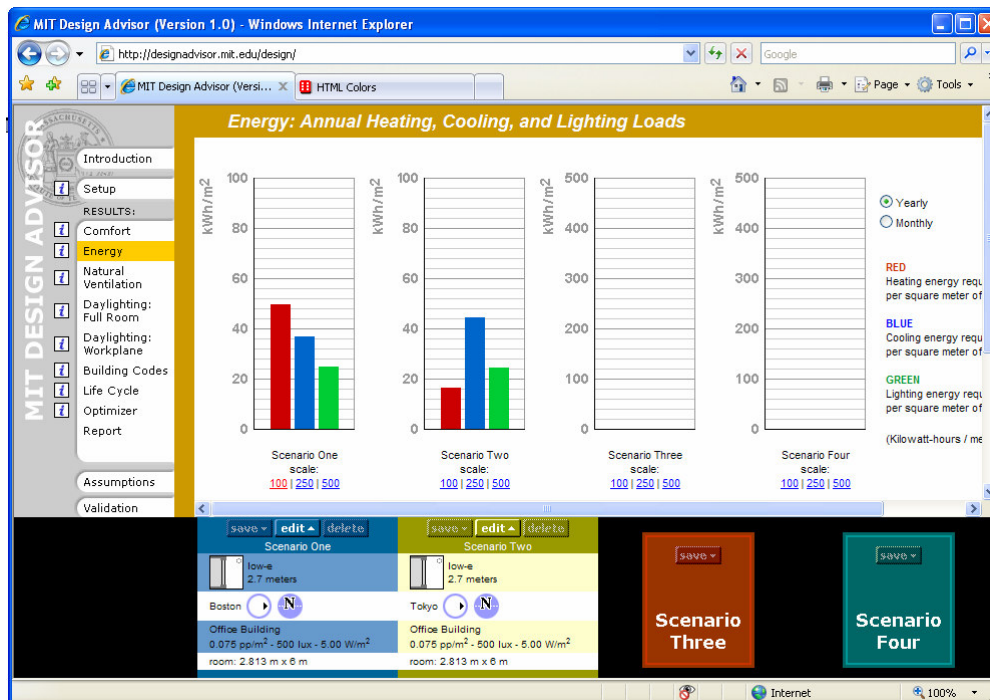


Figure 2-8. A design situated in two different cities: Boston, left and Tokyo, right. Energy bars read left to right: heating, cooling, and lighting.

A sample energy comparison between two scenarios is shown in Fig. 2-8. Design tradeoffs can be analyzed quickly with graphical side-by-side comparisons.

Thermal Comfort: Naturally & Mechanically-ventilated buildings

For mechanically ventilated buildings in which the air temperature is comfortable, occupants can still become uncomfortable due to thermal sensation. If window temperatures or other building surfaces (blinds, walls, etc.) are excessively hot or cold, or if solar radiation is felt directly on the skin, occupants may feel uncomfortable. Because people perceive comfort differently, metrics have been developed to predict the percentage of people dissatisfied, or PPD, for a given condition. The comparison is made by assuming the room's air temperature is set for maximum comfort in the middle of the room. Perceived comfort is then computed for other parts of the room based on the exterior window/wall surface temperature. The PPD metric is graphed as a function of distance from the room and at varying times during the day, and a sample plot is shown in Fig. 2-9.

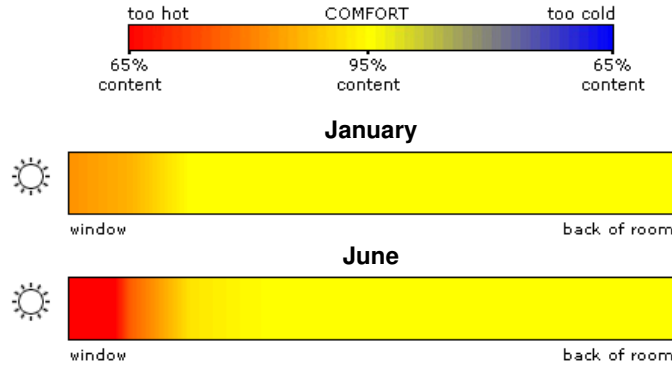


Figure 2-9. Thermal comfort graph of a mechanically-ventilated East-facing room. In June, occupants are excessively warm near the window at 9am.

In the case of strictly-naturally ventilated buildings, comfort is described differently because the air temperature in the room is not bound on the upper end. It is more important to know how many hours of the year a given temperature is exceeded. A room-temperature histogram is given as shown in Fig. 2-10. This graph is useful for determining if natural ventilation is suitable for a given climate.

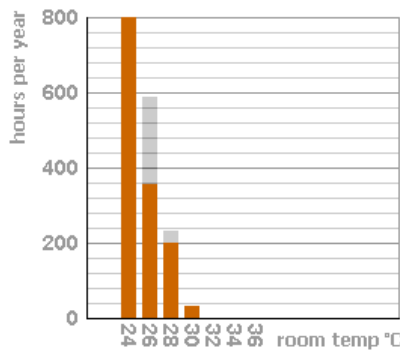


Figure 2-10. Thermal comfort graph of a naturally-ventilated room. Dark bars indicate the number of hours at a given temperature. Light bars indicate the number of hours at-or-above a given temperature.

Daylight Simulation: 2-D and 3-D Representations of the room

Daylighting distribution is computed as part of the model. This can be displayed in two ways: a 2-D view of the workplane surface; and a 3-D view of the room facing the window. The workplane view shows the distribution of daylight reaching an imaginary surface at the typical height of a desk. The 3-D view shows how sunlight falls throughout the room. Both provide values for various times of day and year. Examples are shown in Figs. 2-11 and 2-12.

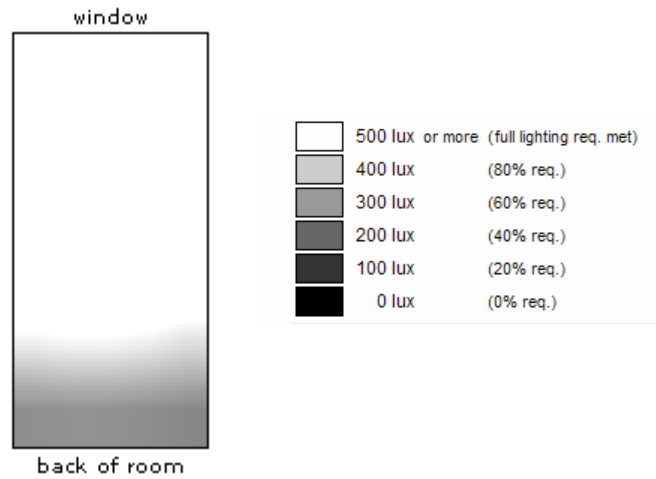
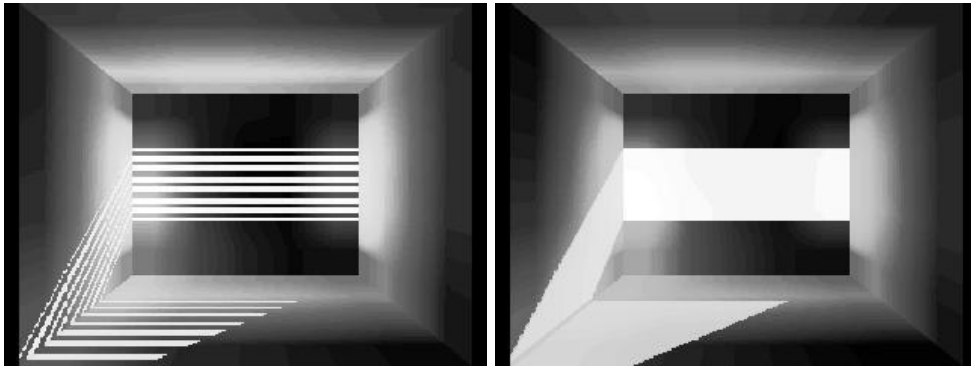


Figure 2-11. Lighting distribution on the 2-D workplane surface.



**Figure 2-12. Three-dimensional lighting distribution facing the window.
Window with blinds on the left, without blinds on the right.**

Building-Codes

Building codes are commonly used as minimal requirements for energy efficiency. Users can compare designs against prescriptive- and performance-based metrics. In cases where the proposed building design fails, the user is notified how and why the building fails and suggestions are presented indicating ways in which the building design could be improved.

Life Cycle Analysis: Energy Cost & CO₂ Emissions

A utility has been devised to allow costs-of-energy and CO₂ emissions comparisons between multiple designs. To make such a comparison basic assumptions about the price of heating fuel, electricity, duration of building operation, cash discount rate, and CO₂ emission rate must be specified. Typical values for each option are given as defaults, and the user is free to make modifications. Because fuel prices can fluctuate substantially, this feature is important. An example of the user-input boxes and the cost graphs is given in Fig. 2-13.

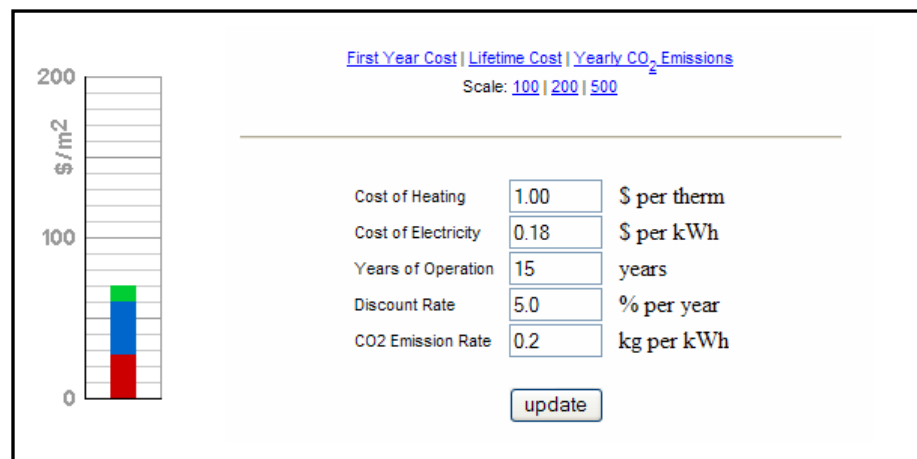


Figure 2-13. Left: lifecycle cost of energy, bars from top to bottom: lighting, cooling, and heating costs. Right: user input options.

Detailed Report File

The report file is useful for technical users wanting to document a simulation and the more-detailed results. It contains all of the information needed to re-create the simulation. It also contains tabular information on the selected simulation's energy results. Hourly-averaged values of technical details are given for each month, and these include incident solar flux, outdoor and indoor temperature, status of blinds (opened or closed), and heating/cooling loads.

Optimizer

An optimizer has been developed to help users find more efficient building design configurations. The user can specify which parameters of the simulation are allowed to vary and which are not. The parameters which are allowed to vary may further be restricted by setting upper and lower bounds, e.g. the user may require that the window area range between 20% and 40% of the wall area. The optimization engine will then predict an improved building design and share the results with the user.

2.7 MORE INFORMATION

This chapter has been meant to familiarize the reader with the software that has been developed. For a better familiarization, the reader is encouraged to try out the tool on the Web at <http://designadvisor.mit.edu>. The remaining chapters are meant to give additional detail regarding the procedures that are used to compute the outputs.

CHAPTER 3

RADIANT SOLAR ENERGY

3.1 INTRODUCTION

Solar radiation is a prominent contributor of energy in buildings. Radiant solar energy can be transmitted directly into a building as through a window, and it can be absorbed by building components. Both cause heat addition to the building interior. The visible portion of the solar radiant spectrum can provide natural lighting to a room. Evaluating the heat-exchange and visible light transmission through the building envelope each requires knowledge of the amount of solar radiation reaching the building at any given time. This chapter will outline and validate a procedure for finding the solar flux incident on any surface of a building at any time of year.

Radiation from the sun travels for roughly eight minutes before reaching the earth. For most of its journey the radiation moves unobstructed through empty space. During the final seconds, however, the radiation encounters the earth's atmosphere where interactions can occur. Just outside the earth's atmosphere a surface positioned normal to the sun's rays will receive, on average, a solar flux of 1367 W/m^2 , Fig. 3-1. A fraction of this energy will be absorbed or reflected by atmospheric particles, another fraction will be scattered by these particles, and still another fraction will reach the earth's surface completely unobstructed. Since most buildings are situated on earth's surface², we are interested in finding out the amount of solar radiation flux arriving there.

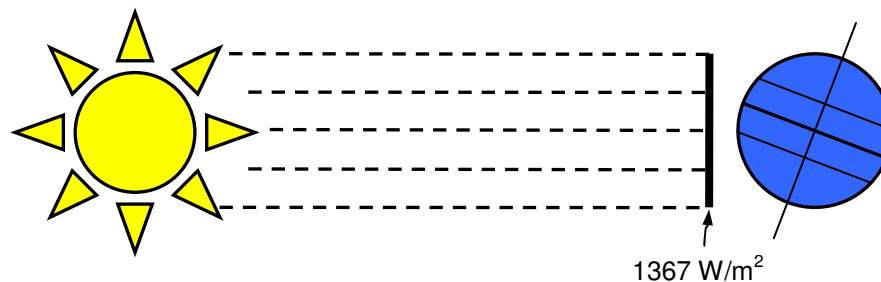


Figure 3-1. Average solar flux reaching the earth's atmosphere.

² Extra-planetary structures would require a modified simulation approach; however, at the time of this writing, such buildings are not very common.

3.2 RADIATION BASICS

Materials respond differently to radiation depending on the wavelength of the radiation and the angle at which the radiation is striking the material's surface. It is therefore necessary to model both the direction and the band of incident radiation to correctly analyze the interaction that occurs when radiation strikes a given building surface. Described in this section are a few basics as to how these differences are considered.

Radiation Wavelength: Total Solar Spectrum vs. Visible vs. Infrared Radiation

Our sun roughly approximates a black body radiating at 5800 K. Solar radiation is concentrated in the wavelength band spanning 200 to 3000 nm, with its peak occurring around 500 nm. Visible light comprises a smaller subset of this band, ranging from about 400 to 700 nm. Building surfaces are typically at temperatures near 300 K and radiation from these surfaces occurs most-strongly in a portion of the infrared band – between 8000 to 12,000 nm. Accordingly, the total-solar-thermal radiation, infrared, and visible portions of the solar radiation must be computed and considered independently. Some glass materials, for example, are effective at transmitting visible radiation while reflecting solar-thermal energy. Using such materials can be help to reduce summer heat gains, while allowing daylight into the space. The tri-band model is used throughout the modeling process to ensure accurate results.

Radiation Direction: Direct vs. Diffuse Radiation

Radiant solar energy reaching the earth's surface can be classified further into two categories: direct radiation and diffuse radiation. Direct solar radiation represents the portion of solar energy that is transmitted directly through the atmosphere unobstructed by atmospheric particles. Its direction remains basically unchanged from the time it was emitted from the sun to the time it strikes the building surface. Diffuse solar radiation represents the portion of the solar energy that has collided with one or more particles in the atmosphere and has been re-

emitted in some new direction. As a first approximation, the diffuse solar radiation consists of solar energy of equal intensity in every direction.

3.3 WEATHER DATA OVERVIEW

Accurately predicting the interactions of solar radiation with the atmosphere is difficult. Reflections from clouds depend on the clouds' type, spatial distribution in the sky, and movement throughout the day. Since meteorologists are unable to accurately predict the weather a few days or weeks in advance, it is unreasonable to model the cloud interactions at a detailed level. A different approach must be taken to capture the effects of atmospheric particles. Fortunately, extensive climate data have been compiled for cities throughout the world and these data can make a practical substitution.

Weather data files contain hourly information on the solar flux reaching the earth's surface throughout a typical year. Data for solar-flux (W/m^2) and illuminance (lux) are available in the direct-normal and diffuse-horizontal components. A direct-normal flux is the amount of power per unit area incident on a surface oriented normal to the direction of solar radiation. To find the component of the direct radiant flux incident on a building surface, the solar angle of incidence, Fig. 3-2, must be determined.

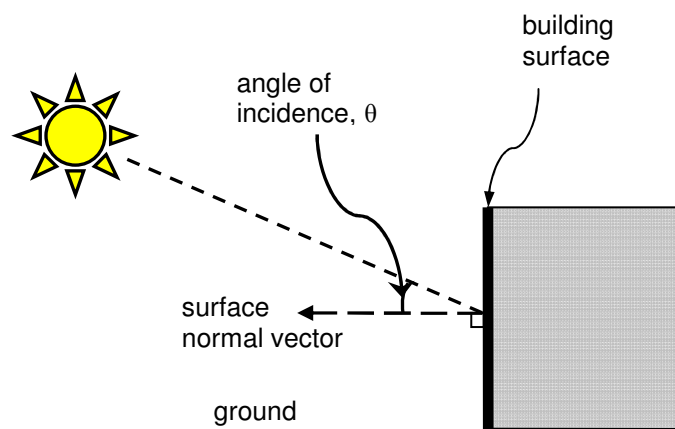


Figure 3-2. The angle of incidence: the angle between direct sunlight and the outward normal to a building surface.

Diffuse-horizontal radiation represents the amount of radiation, less the direct radiation, that is incident on a horizontal surface facing the sky. For non-horizontal building components, an adjustment factor must be included to determine the amount of diffuse-incident radiation.

Due to the high variability of weather systems, typical-year weather data is not useful for predicting the weather on a specific future date. On time scales of months and years, however, the historic data provide a good approximation of average climate behavior. Since buildings operate on time scales of many years, the representative climate data can be effectively used for predicting energy usage patterns over longer time horizons.

3.4 METHOD OF FINDING THE INCIDENT SOLAR FLUX

To find the incident solar flux on a building surface, it is necessary to compute the angle between the sun's rays and the normal to the receiving surface. The angle of incidence θ depends on the cardinal orientation of the building surface, its vertical angle of tilt, latitude and longitude, and the time of day and year. One method for finding the angle of incidence is given by ASHRAE (Fundamentals 31.13 2005). Here the ASHRAE method is presented with the simplifications and assumptions that are used in the MIT Design Advisor model.

3.5 CALCULATION OF THE ANGLE OF INCIDENCE

To determine the solar angle of incidence, it is necessary to first compute the declination, solar altitude, solar azimuth, and solar azimuth angles, relative to building surface orientation. Each of these angles is explained below and a numerical method is given for calculating the solar angle of incidence based on the month, day, hour, and location of a building.

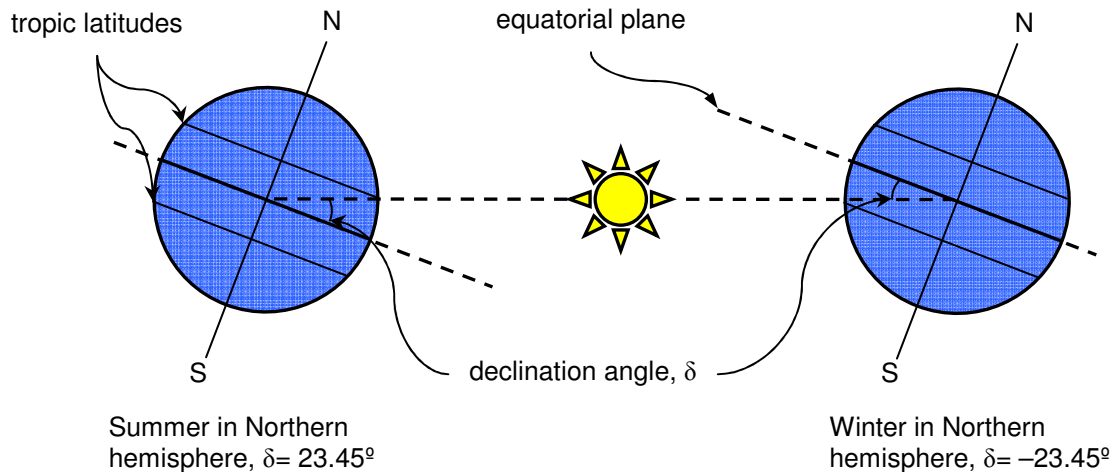


Figure 3-3. Declination angle varies with season as the earth orbits the sun.

Solar Declination

Solar declination is the angle between the earth-sun line and the equatorial plane, Fig. 3-3. Because the earth's axis of rotation is tilted and because its orbit around the sun is slightly eccentric, the declination angle varies throughout the year. An approximation of the declination angle is given by

$$\delta = 23.45^\circ \times \sin \left\{ \frac{360}{365} (284 + D) \right\} \quad (3-1)$$

where D is the day of the year (ASHRAE). Accurate tabular data are available for the declination, and Eq. (3-1) reflects a very good approximation of the data as shown in Fig. 3-4.

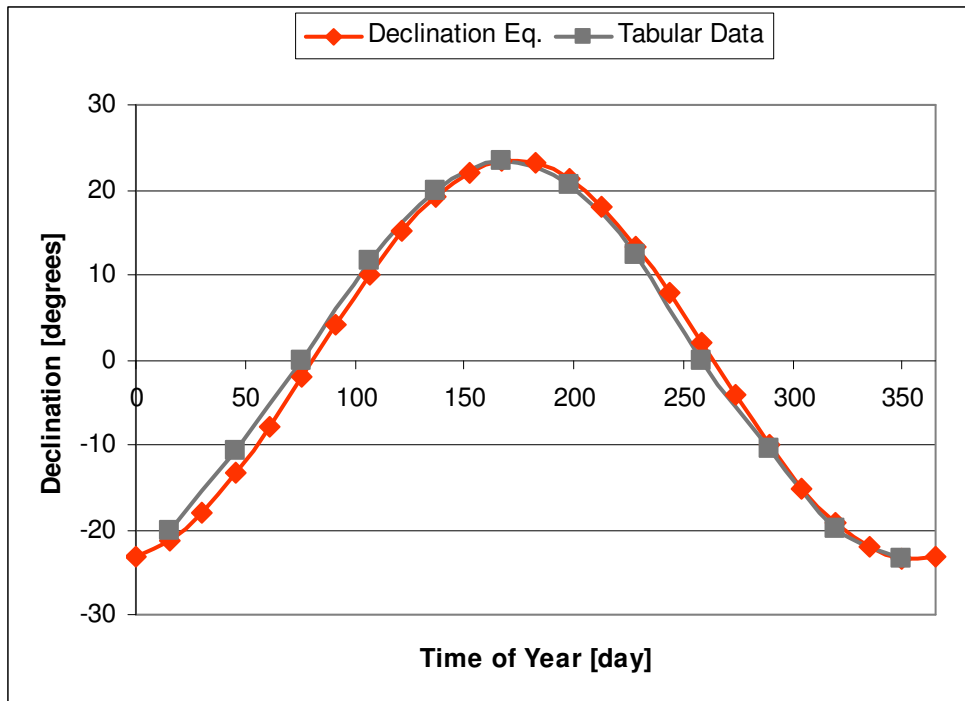


Figure 3-4. Variation of the solar declination with the time of year, 0=January 1st.

Apparent Solar Time

Time read from a clock differs from time read by a sundial. Solar noon occurs when a sundial's shadow points directly to the north in the Northern hemisphere and directly to the south in the Southern hemisphere. Solar noon does not always coincide with noon-time as read on a mechanical or a digital clock, and this is mainly for two reasons. First, time zones have a significant longitudinal width. A person on the east side of a time zone will see the sun rise a full 30 minutes earlier than a person in the center of the same time zone. Second, since the earth rotates obliquely and its orbit around the sun has some eccentricity, the middle of the solar day may be shifted in relation to clock-time.

The first error can be corrected using the difference between the time zone meridian and the building's longitude. A solar day consists of 24 hours and as many time zones are spaced in 15° intervals around the earth³. Since time zone meridians

³ Actual time zone widths may differ based on geographical or political boundaries.

are placed in the center of a time zone, geographic displacement can yield a difference of +/- 30 minutes between solar and clock time for an observer located exactly on the local time meridian. The difference (in hours) between solar time and clock time due to geographic displacement from the local time zone meridian is given as

$$\text{Geographic Difference} = \frac{\text{LSM} - \text{LON}}{15^\circ/\text{hr}} \quad (3-2)$$

A correction for the variation due to orbit irregularity is given by the Equation of Time ET, which relates sundial time to clock time (assuming no geographic displacement from the time zone meridian). Tabular data for monthly values of the ET is given by ASHRAE, and the following approximation yields good agreement

$$ET = 9.87 \sin 2B - 7.53 \cos B - 1.5 \sin B \quad (3-3)$$

where

$$B = \frac{2\pi}{364}(D - 80) \quad (3-4)$$

and

$$D = \text{day number:} \quad 0 = \text{January 1}^{\text{st}}; 1 = \text{January 2}^{\text{nd}}; \text{ etc.} \quad (3-5)$$

The equation of time correction is shown in Fig. 3-5. Taking the two corrections together, the apparent solar time is computed

$$\text{AST} = \text{LST} + \frac{\text{ET}}{60 \text{ min/hr}} + \frac{(\text{LSM} - \text{LON})}{15 \text{ deg/hr}} \quad (3-6)$$

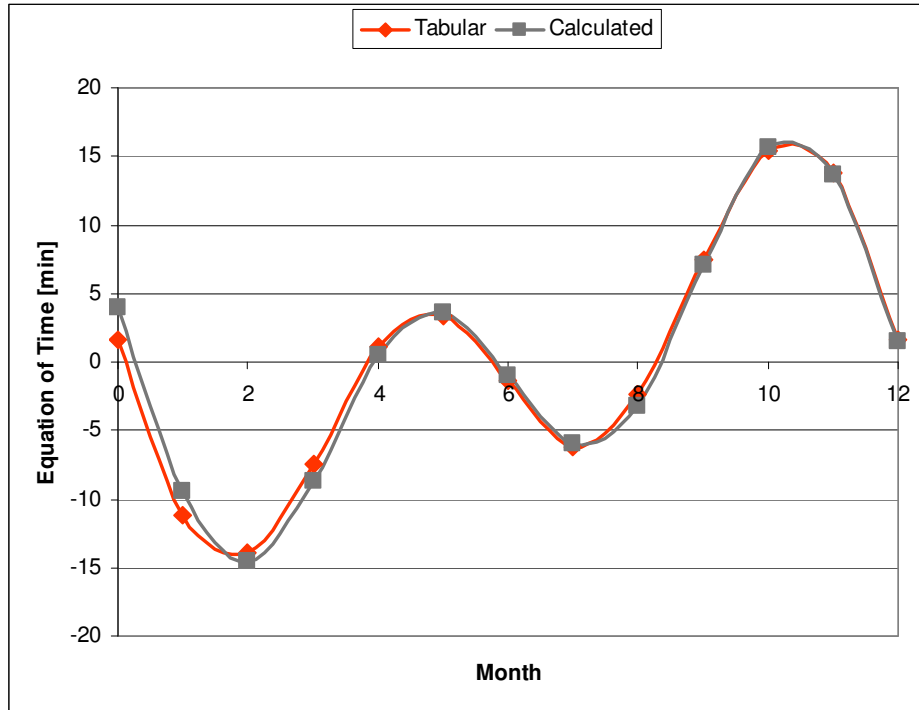


Figure 3-5. Equation of time vs. time of year.

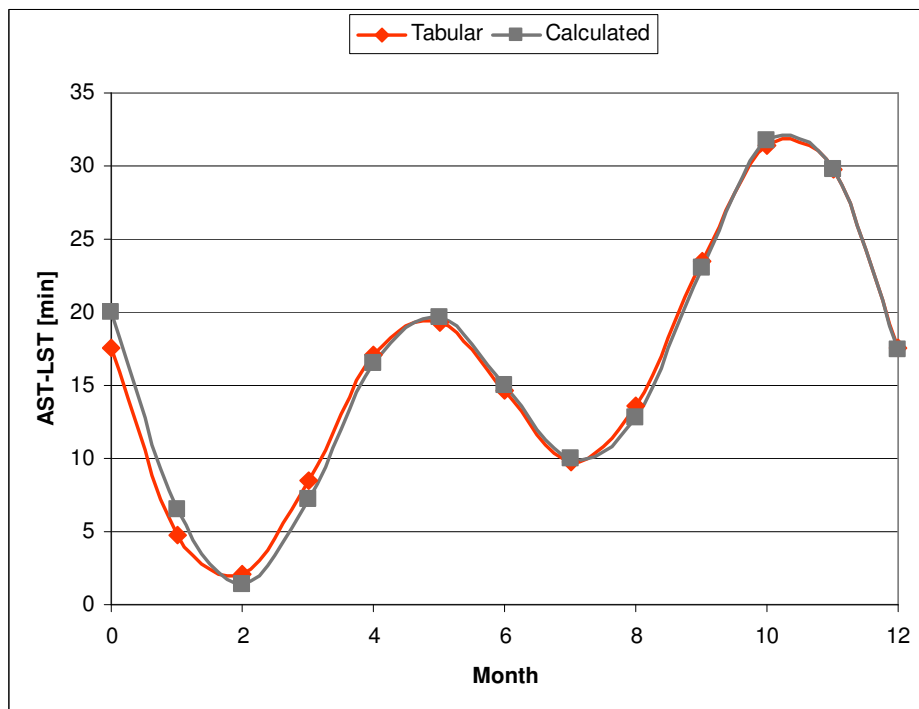


Figure 3-6. The difference between AST and LST in Boston, accounting for both the Equation of Time and geographic displacement from the Local Time Zone Meridian.

An example is given to show the combined effect. Boston, MA has a longitude of 71.1° and resides in the Eastern Standard Time Zone, which lies on the 75° meridian. Geographic displacement from the meridian causes solar time to lead local time by 16 minutes⁴. Adding to this the variation due to the equation of time, one can obtain the difference between Local Time and Apparent Solar Time, see Fig. 3-6. Local time in Boston always lags behind apparent solar time, by an average of about 16 minutes, and by as much as 32 min.

Solar Altitude and Azimuth

Next, two solar angles – the altitude β and azimuth ϕ – must be computed. These angles are depicted in Fig. 3-7. First the terms are defined and then a method is given for calculating their values.

The solar altitude β is the elevation angle between the earth-sun line (QO) and its projection (OH) onto the ground in the direction of the horizon. When solar altitude is positive, the sun is above the horizon and direct sunlight is visible to an observer on the ground. When the solar altitude is negative, the sun is below the horizon and direct sunlight is not visible to a ground observer. As defined the solar altitude can vary between -90° to $+90^\circ$.

The solar azimuth ϕ is the horizontal component of the sun's compass direction. In Fig. 3-7 it is shown as the angle between the N-S vector and segment (OH). The azimuth angles are positive measured from the south towards the west, and negative measured from the south towards the east. When the sun shines from due east, the azimuth angle is -90° ; when the sun shines from due south, the azimuth angle is 0° ; and when the sun shines from due west, the azimuth angle is $+90^\circ$. Solar azimuth can vary between -180° to $+180^\circ$.

⁴ Calculated as: $\frac{(\text{LSM} - \text{LON})}{15^\circ/\text{hr}} = \frac{(75^\circ - 71.1^\circ)}{15^\circ/\text{hr}} = 0.27\text{hr} = 16\text{min}$

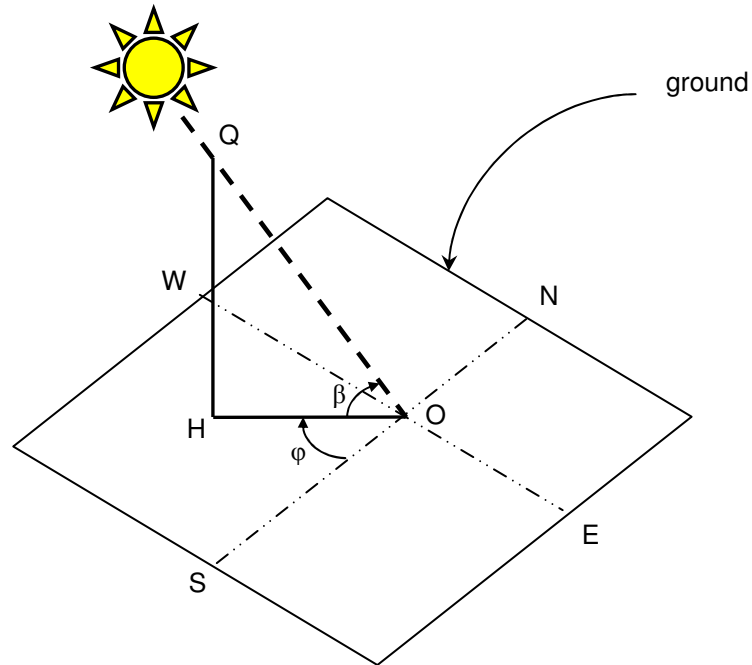


Figure 3-7. Solar altitude and azimuth angles: QOH and SOH, respectively.

To compute the solar altitude and azimuth angles, the time of day must be converted into a geometric angle. The hour-angle H serves this purpose. The hour-angle represents the rotational position of the earth about its axis, and it is based on the apparent solar time. Since the earth rotates at 15° per hour⁵, H is defined as

$$H = \frac{15\text{deg}}{\text{hr}}(\text{AST} - 12) \quad (3-7)$$

As defined above, the hour angle can vary between -180° to $+180^\circ$. Solar noon occurs at an $H=0^\circ$. Negative values indicate morning time and positive values indicate afternoon time. The solar altitude β depends on the hour angle H , the local latitude L , and declination δ

$$\beta = \arcsin(\cos L \cos \delta \cos H + \sin L \sin \delta) \quad (3-8)$$

⁵ This is not strictly true, since the earth is moving around the sun as it rotates about its axis. A solar day is 24 hours, while the earth rotates slightly

With the result of Eq. (3-8) the solar azimuth can be determined

$$\phi = \arccos\left(\frac{\sin \beta \sin L - \sin \delta}{\cos \beta \cos L}\right) \quad (3-9)$$

From the angle conventions above, the solar azimuth angle takes negative values during the morning and positive values during the afternoon.

Building Surface Orientation

Building surface orientation is the only remaining parameter that must be described before the angle of incidence can be computed. Two angles are used to specify surface orientation: surface azimuth Ψ , and surface tilt Σ . The surface azimuth angle is determined in the same manner as the solar azimuth; however, the ground-projection of the outward-surface-normal vector is used in place of the projected direction of the sun. Fig. 3-8 illustrates how the surface azimuth angle is measured, and Table 1 gives values for various surface orientations.

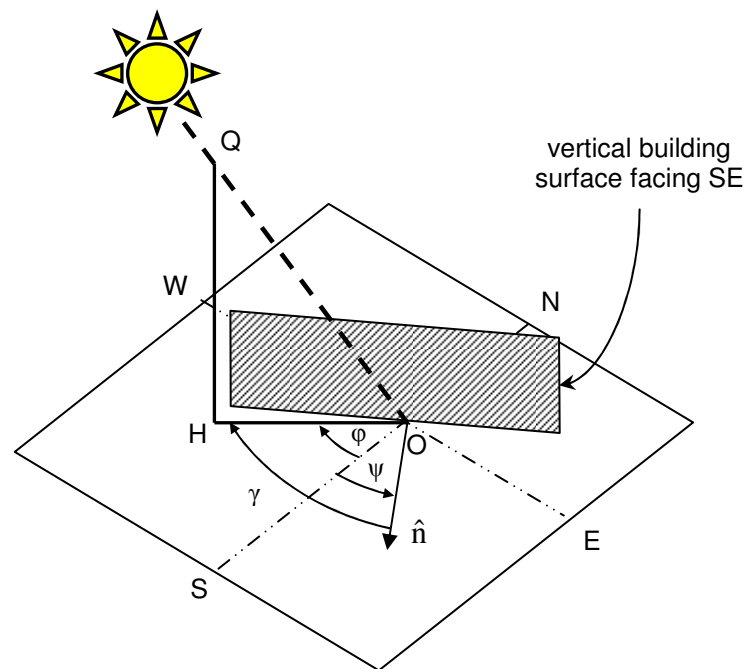


Figure 3-8. Solar azimuth ϕ , surface azimuth ψ , and surface solar azimuth γ . The surface depicted is receiving very little direct sunlight.

Table 3-1. Surface Azimuth for Various Surface Orientations

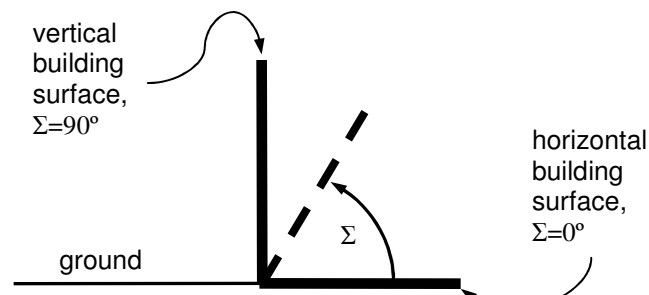
	Surface Orientation							
	N	NE	E	SE	S	SW	W	NW
Surface Azimuth Ψ	180°	-135	-90	-45	0	45	90	135

The surface-solar azimuth angle γ (angle $[\hat{n}-O-H]$ in Fig. 3-8) is the difference between the solar azimuth and the surface azimuth, given as

$$\gamma = \phi - \psi \quad (3-10)$$

A vertical surface is in the shade when γ is greater than 90° or less than -90° . This can be seen in Fig. 3-8. As the sun is setting in the West, the SE-facing surface is receiving less and less direct sunlight.

Surface tilt is simply the angle measured up from the ground to the surface, illustrated in Fig. 3-9. A horizontal surface tilt is 0° and a vertical surface tilt is 90° . Most building surfaces are vertically oriented, but a few (roofs, overhangs, etc.) are not.

**Figure 3-9. Surface tilt angle.**

Surface-Solar Angle of Incidence:

Once the solar and building geometry has been determined using the equations above, the angle of incidence θ between the surface outward normal vector and the incoming radiation vector (angle $[\hat{n}-O-Q]$ in Fig. 3-8) can be computed using

$$\cos \theta = \cos \beta \cos \gamma \sin \Sigma + \sin \beta \cos \Sigma \quad (3-11)$$

The angle of incidence is used directly to determine the amount of incident direct-radiation, and the method is outlined below.

3.6 COMPONENTS OF SOLAR RADIATION

Direct-Incident Radiation

Climate data in the TMY2 format include hourly values for direct-normal and diffuse-horizontal solar radiation and illuminance. The component of the direct-normal radiation incident on a surface is given by the cosine of the angle of incidence. The relations for direct-incident radiation and illuminance are given by

$$E_{dir,i} = E_{dir,n} \cos \theta \quad (\text{solar thermal radiation}) \quad (3-12a)$$

$$I_{dir,i} = I_{dir,n} \cos \theta \quad (\text{visible illuminance}) \quad (3-12b)$$

Diffuse-Incident Radiation

For horizontal surfaces, the diffuse-horizontal radiation can be used directly. For vertical surfaces, however, the diffuse-horizontal radiation must be converted into diffuse-vertical radiation. ASHRAE provides a conversion ratio Y of vertical:horizontal incidence values. The relations for diffuse-vertical radiation and illuminance are given by

$$E_{dif,vertical} = Y \cdot E_{dif,horizontal} \quad (\text{solar thermal radiation}) \quad (3-13a)$$

$$I_{dif,vertical} = Y \cdot I_{dif,horizontal} \quad (\text{visible illuminance}) \quad (3-13b)$$

where

$$\begin{aligned} Y &= 0.55 + 0.437 \cos \theta + 0.313 \cos^2 \theta && \text{for } \cos \theta > -0.2 \\ Y &= 0.45 && \text{for } \cos \theta \leq -0.2 \end{aligned} \quad (3-14)$$

The behavior of Y with angle of incidence is illustrated in Fig. 3-10. At small incidence angle a vertical surface may receive slightly more diffuse radiation than a horizontal surface ($Y > 1$). This can occur when the sun is low in the sky (usually sunrise or sunset for east- or west-facing surfaces), and the majority of the diffuse energy is not coming from overhead, but directionally instead.

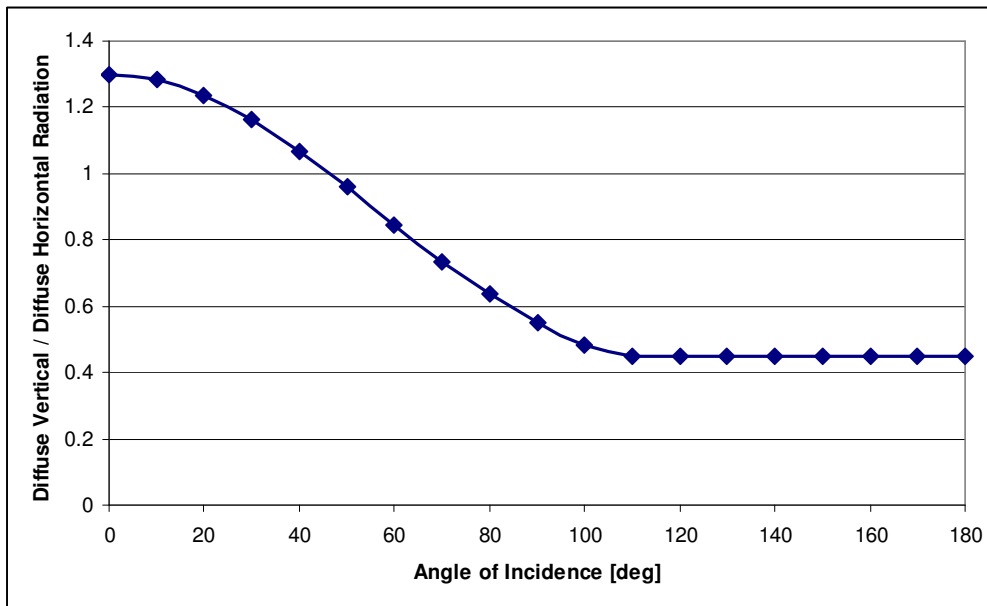


Figure 3-10. Ratio Y of diffuse-vertical to diffuse-horizontal radiation (or illuminance).

Reflected-Incident Radiation

Some portion of the direct radiation can be reflected from the ground before it strikes a building surface. The amount of reflected radiation depends on the properties of the ground, and whether or not there are surrounding objects – tall trees, structures, etc. – that could shade the reflections. It is assumed that ground reflections are diffuse. ASHRAE gives an expression for the reflected-incident radiation

$$E_{ref,i} = E_{dir,n} (C + \sin \beta) \rho_g \frac{1 - \cos \Sigma}{2} \quad (\text{solar thermal radiation}) \quad (3-15a)$$

$$I_{ref,i} = I_{dir,n} (C + \sin \beta) \rho_g \frac{1 - \cos \Sigma}{2} \quad (\text{visible illuminance}) \quad (3-15b)$$

where ρ_g is the reflectivity of the mixture of ground materials (typically 0.20), and C is a dimensionless astronomical ratio which varies slightly by month, Fig. 3-11. Using the yearly average value $C=0.118$ yields only slight differences in the reflected fraction, as compared with using minimum or maximum values, as shown by Fig. 3-12.

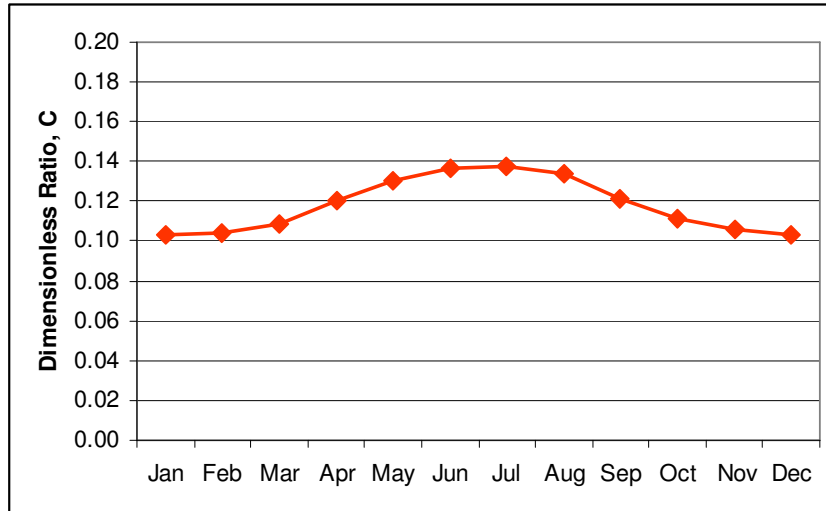


Figure 3-11. Astronomical parameter C.

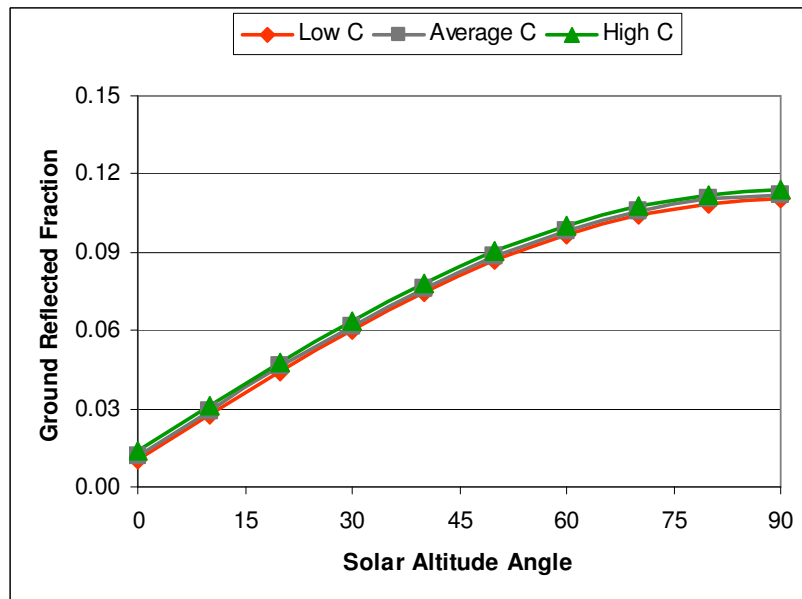


Figure 3-12. Ground reflected fraction of direct radiation using different values of C.

3.7 VALIDATION

The hourly data used in the MIT Design Advisor software must be consistent with other reliable sources of weather data, and the calculation method for resolving components of radiation must be accurate. To check the climate data, a comparison has been made against an alternative data source. A qualitative comparison between two differing climates also provides some sense of correctness. Finally, a comparison has been made between third-party software for hourly incident load computation. Agreement in all cases is satisfactory.

Weather File Data Comparison

The METEONORM software has been used to generate weather files in the TMY2 data format. To ensure the data are interpreted properly and consistent with other data sources, a comparison has been made with climate data from the National Renewable Energy Lab (NREL). Values of direct-normal and diffuse-horizontal solar radiation have been explored. A comparison of the yearly average of the hourly solar flux shows good agreement, Fig. 3-13.

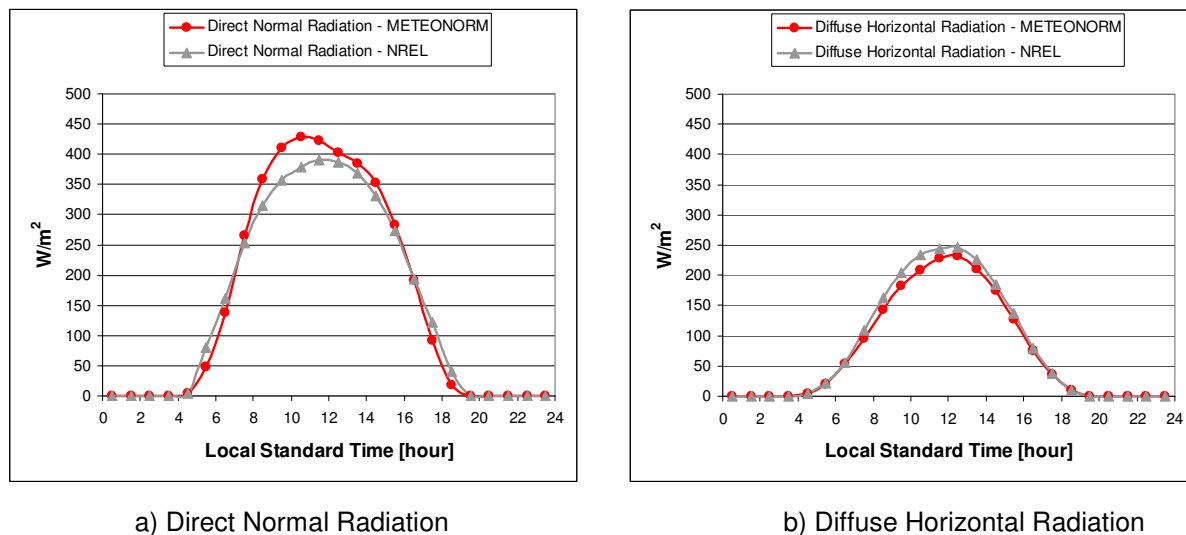


Figure 3-13. Comparison of two sources of TMY2 weather data for Boston, MA METEONORM vs. NREL data.

The METEONORM data report slightly higher direct-normal radiation values, while the NREL data report slightly higher diffuse-horizontal radiation. The small differences for identical locations underline the variability inherent to weather-file-type simulations. Differences are reasonable.

Climate Comparison

Next comparisons are made between differing climates and in different hemispheres to underscore some possible variations and patterns. Figs. 3-14 to 3-16 illustrate solar data for two locations: Boston, MA and Johannesburg, South Africa. A yearly average of the hourly solar flux, Fig. 3-14, indicates that the diffuse radiation is similar for the two locations. Direct radiation, however, is modestly higher in Johannesburg as compared with Boston – owing to a closer proximity to the equator and to a reduced cloud cover. Data for each city shows approximate symmetry about the solar noon, which is consistent with expectation.

Some of the daytime symmetry is lost when considering the monthly averaged data, most notably in the direct radiation, Figs. 3-15 and 3-16. Daily patterns in cloud cover can help to explain such results. Over an entire year these patterns average out, but on a monthly scale results are noticeably affected. Solar flux data on the daily scale presents an even higher variability.

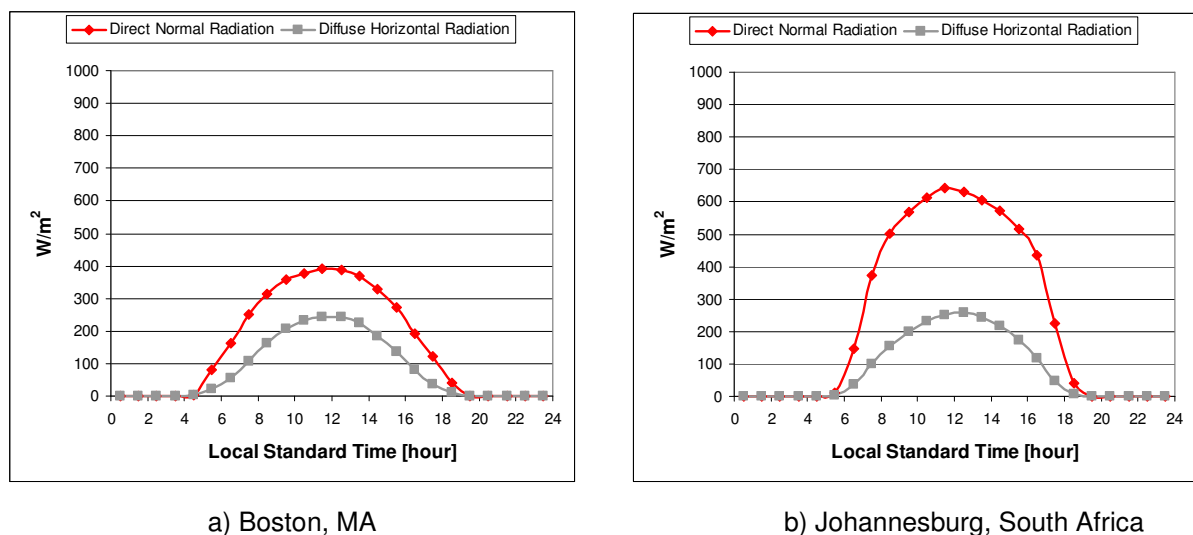


Figure 3-14. Yearly-averaged hourly solar flux data for two very different climates.

Monthly trends again follow expectations. In Boston, Fig. 3-15, there is more direct sunlight in the colder, drier months – January, October – than in the warmer, more humid months – April and July. More of the direct radiation is scattered by clouds in the warmer humid seasons, and this is seen as diffuse-horizontal radiation increases at this time. In Johannesburg, Fig. 3-16, the climate differs – monthly trends are opposite that of Boston due to its location in the Southern Hemisphere.

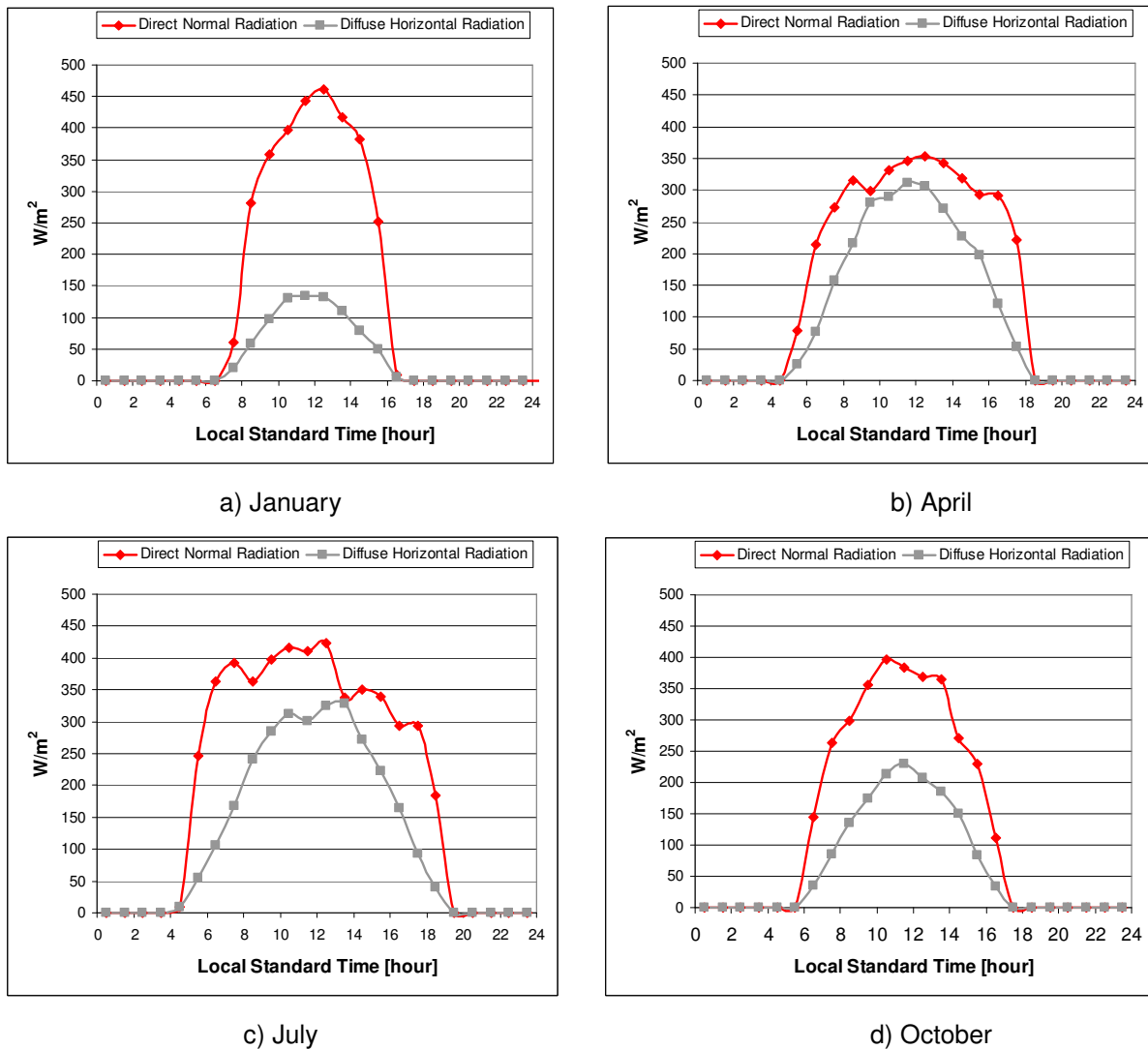


Figure 3-15. Monthly-averaged hourly solar flux in Boston, MA.

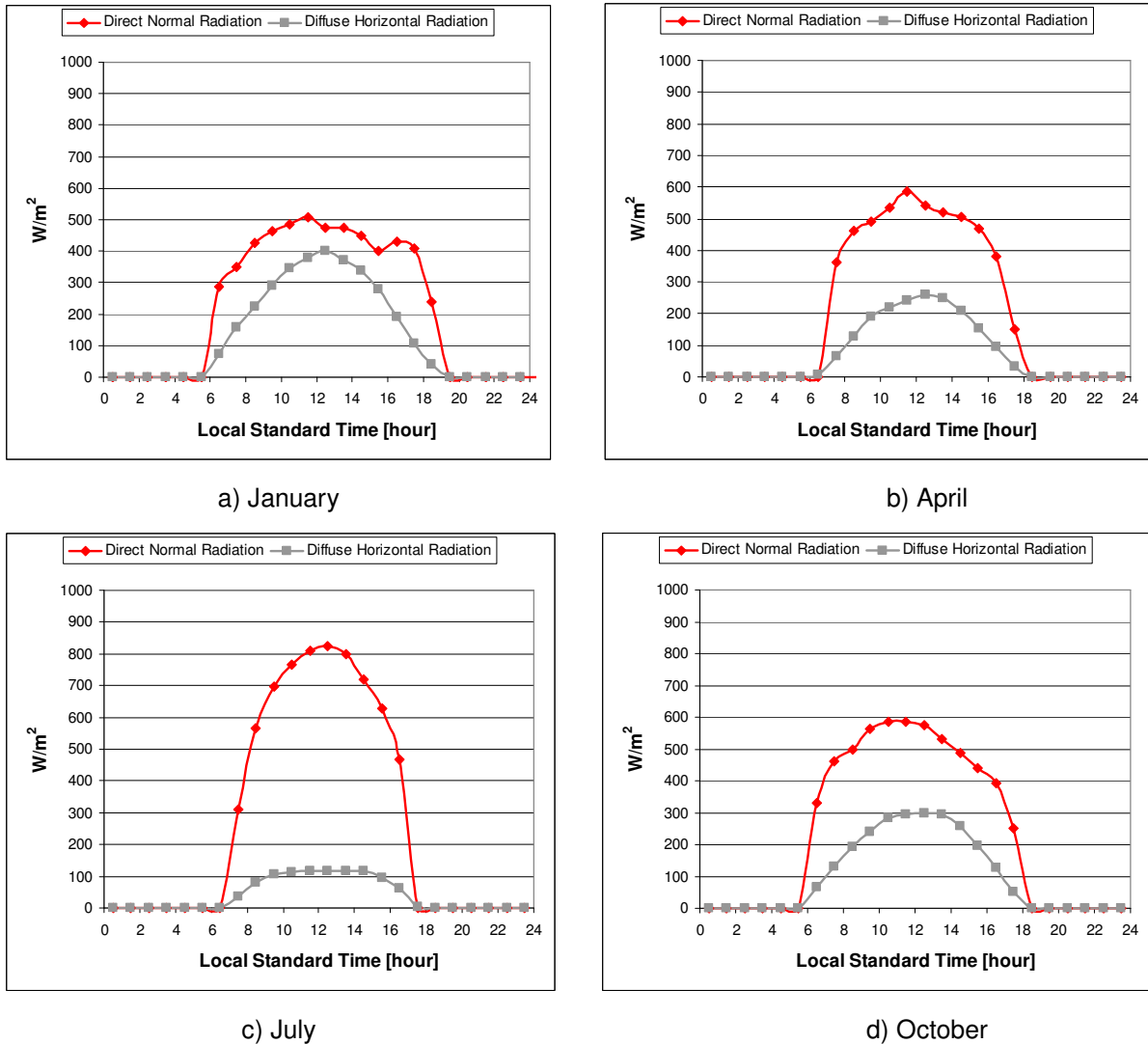


Figure 3-16. Monthly averaged hourly solar flux in Johannesburg, South Africa.

Energy Plus Comparison

Finally, a comparison is made with the Energy Plus software. Fig. 3-17 illustrates the total incident solar energy upon an East-Facing vertical surface in Boston, MA. Both programs used the same weather data files as inputs. The shape of the graph is similar for both programs. Energy Plus predicts a modestly-lower total incident solar energy over the day. One possible explanation for this difference could be differences in assumption for the reflectivity of the ground. Still, results are modestly close and agreement is satisfactory.

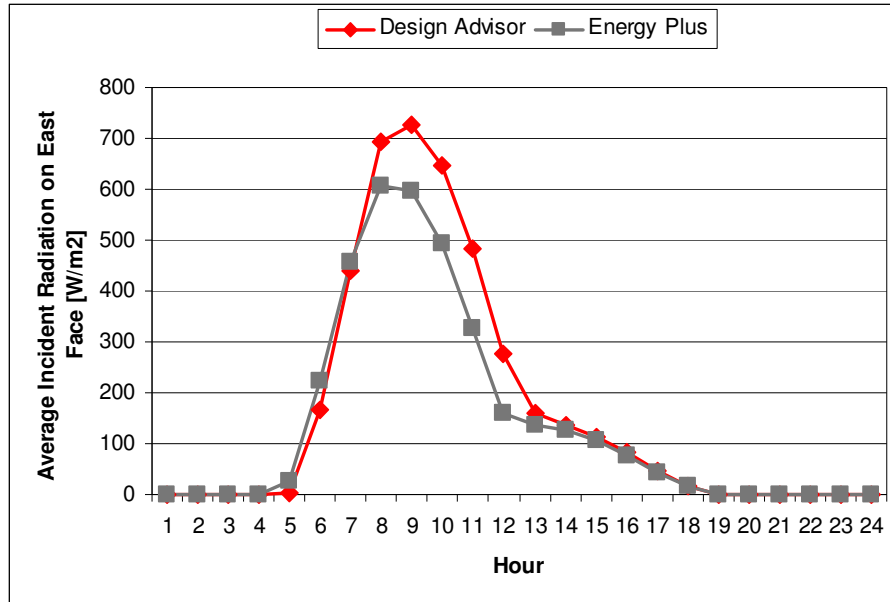


Figure 3-17. Total incident solar radiation on an East-Facing vertical building surface. (sum of direct-, diffuse-, and reflected- incident flux), an Energy Plus comparison.

Conclusion

Technique for computing direct-incident, diffuse-incident, and reflected-incident radiation and illuminance has been demonstrated and validated. Some fraction of incident thermal radiation is absorbed by building surfaces, some is reflected, and some can be transmitted through transparent or semi-transparent surfaces into the building. The interaction of absorbed and transmitted radiation with building components is the subject of subsequent chapters.

CHAPTER 4

WINDOW OPTICS

4.1 INTRODUCTION

Spectral properties of window systems play a key role in determining how much solar energy reaches the inside of a building. In Chapter 3, a detailed method was given for how to compute the amount of solar radiation falling on a given building surface. The next step in computing a building's solar-radiation gains requires the incident radiation be resolved into three components: the transmitted, reflected, and absorbed fractions. Transmitted radiation passes through the material and into the building. Absorbed radiation causes a building's material temperature to rise and this affects the amount of heat conducted or radiated into the zone or out to the external environment. Reflections are important in multi-layered glazing systems, as energy reflected from one layer may be absorbed, reflected, or transmitted through a subsequent layer. A simplistic visual representation of radiation interactions on a single pane is given in Fig. 4-1.

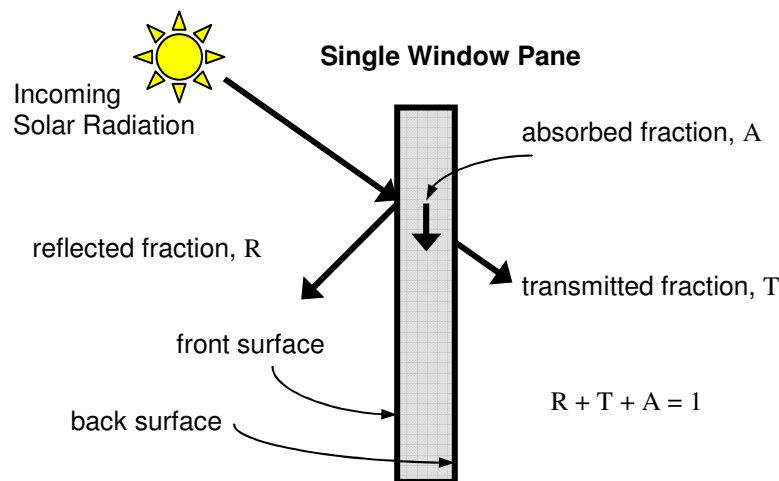


Figure 4-1. A simplified radiation diagram for reflectance, transmittance, and absorptance.

The fraction of incident radiation that is reflected, transmitted, or absorbed depends on material properties, the wavelength of radiation, and the angle of incidence. Data for glass reflectance, absorptance, and transmittance are often available only at normal incidence angle. Because these properties change with incidence angle, and because solar angles change widely during the day and throughout the year, the angular dependence must be carefully considered. Using the Fresnel equations for reflection, a method is given for converting reflectance, transmittance, and absorptance values at normal incidence angle into the corresponding angular-dependent values.

4.2 RADIATION AND OPTICS BACKGROUND

First, we make the important distinction that reflectivity ρ , absorptivity α , and transmissivity τ are physical properties. The terms reflectance R , absorptance A , and transmittance T are convenient expressions for the bulk-behavior of a window system, and are based on ρ , α , τ , and the window configuration.

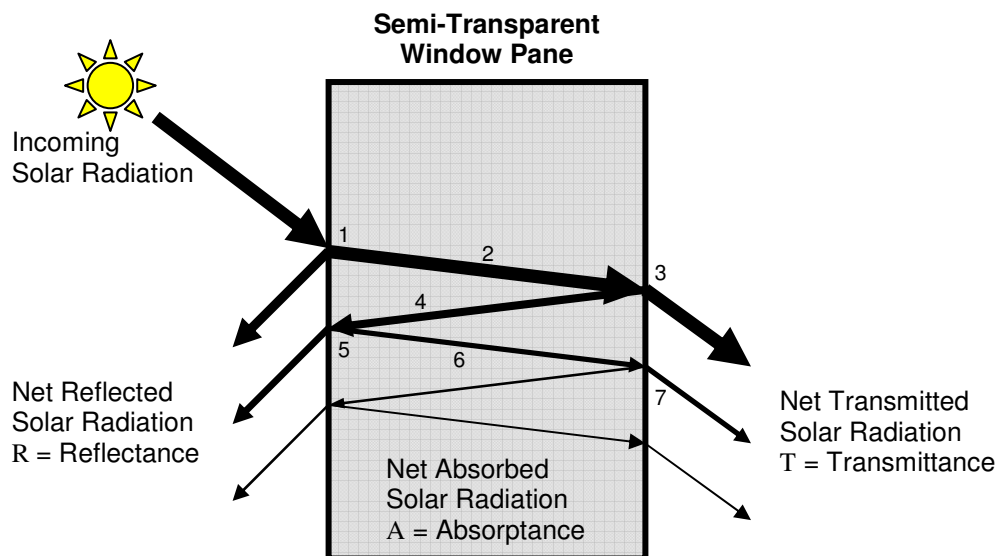


Figure 4-2. Detailed illustration of reflectance, transmittance, and absorptance.

In Fig. 4-2 the path of an incident beam of solar radiation is traced as it travels through a pane of glass. First, the incident radiation falls upon the air-glass interface (1). A fraction ρ_f is immediately reflected away from the surface, and the

remaining fraction τ_f enters the glass. As the transmitted portion travels through the glass material towards the back surface (1 to 3), a fraction α is absorbed by the atoms in the glass (2) causing them to heat up. At the second interface (3) another interaction occurs: some energy is reflected back into the glass towards the first interface, while the rest is refracted into the room. Again a portion of the reflected energy traveling through the glass is absorbed (4) and the remainder strikes the first interface (5). A portion is transmitted, and the remainder is again reflected back. The process repeats until all the energy has been reflected back, absorbed as heat, or transmitted into the room. A step-by-step illustration is given in Table 4-1 for a normal incidence beam striking a glass surface. Identical front and back surface properties are assumed ($\rho_f = \rho_b = \rho$ and $\tau_f = \tau_b = \tau$). As the number of bounces progresses, the amount of energy left traveling in the glass readily approaches zero.

Table 4-1. Bounce-by-bounce accounting of radiation in a single pane, and the infinite series of reflectance, absorptance, and transmittance.

Interaction	Reflected Away	Absorbed by Glass	Transmitted into Room	Still Traveling in Glass	Location
1	ρ	-	-	τ	Surface 1
1 to 3	-	$\tau \alpha$	-	$\tau (1-\alpha)$	Inside Glass
3	-	-	$\tau^2 (1-\alpha)$	$\tau \rho (1-\alpha)$	Surface 2
3 to 5	-	$\tau \rho \alpha (1-\alpha)$	-	$\tau \rho (1-\alpha)^2$	Inside Glass
5	$\tau^2 \rho (1-\alpha)^2$	-	-	$\tau \rho^2 (1-\alpha)^2$	Surface 1
5 to 7	-	$\tau \rho^2 \alpha (1-\alpha)^2$	-	$\tau \rho^2 (1-\alpha)^3$	Inside Glass
7	-	-	$\tau^2 \rho^3 (1-\alpha)^3$	$\tau \rho^3 (1-\alpha)^4$	Surface 2
etc.	etc.	etc.	etc.	etc.	etc.
Totals:	R	A	T	-	-

4.3 COMPUTING THE ANGLE DEPENDENT PROPERTY VARIATION

Frequently the values for transmittance, reflectance, and absorptance of a glass pane are known only at normal incidence angles $[T(0,\lambda), R(0, \lambda), \text{ and } A(0, \lambda)]^6$. These values must be converted into angle-dependent values for making thermal gain calculations. The Fresnel equations offer a way to make this conversion. The following analysis is outlined in the literature (ASHRAE, Energy Plus) and is included here with comments for completeness.

When radiation strikes a surface, it can be either reflected back or transmitted through that surface. An energy balance around the surface yields

$$\tau(\theta) + \rho(\theta) = 1 \quad (4-1)$$

where τ is the transmitted fraction, ρ is the reflected fraction, and θ is the angle of incidence of the incoming radiation measured with respect to the surface normal, Fig. 4-3. As radiation travels through a material, it can be reflected many times as it interacts with each surface. This happens until all of the energy is reflected, absorbed, or transmitted (see Fig. 4-2). Conservation of energy yields

$$R(\theta) + A(\theta) + T(\theta) = 1 \quad (4-2)$$

for the entire process, where R is the total amount reflected, A is the total amount absorbed, and T is the total amount transmitted. Given the values for normal incidence $R(\theta=0)$, $A(\theta=0)$, and $T(\theta=0)$, we wish to find a simple relationship for $R(\theta)$, $A(\theta)$, and $T(\theta)$. The expressions for angular transmittance and reflectance are

$$T(\theta) = \frac{\tau_f(\theta)\tau_b(\theta)e^{-at/\cos\theta}}{1 - \rho_f(\theta)\rho_b(\theta)e^{-2at/\cos\theta}} \quad (4-3)$$

$$R_f(\theta) = \rho_f(\theta)\left(1 + T(\theta)e^{-at/\cos\theta}\right) \quad (4-4)$$

⁶ Optical properties vary with both radiation wavelength λ and angle of incidence θ . From now on, the λ dependence will be omitted from equations to improve readability. It is implied that angle-dependent values of R , T , and A , must be computed separately for each radiation band: solar-thermal, visible, and infrared.

$$R_b(\theta) = \rho_b(\theta) \left(1 + T(\theta) e^{-\alpha t / \cos \theta'} \right) \quad (4-5)$$

where t is the thickness of the pane and θ' is the refracted angle of incidence (θ_2 in Fig.3). The absorption coefficient of the material α (typically on the order of 0.1 m^{-1}) is given by the expression

$$\alpha = \frac{4\pi\kappa}{\lambda} \quad (4-6)$$

where κ is the extinction coefficient of the material and λ is the wavelength of the radiation. Representative values of λ for the solar spectrum and visible spectrum are 898 nm and 575 nm, respectively. In the case of uncoated glass, the front and back surface properties are identical (i.e., $\rho_f = \rho_b = \rho$; and $\tau_f = \tau_b = \tau$). The analysis is pursued for the uncoated case. The impact on accuracy for coated glass is investigated later in this chapter. Eqs. (4-3) and (4-5) can then be expressed as

$$T(\theta) = \frac{\tau(\theta)^2 e^{-\alpha t / \cos \theta'}}{1 - \rho(\theta)^2 e^{-2\alpha t / \cos \theta'}} \quad (4-7)$$

and

$$R(\theta) = \rho(\theta) \left(1 + T(\theta) e^{-\alpha t / \cos \theta'} \right) \quad (4-8)$$

where t is the thickness of the pane of glass or other window material. From Eq. (4-2), absorptance can be computed from T and R

$$A(\theta) = 1 - T(\theta) - R(\theta) \quad (4-9)$$

These expressions can be used to find angular dependence, however, it is first necessary to find expressions for the variables ρ , α , and θ' in terms of $T(\theta)$ and $R(\theta)$.

The Fresnel equations for angle-dependence of reflectivity can be used when the front and back surface reflectivities ρ are identical, and when the material in

question is a dielectric. For the two polarizations⁷ of radiation (subscripts s- and p-) the Fresnel equations for reflectivity are

$$\rho_s(\theta) = \left(\frac{\sin(\theta - \theta')}{\sin(\theta + \theta')} \right)^2 \quad (4-10)$$

$$\rho_p(\theta) = \left(\frac{\tan(\theta - \theta')}{\tan(\theta + \theta')} \right)^2 \quad (4-11)$$

It is assumed that the polarizations of energy are received in approximately equal amounts. Eqs. (4-10 and 4-11) are averaged together to obtain a representative value of ρ

$$\rho(\theta) = \frac{1}{2}(\rho_s(\theta) + \rho_p(\theta)) = \frac{1}{2} \left[\left(\frac{\sin(\theta - \theta')}{\sin(\theta + \theta')} \right)^2 + \left(\frac{\tan(\theta - \theta')}{\tan(\theta + \theta')} \right)^2 \right] \quad (4-12)$$

The angular dependence $\tau(\theta)$ can be obtained directly by substituting Eq. (4-12) into (4-1). Computing $\rho(\theta)$ from Eq. (4-12) requires knowledge of θ' , the refracted angle of incidence. Using Snell's Law of Refraction

$$n \sin \theta = n' \sin \theta' \quad (4-13)$$

where, n and n' are the indexes of refraction⁸, θ is the angle of incidence, and θ' is the refracted angle, Fig. 4-3.

⁷ Radiation "[has] two wave components vibrating at right angles to each other and to the propagation direction" (Howell). The s- and p- subscripts each represent one of the two components.

⁸ Typical values are $n=1.0$ for air and $n'=1.55$ for glass. The analysis requires knowing the n for air (which is assumed to be 1.0), but for glass – n' is calculated in Eq. (4-16) from the glass properties.

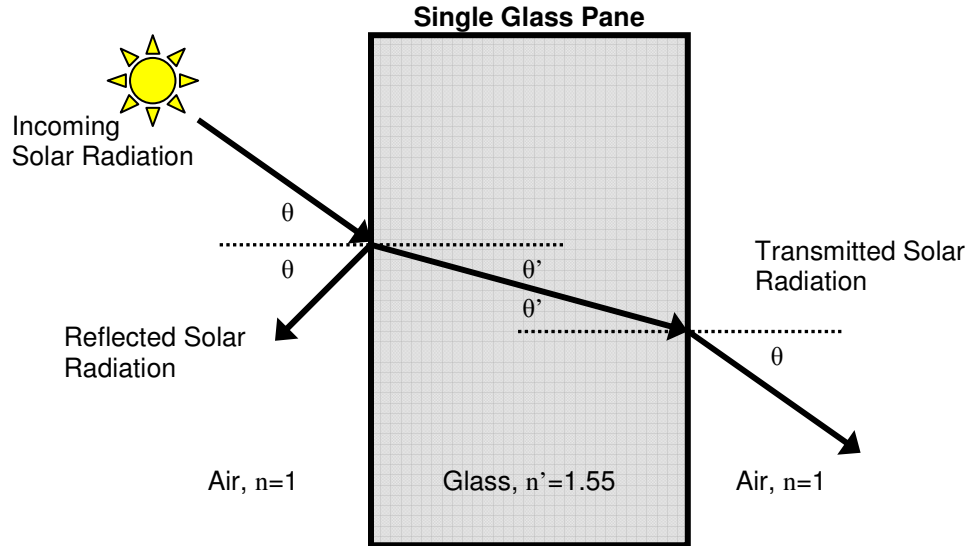


Figure 4-3. Snell's Law of Refraction.
Light changes direction as it passes through a glass pane.

This relation permits the elimination of the refracted angle θ' from Eq. (4-12). Substituting Eq. (4-13) into (4-12) yields

$$\rho(\theta) = \frac{1}{2} \left[\left(\frac{n \cos(\theta) - n' \cos(\theta')}{n \cos(\theta) + n' \cos(\theta')} \right)^2 + \left(\frac{n \cos(\theta') - n' \cos(\theta)}{n \cos(\theta') + n' \cos(\theta)} \right)^2 \right] \quad (4-14)$$

At normal incidence, Eq. (4-14) reduces to

$$\rho(0) = \left(\frac{n' - n}{n' + n} \right)^2 \quad (4-15)$$

which can be solved for the index of refraction of glass n' at normal incidence ($\theta = \theta' = 0$)

$$n' = \left(\frac{1 + \sqrt{\rho(0)}}{1 - \sqrt{\rho(0)}} \right) n \quad (4-16)$$

Setting $\theta=0$ and using the known properties of $R(0)$ and $T(0)$, Eqs. (4-1, 4-7, and 4-8) together can be solved for $\rho(0)$ and α

$$\rho(0) = \frac{P - \sqrt{P^2 - 4[2 - R(0)]R(0)}}{2[2 - R(0)]} \quad (4-17)$$

where

$$P = [T(0)]^2 - [R(0)]^2 + 2R(0) + 1 \quad (4-18)$$

and

$$\alpha = -\frac{1}{t} \ln \left[\frac{R(0) - \rho(0)}{\rho(0)T(0)} \right] \quad (4-19)$$

To compute the value of n' from Eq. (4-16), use $n=1.0$ (for air) and the value of $\rho(0)$ determined by Eq. (4-17). At this point, values for $\rho(0)$, $\tau(0)$, α , n , n' , and t are known; and Eqs. (4-7, 4-8, and 4-9) can be used to determine the values of T , R , and A for all angles.

4.4 DIFFUSE HEMISPHERICAL VALUES OF OPTICAL PROPERTIES

The angular relations discussed above yield accurate results for direct sunlight, which has a distinctive angular direction associated with it. A significant portion of sunlight that reaches the earth's surface is diffuse, or scattered light. For this type of radiation, a separate coefficient must be used to describe optical interactions. By assuming that diffuse solar radiation is scattered and incoming at all angles equally, it is then possible to perform a weighted average of over all angles of incidence to capture the diffuse effect. Coefficients can be generated by integration over the solid angles

$$T_D = 2 \int_0^{\pi/2} T(\theta) \sin(\theta) \cos(\theta) d\theta \quad (4-20)$$

$$R_D = 2 \int_0^{\pi/2} R(\theta) \sin(\theta) \cos(\theta) d\theta \quad (4-21)$$

$$A_D = 2 \int_0^{\pi/2} T(\theta) \sin(\theta) \cos(\theta) d\theta \quad (4-22)$$

Differing Front and Back Pane Properties

A simplification in the analysis was made, in which front and back properties were assumed identical. It is possible for a window pane to have different front and back optical properties due to the application of a metallic coating to one surface, which can help improve a window's thermal performance. When the front and back properties R_f and R_b and T are known to be different, an engineering approximation⁹ can be made with modest agreement to known data. First, set the value of R to either R_f or R_b depending on the direction of incoming radiation (e.g. if radiation is striking the front surface, use R_f ; if it has been reflected from another surface and is striking the back surface, use R_b). Use the same equations to compute $R(\theta)$, $A(\theta)$, and $T(\theta)$ for the given direction. This method will produce differing values for R_f and R_b , T_f and T_b , and A_f and A_b , which can be used to predict thermal behavior of the window system.

4.5 USING PANE PROPERTIES IN MULTI-LAYERED GLAZINGS

A method has been demonstrated to compute the angular and diffuse optical properties of a single pane of glass. In practice windows can be made of more than one layer of glass. When multiple glazing layers are present, the path of incoming radiation must be traced from one pane to the next. Reflections of radiation from one pane may be absorbed or transmitted through subsequent panes, Fig. 4-4. When front and rear properties of each individual pane are identical, the above set of equations can be used with the angle of incidence to determine the fraction of incoming radiation that is absorbed by each pane, and the net radiant energy transmitted into the room. Example outcomes for the radiation transmitted into the room, reflected to the outside, and absorbed by each pane are illustrated in Table 4-2. After computing the first sets of reflections, nearly all (99.28% in the example) of the radiation has been accounted for, and this is sufficient for simulation purposes.

⁹ Note: this engineering approximation violates the assumption made in the analysis and is not physically correct. Indeed, it results in different values of n' being computed for the same pane of glass for different directions of radiation. Nevertheless, modestly accurate results are produced from this method, as is shown in the validation section.

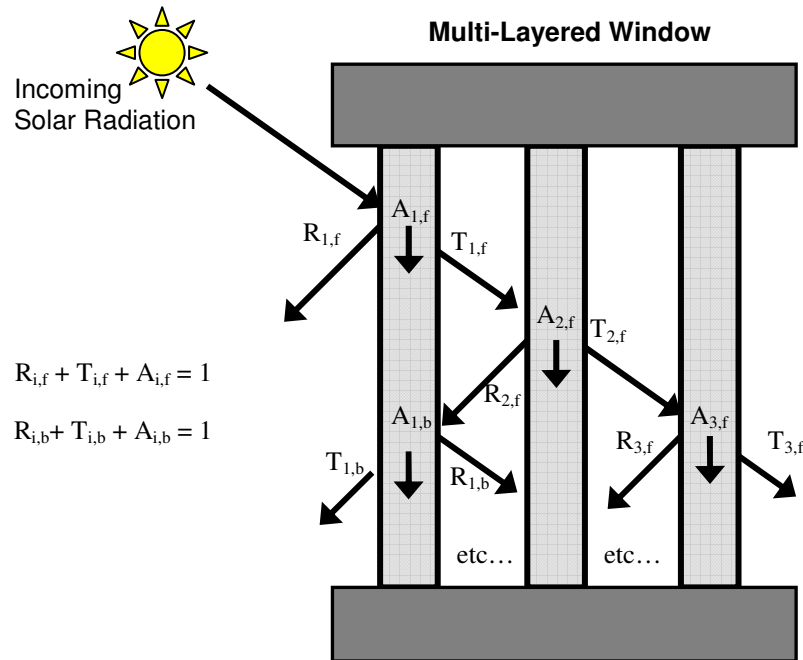


Figure 4-4. Reflections between panes occur in multi-layered windows.

Table 4-2. Radiation Interaction Accounting for a Triple-Pane Window.

Interaction	Transmitted to Room	Reflected Outside	Absorbed by Pane 1	Absorbed by Pane 2	Absorbed by Pane 3	Total:
No internal reflections	$T_1 T_2 T_3$	R_1	A_1	$T_1 A_2$	$T_1 T_2 A_3$	
Sample*	51.2%	10%	10%	8%	6.4%	85.6%
1 st set of internal reflections	$T_1 R_2 R_1 T_2 T_3$ + $T_1 T_2 R_3 R_2 T_3$	$T_1 R_2 T_1$ + $T_1 T_2 R_3 T_2 T_1$	$T_1 R_1 A_1$ + $T_1 T_2 R_3 T_2 A_1$	$T_1 R_2 R_1 A_2$ + $T_1 T_2 R_3 A_2$	$T_1 T_2 R_3 R_2 A_3$ + $T_1 R_1 R_2 T_2 A_3$	
Sample*	1.024%	10.496%	1.312%	1.28%	0.128%	13.68
Totals:	52.224%	20.496%	11.312%	9.28%	6.528%	99.28%

*example totals are found using $T=0.80$, $R=0.10$, and $A=0.10$ for all three panes, front and back.

4.6 SOLAR SHADING DEVICES

Often shading devices are used to vary the amount of sunlight entering a room. Such shading can be useful to prevent glare on a computer screen, improve thermal comfort, or simply to ensure privacy from the neighbors. Modeling the interaction of blinds with windows is important for computing thermal loads and visible light transmittance to the room. Reflectance, transmittance, and absorptance values for the blind system must be computed based on the slat properties (absorptivity and reflectivity) and blind geometry (slat width, angle, and spacing).

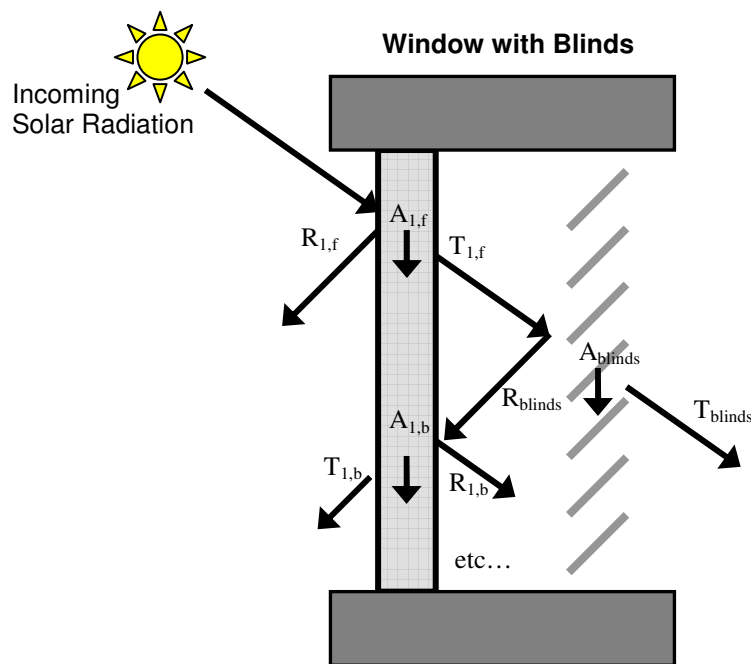


Figure 4-5. Reflections and interaction between a window pane and blinds.

The calculation method and equations used for computing the transmitted, absorbed, and reflected radiation fractions through the blinds is given in great detail in Dan Arons' Masters Thesis (2000). The method and assumptions are included for completeness. For calculations, see Arons.

Bulk optical properties of blind systems are calculated based on the distance between adjacent blind slats. Computed first is the fraction of solar radiation that passes unobstructed between adjacent blinds, Fig. 4-6. The remainder of the incoming radiation strikes the upper surface of a blind slat, where a fraction is

absorbed and a fraction is reflected. The reflected portion is divided into four equal parts, and the direction of the reflection is traced. Some radiation may be reflected away from the blinds, some may be absorbed by the adjacent blind's lower surface, and some may be reflected in the direction of the room, Fig. 4-7. During the reflection process, the direct-radiant energy may become diffuse. It is assumed that 60% of the reflected solar energy becomes diffuse, while the remaining 40% retains its specular (directed) properties.

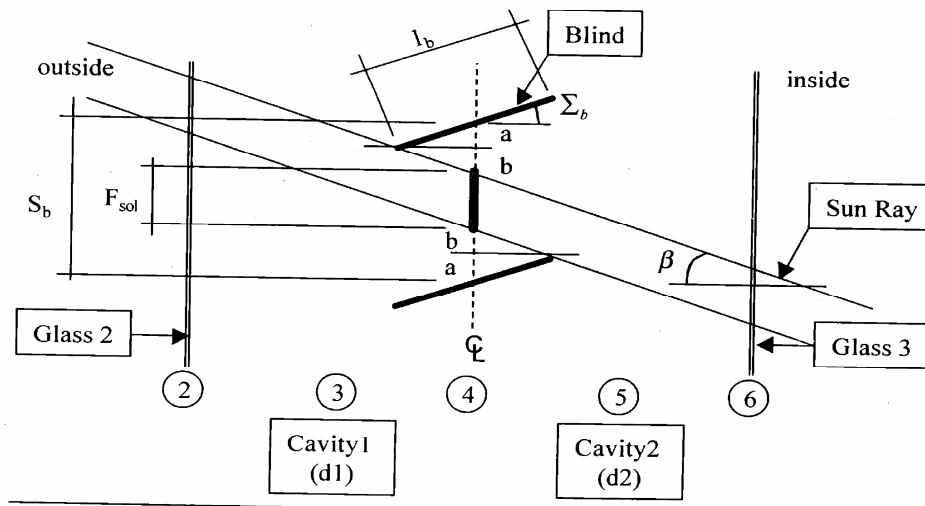


Figure 4-6. Radiation passing between two adjacent blinds (Arons 2000).

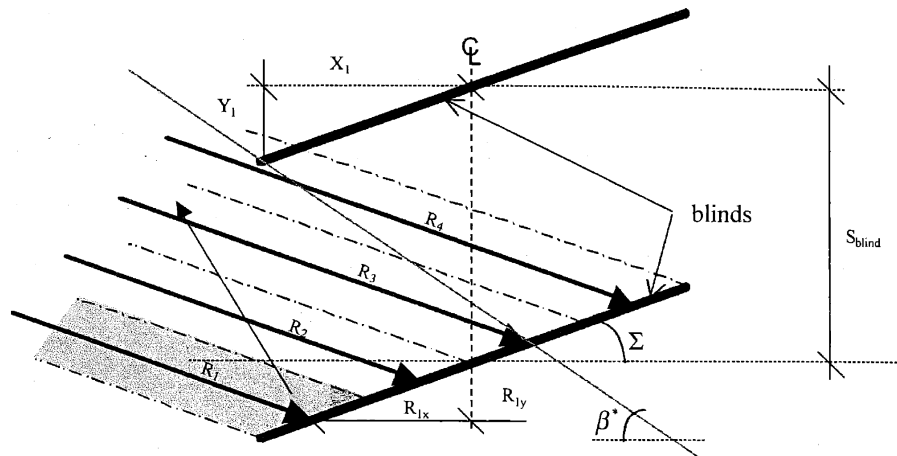










Figure 4-7. Radiation reflected from the top surface of one blind: some is reflected back (R_1) and some is absorbed by the blind above (R_2 - R_4) (Arons 2000).

4.7 OPTICAL PROPERTIES OF WINDOW PANES AND BLINDS

Typical optical properties of glass window panes and blinds are given in Tables 4-3 and 4-4. A few assumptions are made about the nature of the materials. First, for both window panes and blinds, it is assumed that the materials are opaque to IR radiation, such that the transmissivity of the material is zero in the IR band. Blind slats are further assumed to be opaque to visible radiation, such that the visible transmittance is also zero. Finally, for blinds, emissivity is assumed to be the same as absorptivity?

Table 4-3. Pane Properties as Defined in the MIT Design Advisor Software.

Pane Description		t	T _{sol}	R _{sol,f}	R _{sol,b}	T _{vis}	R _{vis,f}	R _{vis,b}	ε _{ir,f}	ε _{ir,b}
Clear		6	0.79	0.07	0.07	0.89	0.08	0.08	0.84	0.84
Low-e1		6	0.56	0.22	0.16	0.84	0.04	0.06	0.10	0.84
Low-e2		6	0.34	0.29	0.44	0.67	0.12	0.12	0.84	0.04
Blue		6	0.38	0.05	0.05	0.57	0.06	0.06	0.84	0.84
Bronze		6	0.45	0.05	0.05	0.49	0.05	0.05	0.84	0.84
Green		6	0.46	0.05	0.05	0.75	0.07	0.07	0.84	0.84
Grey		6	0.45	0.05	0.05	0.44	0.05	0.05	0.84	0.84

Variables:

t = pane thickness (mm)

T_{sol} = solar transmittance

R_{sol,f} = solar reflectance, front

R_{sol,b} = solar reflectance, back

ε_{ir,f} = IR emissivity, front

ε_{ir,b} = IR emissivity, back

T_{vis} = visible light transmittance

R_{vis,f} = visible light reflectance, front

R_{vis,b} = visible light reflectance, back

IR transmissivity is assumed equal to zero;

IR absorptivity is assumed equal to emissivity;

Table 4-4. Blind Slit Properties as Defined in the MIT Design Advisor Software.

Blind Slit Description	α_{sol}	ϵ_{ir}
Shiny Aluminum	0.20	0.22
White Plastic	0.38	0.77
Painted Silver Aluminum	0.45	0.67
Blue Plastic	0.85	0.84

Variables:

α_{sol} = Solar absorptivity, upper and lower blind surfaces

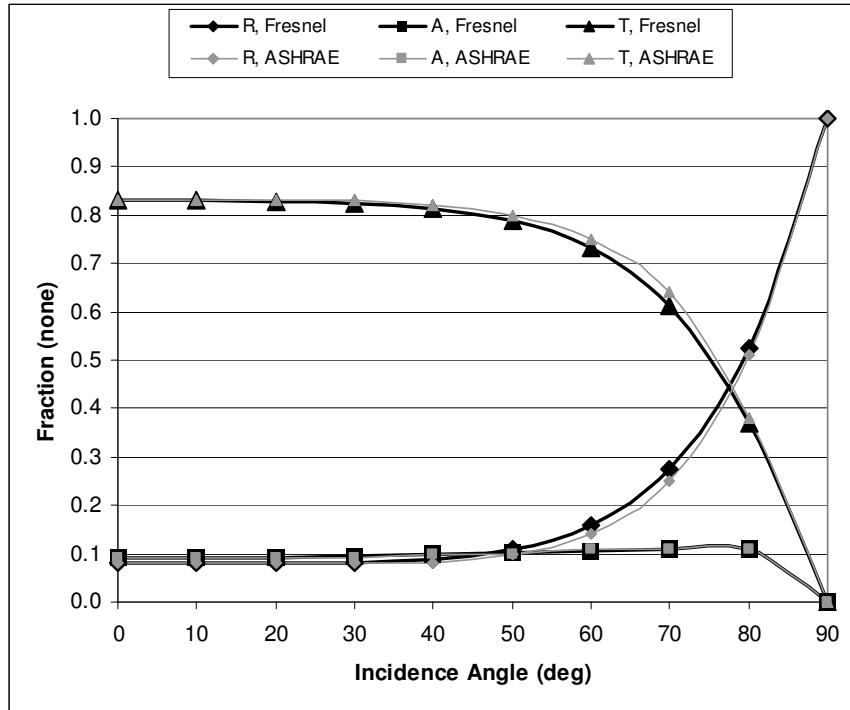
ϵ_{ir} = IR emissivity, upper and lower blind surfaces

Solar and IR transmissivity of slit material is assumed equal to zero (opaque);

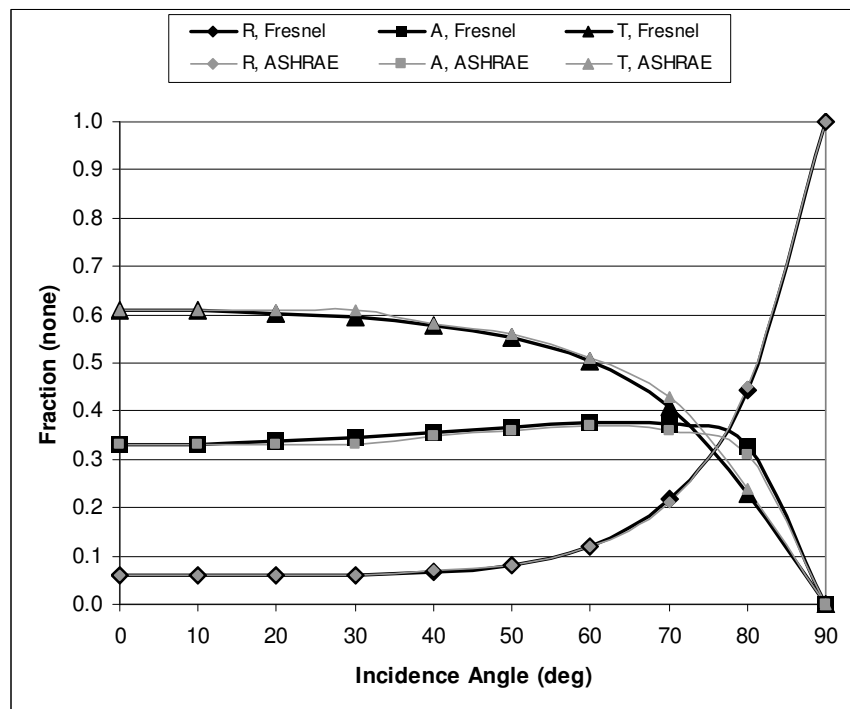
Emissivity and absorptivity are assumed equal for IR radiation

4.8 VALIDATION

The procedure for finding angular dependence of spectral properties must be tested for accuracy. Glass property variation with incidence angle is presented in tables in the ASHRAE Fundamentals (2005). Comparisons of predictions using the above method have been made against the ASHRAE data, Fig. 4-8. In most cases agreement is good to within 10% of published values. Figures 4-8a and 4-8b indicate results for uncoated glass (identical front and back pane properties). Figures 4-8c and 4-8d show results for a titanium-coated glass (differing front and back pane properties). Even though the identical front/back property assumption no longer holds, the agreement is still modestly good for predicting front and back optical properties. In cases where front/back properties differ, the largest differences occur in predicting T and A at high angles of incidence. This corresponds to the times that the least amount of sunlight is striking the window surface, so the error impact on the energy balance is minimal.

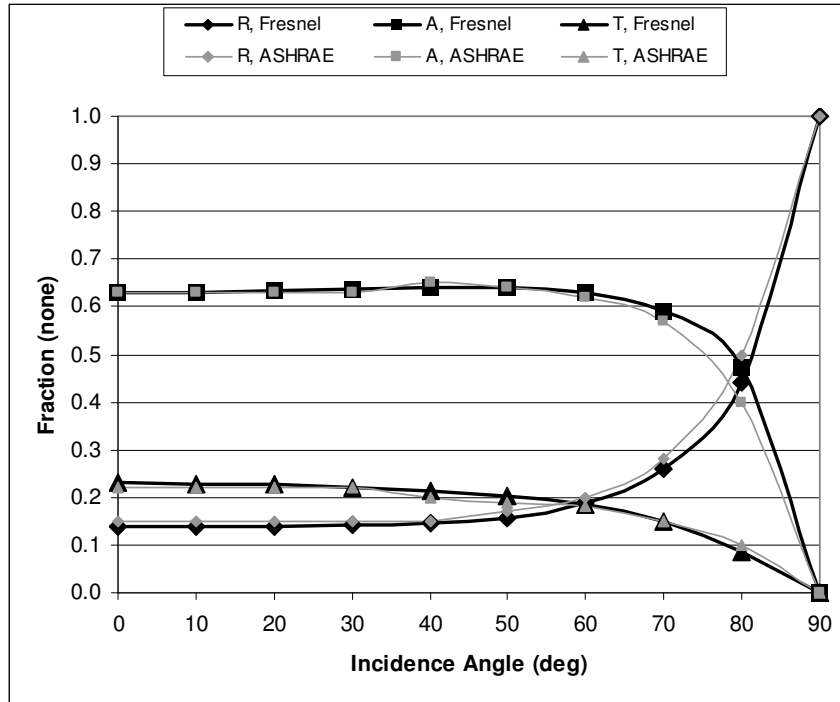


a) Clear glass, 1/8" ASHRAE

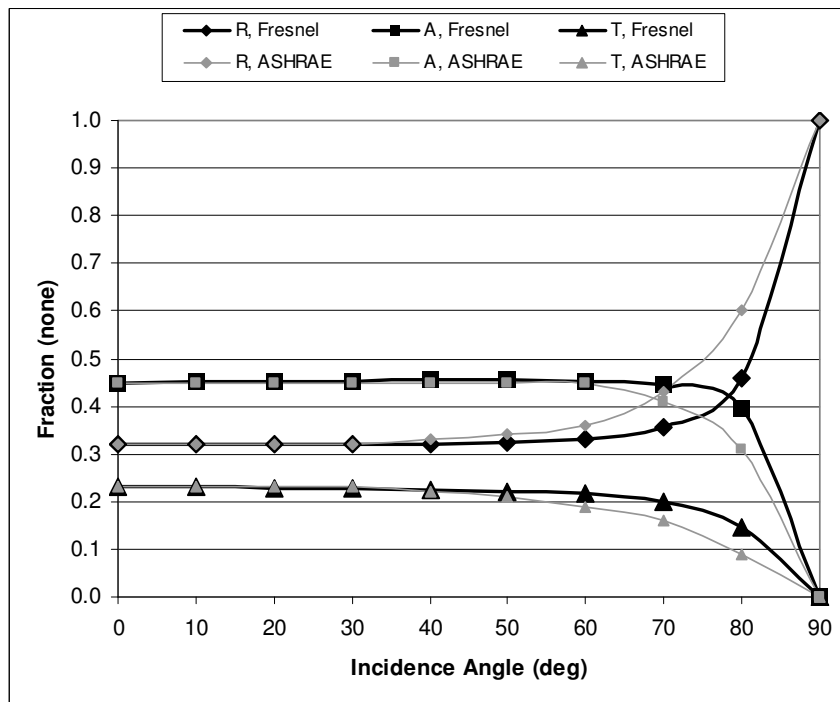


b) Green glass, 1/8" ASHRAE

Figure 4-8. Fresnel vs. ASHRAE spectral property comparison.



c) Titanium coated glass, 1/4" ASHRAE (Front Radiation)



d) Titanium coated glass, 1/4" ASHRAE (Back Radiation)

Figure 4-8. Fresnel vs. ASHRAE spectral property comparison.

4.9 QUICK REFERENCE

HOW TO COMPUTE ANGLE DEPENDENCE OF OPTICAL PROPERTIES

Given R_f , R_b , T at normal incidence, find $R(\theta)$, $T(\theta)$, $A(\theta)$

1. Compute P :

$$P = [T(0)]^2 - [R(0)]^2 + 2R(0) + 1$$

2. Compute $\rho(0)$:

$$\rho(0) = \frac{P - \sqrt{P^2 - 4[2 - R(0)]R(0)}}{2[2 - R(0)]}$$

3. Compute α :

$$\alpha = -\frac{1}{t} \ln \left[\frac{R(0) - \rho(0)}{\rho(0)T(0)} \right]$$

4. Compute n :

$$n = \frac{1 + \sqrt{\rho(0)}}{1 - \sqrt{\rho(0)}}$$

5. To compute the angle-dependence of properties, use α and n in

$$T(\theta) = \frac{\tau(\theta)^2 e^{-\alpha t / \cos \theta'}}{1 - \rho(\theta)^2 e^{-2\alpha t / \cos \theta'}}$$

$$R(\theta) = \rho(\theta) \left(1 + T(\theta) e^{-\alpha t / \cos \theta'} \right)$$

$$\rho(\theta) = \frac{1}{2} \left[\left(\frac{n \cos(\theta) - \cos(\theta')}{n \cos(\theta) + \cos(\theta')} \right)^2 + \left(\frac{n \cos(\theta') - \cos(\theta)}{n \cos(\theta') + \cos(\theta)} \right)^2 \right]$$

6. Compute absorptance based on R and T :

$$A(\theta) = 1 - T(\theta) - R(\theta)$$

Note: When R_f and R_b are different, simply use the value for the direction in which light is traveling. Although this procedure yields different calculated values of n' (glass) for front vs. back radiation (which is not physically meaningful), acceptable results are nevertheless obtained.

[this page intentionally left blank]

CHAPTER 5

ARTIFICIAL LIGHTING

5.1 INTRODUCTION

Maintaining sufficient lighting levels is necessary for the productive operation of a building. Considering the artificial lighting needs is important to an energy analysis for two main reasons: 1.) lights consume energy, and 2.) lights produce heat. This chapter describes a method for computing the electricity required to power the lights in a building, and equivalently, the thermal output that is produced. Several questions help to determine the required amount of artificial light:

1. What minimum light level is required?
2. When is the building occupied?
3. What type of light bulb/fixture is used, and what is its efficiency?
4. How are the lights controlled?
5. How much daylight is available?

In buildings with windows, sunlight can provide some or all of the lighting demand. When insufficient sunlight is available, artificial lighting must be supplied to provide a comfortably-lit working and living environment for the occupants.

In developed countries, electric lights are used almost exclusively to meet supplementary lighting needs. In underdeveloped regions, where electricity may not be readily available, lighting is often accomplished by burning wax candles, kerosene, or paraffin in lamps. This chapter will focus explicitly on electric lighting.

This chapter is organized as follows. First, the significance of lighting energy is outlined. Next, a brief background of visible light is given. A model is then introduced for computing the daylight distribution in a room with a window. Taking the results of the daylight model together with information about the lights and control schemes, a method is constructed for estimating a building's lighting energy load throughout a typical year. An overview of the user-defined lighting system options is given, along with sample pictures of the input interface. Finally, some examples are given to show the influence of design parameters on lighting energy consumption, demonstrating the potential for energy savings through better design.

Significance of Lighting Energy

Artificial lighting comprises a significant portion of the average building's total energy usage. Of the total electricity consumed in a building, lighting is 8.8% for residential (EIA 2001) and 23% for commercial buildings (EIA 1999). On the aggregate scale artificial lighting represents one-fifth of the total US electricity production. Collectively, commercial and residential buildings constitute over 75% of this demand, Fig. 5-1. More than half is used in commercial buildings where demand is during the daytime and coincides with peak electricity demand. Ironically, this is the same time that the most natural daylight is available. From a design perspective there is ample opportunity to reduce this consumption by taking advantage of the available daylight resource. Adding windows to buildings can help, but only if the lighting controls are properly managed. No savings can be realized if lights are left on at full intensity all day long, regardless of sunlight levels. Installing more efficient bulbs and fixtures can also reduce lighting loads substantially. The lighting simulation tool can allow building designers and managers to compare the energy-saving and money-saving potential of improved lighting options.

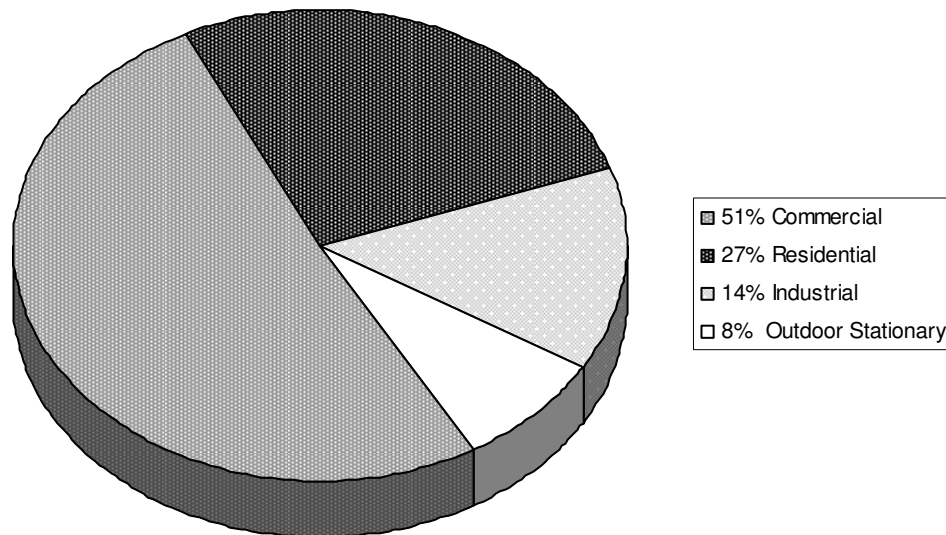


Figure 5-1. US lighting energy end-use by sector. Commercial and residential consumption is dominant (DOE 2006).

5.2 LIGHTING BASICS

Illuminance or light intensity – symbol E_v (v for visible) – is measured in lux. One lux is defined as one lumen per square meter. A lumen is the unit of luminous flux or luminous power, a measure of the perceived power of light by a typical human eye. Consider a common 60-watt incandescent light bulb, which when turned on, continuously emits about 1000 lumens. If the bulb emits light equally in all directions, then at a distance of one meter, 1000 lumens would be distributed over the area of a sphere of radius $r=1$ m. Assuming no reflections from walls or other objects, the luminous intensity at one meter is 80 lux, Fig. 5-2.

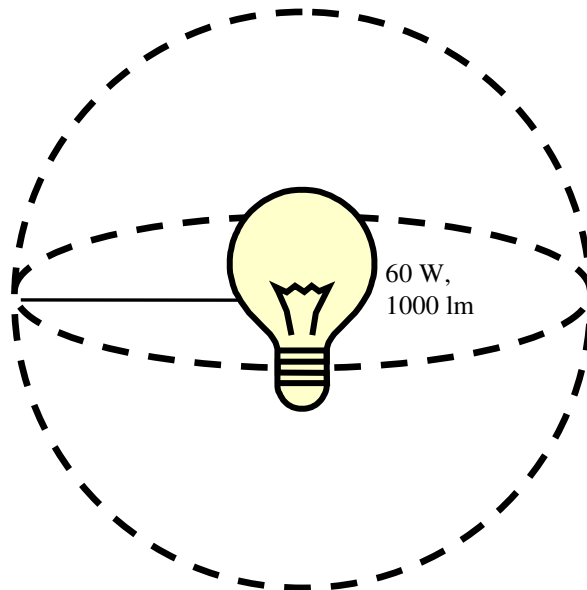


Figure 5-2. A 60-watt incandescent bulb emitting 1000 lumens will produce a light intensity of 80 lux at one meter. Intensity drops with distance squared.

Visible Spectrum – the Colors We Can See

The visible spectrum for humans is comprised of light in the band of colors from the violet to the deep red – wavelengths between 400 to 700nm. Outside these bands, our vision generally cannot detect light. Within the visible spectrum, human vision responds selectively: our eyes respond better to green light than to blue light. Perhaps not surprisingly, green is also the brightest color in sunlight at the surface of the earth (MSN Encarta). This is important because the efficiency of a light source is

based on the minimum amount of power required to continuously produce monochromatic green light.

Workplane Surface

The workplane is defined as an imaginary horizontal plane at the height at which work is typically done, Fig. 5-3. This concept is useful for determining where light is needed within a building. In office buildings the workplane generally represents the surface of a desk where a worker is situated. European and US standard values for the height of the workplane are 0.85 and 0.76 meters (2.8 and 2.5 ft), respectively, measured up from the floor (Mischler). For simplicity and to give modest agreement with both standards, 0.8 m is used as the standard workplane height.

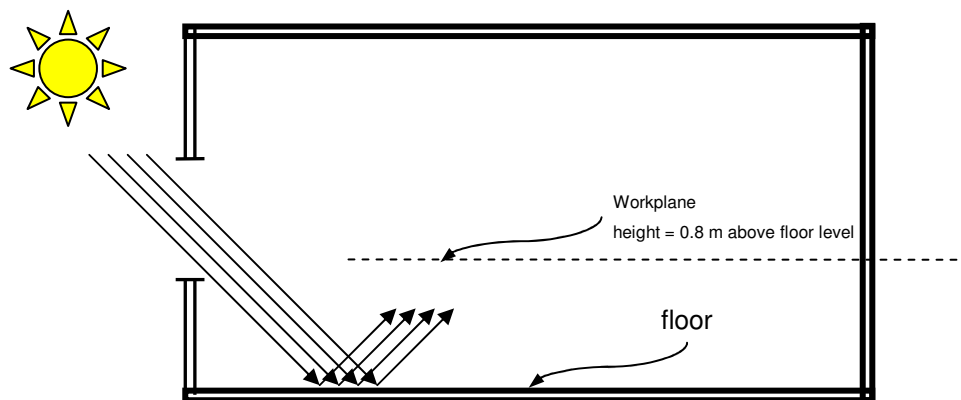


Figure 5-3. Simple lighting diagram.
Minimum lighting levels must be met at the workplane surface.

Light Source Efficiency

Two types of efficiency are commonly associated with sources of visible light: the dimensional luminous efficacy ε (lm/W) and the dimensionless overall lighting efficiency η . The luminous efficacy ε of a light source relates its luminous output F (lm) to the supplied power input Q_e (W)¹⁰

¹⁰ The supplied power is assumed to be electrical energy, though it could be thermal energy in the case of a combustion-style light source as with a candle flame.

$$\epsilon_{\text{source}} = \frac{F (\text{lm})}{Q_e (\text{W})} \quad (5-1)$$

Luminous efficacy is the quantity that must be known to make predictions of light source energy requirements. Manufacturers typically list the luminous output and wattage on the product information.

Sometimes lighting efficiency is given as a percentage (e.g. “this incandescent bulb is 2.5% efficient”). Percentages generally refer to the overall lighting efficiency η , which is the ratio of luminous efficacies of the light source to that of an ideal source of monochromatic green light

$$\eta_{\text{source}} (\%) = \frac{\epsilon_{\text{source}}}{\epsilon_{\text{ideal},555\text{nm}}} = \frac{\epsilon_{\text{source}} (\text{lm/W})}{683 (\text{lm/W})} \quad (5-2)$$

A perfectly efficient source of monochromatic green (555nm) light has a luminous efficacy $\epsilon_{\text{ideal},555\text{nm}}=683 \text{ lm/W}$. The overall lighting efficiency η of a light source (bulb, LED, flame, etc.) is the ratio of the source’s luminous efficacy to that of the ideal 555nm source. When η_{source} is known, ϵ_{source} can be computed directly as

$$\epsilon_{\text{source}} = \eta_{\text{source}} \epsilon_{\text{ideal},555\text{nm}} = \eta_{\text{source}} 683 (\text{lm/W}) \quad (5-3)$$

Thus, a typical incandescent bulb with $\eta=2.5\%$ would have a luminous efficacy of $\epsilon_{\text{incandescent}}=2.5\% \times 683 \text{ lm/W}=17 \text{ lm/W}$. Sample product luminous efficacy and lighting efficiencies are given in Table 5-1.

Table 5-1. Luminous efficiency of select light sources¹¹.

Fixture Type	Luminous Efficacy, ϵ (lm/W)	Overall Lighting Efficiency, η (%)
Candle flame	0.3	0.05
Halogen	12	1.8
Incandescent	17	2.5
White LED bulb	34	5.0
Compact fluorescent	63	9.2
Tube fluorescent	88	13.0
High pressure sodium	130	19.0

Light Fixture Efficiency

It is rare for a bulb to be directly exposed to the lit-environment. Lamps often have shades, lights can be recessed into the ceiling, and fluorescent bulbs can be housed with a reflective metal cover. Each time a beam of light is reflected from a surface, some energy is absorbed as heat and this reduces the beam's intensity. Further, light does not travel directly from the ceiling down to the workplane surface. As an example, consider a room with fluorescent tube lighting. The lights are spaced several on the ceiling, and this could produce a pattern of light and dark areas on the workplane surface (and/or floor) depending on just how far apart the lights are spaced.

For the purposes of an energy estimation tool, these considerations are not included in the model. Instead, the best case is assumed: electric lights are positioned on the ceiling, and are housed inside of an ideally reflective casing that directs light downward towards the workplane without any loss of intensity. Thus, if a light bulb were positioned directly above a 1m x 1m box, it would illuminate that 1m x 1m box evenly, and no light would reach any other area of the room. This idealization offers an effective way to estimate the lighting needs for an entire room as will be shown.

¹¹ Values computed from product data listed on a supplier web site: White LED bulb data taken from <http://www.ccrane.com/lights/led-light-bulbs/index.aspx>, all others from <http://www.1000Bulbs.com>.

Luminous Intensity – How Much Light is Required

Humans require specific light intensity levels for comfortable vision. Outdoor light intensity can reach values as high as 110,000 lux for direct-normal illuminance and 80,000 lux for diffuse-horizontal illuminance. These levels are uncomfortably bright for most activities. When light levels reach 50,000 lux, glare can occur making it difficult to perform common tasks such as reading a computer screen. The use of adjustable shades or blinds can prevent glare in an indoor environment when the luminous intensity is too high. For various activities, the typical minimum values of luminous intensity are shown in Table 5-2.

Table 5-2. Minimum luminous intensity for common environments.

Environment / Activity	Minimum lighting $E_{v,min}$ (lux)
Storage	0 to 150
Residential living room	50
Kitchen	300
Office	400 to 500
Television studio	1000
Detailed work	1000 to 1500

Computing Electrical Lighting Loads

The amount of electricity Q_e required for a light source to illuminate a given area can be computed using

$$\frac{Q_e}{A} = \frac{E_{v,min} \text{ (lm/m}^2\text{)}}{\epsilon_{\text{source}} \text{ (lm/W)}} \quad (5-4)$$

where A is the area in m^2 to be illuminated and $E_{v,min}$ is the minimum required luminous intensity. As stated earlier, Eq. (5-4) assumes that all light emitted from the source travels in equal amounts in the direction of the surface to be illuminated and that no light reaches other parts of the room.

An example illustrates how one may convert a lighting requirement into an electrical requirement. Suppose a light source shines towards a flat 1 m x 1 m square with perfect fixture efficiency (described above). The light source has a light

efficacy $\epsilon_{\text{source}}=17$ (lm/W). A lighting requirement of 300 lux, or 300 lumens per square meter is imposed. Using Eq. (5-4) and solving for Q_e

$$Q_e = 300 \text{ (lm/m}^2\text{)} \times 1 \text{ (m}^2\text{)} / 17 \text{ (lm/W)} = 17.6 \text{ (W)} \quad (5-5)$$

it is found that 17.6 W of electricity is required to illuminate the area to the proper level. If a room were comprised of many 1 m x 1 m squares, then each square would require this amount of electricity. In that case the lighting energy per unit area would be 17.6 W/m².

5.3 MODELING LIGHT REQUIREMENTS OF BUILDINGS

Since sunlight can provide some or all of a building's lighting need, the first step in the modeling process is to compute the sunlight illuminance levels throughout a representative room. Matthew Lehar, a former MIT graduate student, has developed and implemented a method for rapidly computing the daylight illuminance throughout a room. The reader is encouraged to seek out Lehar's references for more detail.

Weather data files provide hourly values for direct-normal and diffuse-horizontal illuminance for the outdoor environment. During each hour, the amount and direction of visible light entering a room must be computed using the weather data, solar geometry functions (Chapter 3), and window optical properties (Chapter 4). The path of the direct illuminance is traced as it travels throughout the room. If the room is very deep, the portion of the room closest to the window may be well-lit, while the back of the room may be quite dark. It is not sufficient to compute the average daylighting level in the room to determine the required amount of supplemental lighting load.

Lehar's daylight model considers the visible light transmitted into the room through a window. Windows are modeled as horizontal strips spanning the entire width of the room and centered vertically on the wall, Fig. 5-4. Solar geometry functions are used to determine the angle which direct light enters the room. Three-

dimensional reflections from building surfaces¹² (walls, ceiling, and floor) are used to generate a grid of illuminance values on the workplane.

Workplane illuminance levels from incoming daylight are computed by an iterative radiosity calculation for each square of the discretized workplane surface. It is assumed that all reflections in the room are spectrally diffuse. The daylight model allows for multiple reflections of solar illuminance within the room.

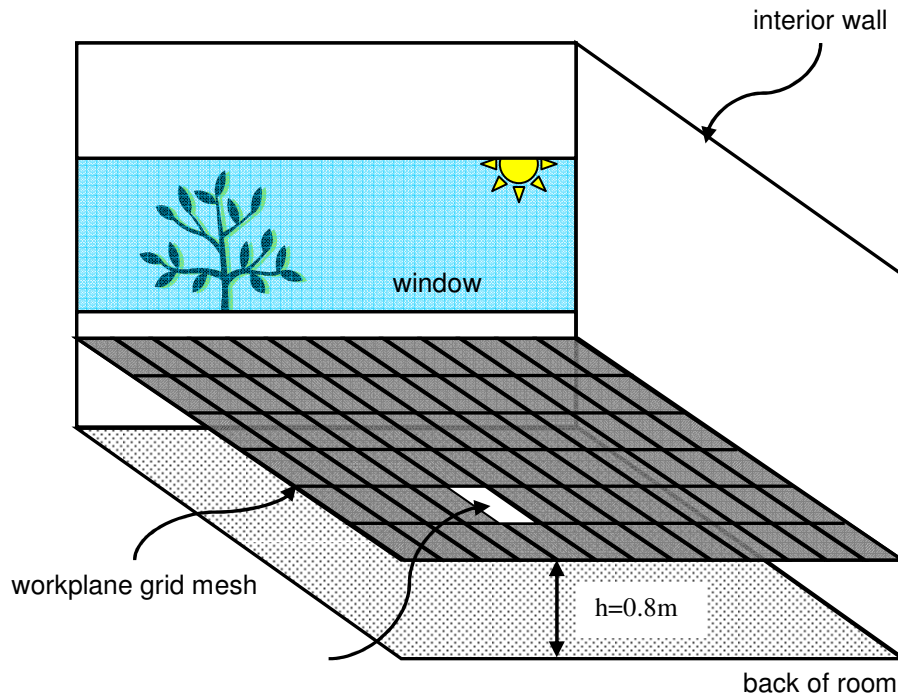


Figure 5-4. Two-dimensional workplane grid.
Illuminance values are computed for each grid box (i,j) .

Based on the user-specified minimum lighting level requirement $E_{v,\min}$ (lux), a local lighting deficit $E_{v,\text{deficit}(i,j)}$ is computed for each grid square by subtracting the local daylight illuminance $E_{v,\text{daylight}(i,j)}$ from the minimum required illuminance

$$\begin{aligned}
 E_{v,\text{deficit}(i,j)} &= E_{v,\min} - E_{v,\text{daylight}(i,j)} && \text{for } (E_{v,\min} > E_{v,\text{daylight}(i,j)}) \\
 E_{v,\text{deficit}(i,j)} &= 0 && \text{for } (E_{v,\min} \leq E_{v,\text{daylight}(i,j)})
 \end{aligned}
 \tag{5-6}$$

¹² Internal building surfaces are modeled with a reflectivity of 0.5, and all reflections are assumed to be diffuse.

When the minimum requirement is met or exceeded, the local lighting deficit is zero (negative lighting deficits are not allowed). The illuminance deficit values $E_{v,deficit(i,j)}$ (lux) are computed for each grid box of the room, where i and j represent the grid box indexes. The local illuminance deficits determine the minimum required amount of supplemental light. A shaded plot of a sample workplane surface lighting deficit $E_{v,deficit(i,j)}$ is pictured in Fig. 5-5.

The method for turning this set of ($i \times j$) electrical loads into an approximate hourly electric loads depends on the lighting control system. Three lighting control strategies are offered as options to the user (always-on, single-dimmer, and multiple-dimmer), each with an appropriate calculation method. The control strategy options are discussed in more detail in the next section, and the associated calculation methods are given here

1. Lights all always on

$$Q_{e,total} = \sum_{i,j} \frac{E_{v,min} A_{(i,j)}}{\epsilon_{source}} = \frac{E_{v,min} A_{total}}{\epsilon_{source}} \quad (5-7)$$

2. Lights all dim together (more efficient)

$$Q_{e,total} = \frac{\max\{E_{v,deficit(i,j)}\} A_{total}}{\epsilon_{source}} \quad (5-8)$$

3. Lights all dim independently (most efficient)

$$Q_{e,total} = \sum_{i,j} \frac{E_{v,min} A_{(i,j)}}{\epsilon_{source}} \quad (5-9)$$

The thermal energy generated by the lights is exactly equal to the electrical load. All light and wasted thermal energy is ultimately absorbed by objects, walls, and other building components and contributes to the HVAC loads. These thermal gains are considered in the energy balance (Chapter 8).

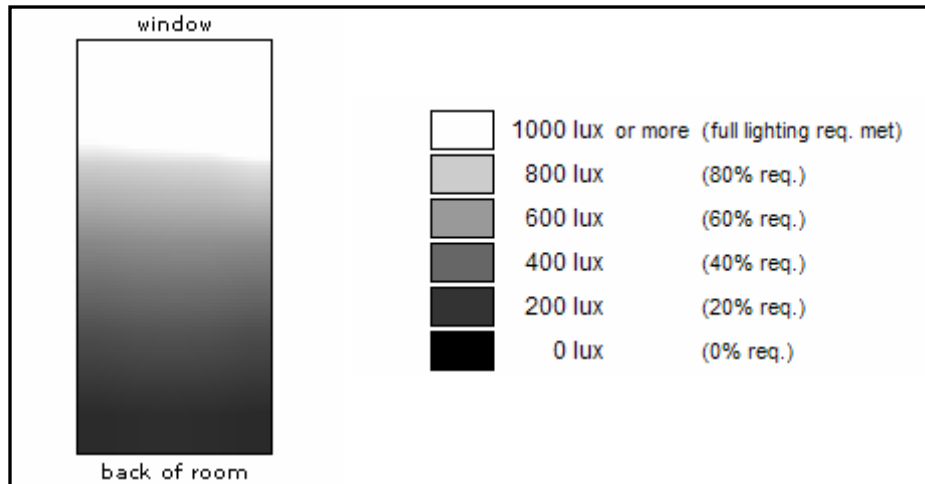


Figure 5-5. Top view of workplane daylight levels for a room with a 1000 lux minimum lighting requirement.

5.4 LIGHTING INPUT OPTIONS AND THE USER INTERFACE

Outlined in this section, are the parameters that are used in the model above to determine required amounts of lighting energy. Users must specify a minimum light intensity, a lighting control strategy, and an lighting schedule. Each of these is described with a figure depicting the options as presented on the user-interface.

Minimum Light Intensity

The minimum amount of light required by the occupants of a given space varies depending on what the occupants want to do. Typical activities require anywhere from 50 to 500 lux, but special conditions could require up to 1500 lux, Table 5-2. The user must specify the minimum lighting requirement of a representative room when it is occupied. Fig. 5-6 illustrates a simplified input field for specifying minimum lighting requirements. Adequate supplementary lighting is applied to the room such that this minimum light level is met during each hour. The method for computing the amount of lighting energy is based on the selected lighting control strategy (three strategies are described in a later subsection of this chapter).

Occupancy

Occupancy Load: people per m²

Lighting Requirements: lux

Equipment Load: W/m²

Occupancy Schedule: End Hour

Representative Room

Window Orientation

Window Orientation: N, S, E, W

Window Orientation: perpendicular to windowed surface, parallel to windowed surface, vertically parallel to windowed surface

Figure 5-6. Lighting requirement input field on the MIT Design Advisor interface.

Occupancy Schedule: Occupancy Begins to Occupancy Ends

Occupancy Schedule: 12:00 midnight, 1:00 AM, 2:00 AM, 3:00 AM, 4:00 AM, 5:00 AM, 6:00 AM, 7:00 AM, 8:00 AM, 9:00 AM

Window Orientation: N, S, E, W

Window Orientation

Pure Mechanical E... Pure Naturally Ven... Joint Natural Ventil...

m - perpendicular to windowed surface m - parallel to windowed surface m - vertically parallel to windowed surface

Energy System

Figure 5-7. Occupancy schedule input field on the MIT Design Advisor interface.

Occupancy Schedule

Understanding when the lights are on or off is an important factor in determining lighting loads. The present model assumes that when a building is unoccupied, all the lights are switched off¹³. In practice occupancy schedules can vary from day to day (e.g. office buildings closing on weekends, holidays, etc.). Presently, a fixed occupancy schedule is assumed throughout the year, though future interfaces may allow the user to specify the number of occupied days per week. The user specifies the hour in which the building is first occupied and the hour in which the building is vacated by selecting values from a drop-down menu depicted

¹³ This is often not true of many buildings. Some building operators keep some or all lights on regardless of occupancy. By varying the occupancy schedule, the user can see just how much electricity can be saved by making changes to the lighting policy.

in Fig. 5-7. To specify overnight occupancy the user can select an occupancy-begin hour that is later in the day than the occupancy-end hour (e.g. 9pm to 6am indicates overnight occupancy).

Light Fixture Efficiency

Producing visible light from electrical energy is not a perfectly efficient process. Some light will inevitably be emitted by a fixture in portions of the electromagnetic spectrum that the human eye cannot detect. This wasted energy contributes to the heat load in a room. Different types of lighting fixtures produce differing amounts of light per unit energy input. Table 5-1 shows representative values of light conversion efficiency for popular types of indoor lighting available at the time of this writing.

The MIT Design Advisor presently assumes an aggressive overall lighting efficiency of 13.5% (92.2 lm/W), typical of a highly efficient fluorescent bulb. It is possible to allow the user to specify the bulb type or the efficacy of the fixture to improve model accuracy; however, at the time of this writing this feature has not been implemented.

Lighting Control Strategies: Dimming Lights with Sunlight

Since artificial lighting is generally designed to provide the minimum lighting requirement when there is complete darkness, there may often be times when sunlight can reduce or completely eliminate the need for artificial lighting in some parts of the building. Practically, this amounts to someone or *something* that can switch off or adjust the output of the lights. The 'someone' could be an occupant who turns off the lights nearest the window when it is sunny. The '*something*' could be a light-sensing electronic controller that dims some or all of the lights in the room in response to measured light levels. Both behaviors will reduce the lighting load, and consequently the electricity load within the zone.

Because occupant behavior can be unpredictable, no attempt has been made by the author to model occupant-controlled lighting. Instead the focus has been on

modeling the automated control options¹⁴. From a modeling perspective the focus has been on producing simple ways of estimating upper and lower bounds of energy consumption. In order of increasing efficiency, the three control schemes are 1. Lights do not dim; 2. Lights all dim together; and 3. Lights dim independently, Fig. 5-8.

The screenshot shows a software interface for configuring room ventilation and lighting control. The 'Room Ventilation' section includes a dropdown menu for 'Air Change Rate Per Occupant' set to 15 (labeled 'liters / sec per person') and a text input for 'Total Air Changes' set to 1.5 (labeled 'per hour'). The 'Lighting Control' section has three radio button options: 'Always on (least efficient): During occupancy hours, all lights are on at full brightness'; 'Lights all dim together (more efficient): A single light sensor controls all lights together' (which is selected); and 'Lights dim independently (most efficient): All lights in room dimmed independently to supplement sunlight'.

Figure 5-8. Lighting control input field on the MIT Design Advisor interface.

1. Lights do not dim (least efficient)

This is the simplest and least-efficient of the control strategies. While the building is occupied, all the lights are always on at their full levels. When the building is unoccupied, the lights are all switched off. Many commercial and industrial buildings are operated this way. As a worst-case lighting scenario, this option allows the user to see the maximum possible lighting energy consumption.

2. Lights all dim together (more efficient)

In this case it is assumed that all of the lights in a room are controlled simultaneously by a single light-sensing controller. The sensor measures the illuminance of the darkest part of the room and computes the difference in lux between the minimum required lighting level and the darkest part of the room's workplane. All lights are then adjusted to this new level.

¹⁴ Although the automated control options can approximate the behavior of a pro-active light-controlling person.

As an example, suppose a room has a 500 lux minimum lighting requirement. Sunlight provides some of this requirement to the room: the part of the room nearest the window receives more than 500 lux, but the rear part of the room receives only 200 lux. In this case the maximum lighting deficit is $500-200=300$ lux. All the lights throughout the room are then adjusted to provide 300 Lux, even though the 300 lux is only needed by the back half of the room. This is 40% more efficient than having all the lights provide a full 500 lux, but the part of the room nearest the window has excess lighting.

3. Lights all dim independently (highly efficient)

This most efficient lighting control strategy monitors the available daylight on the workplane at all parts of the room and adjusts each light bulb individually to provide just enough light to meet the minimum requirement. The simplified example described above in control strategy 2 is re-examined with the present strategy.

The part of the room nearest the window has more than enough daylight, the darkest portion of the room requires an additional 300 lux, and the places in between require supplemental light somewhere between 0 and 300 lux. In this case, the lights farthest from the window would still produce the lighting deficit of 300 lux. But now the lights nearest the window would sense that enough daylight is present and would turn themselves off. Similarly, at each point on the workplane, the lighting deficit is computed and the artificial lights are adjusted to just meet the minimum lighting requirement.

5.5 SAMPLE OUTPUT

Shown in Fig. 5-9 is the electric lighting load variation for an east-facing room located in Delhi, India. The minimum lighting requirement is set to 1000 lux, the room has a small window (10% of the wall area) and is occupied from 7am to 8pm. The lighting control system has much to do with the actual energy requirement.

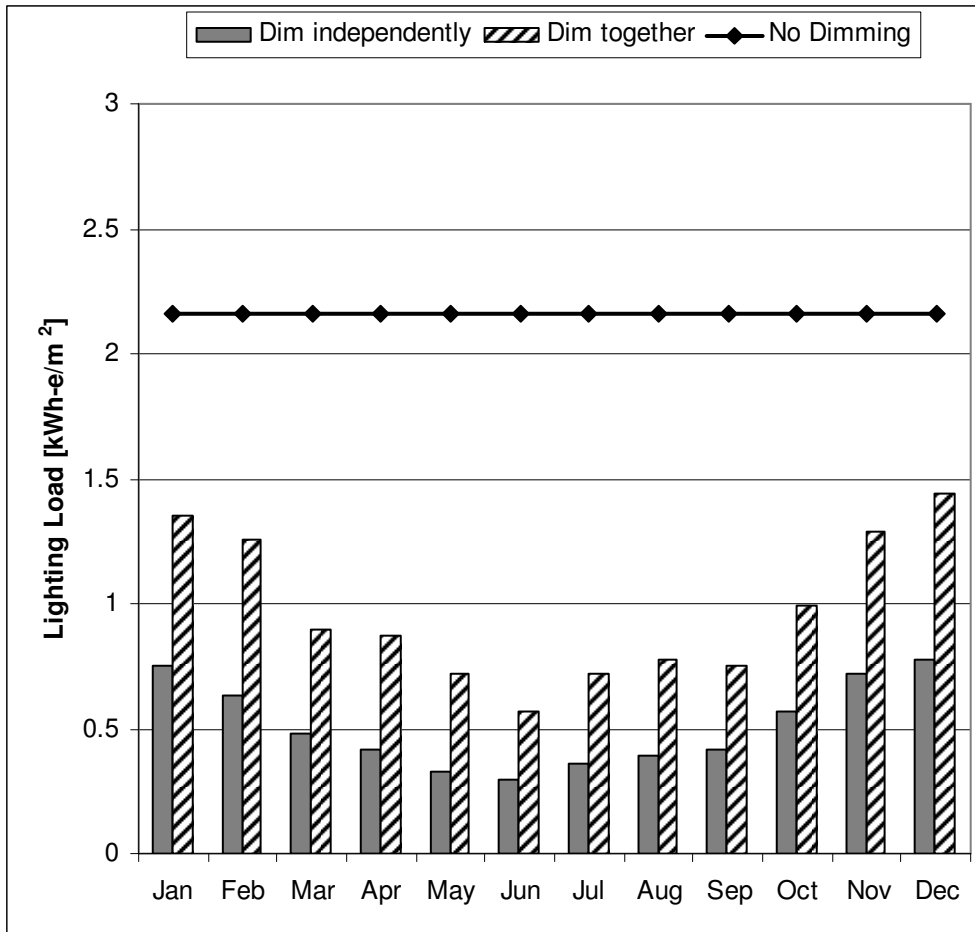


Figure 5-9. Lighting loads: 3 lighting control schemes, for an East-facing window.

As expected, the case without dimmable lights results in the highest use of lighting energy with a consistent consumption throughout the year. When dimming is controlled by a single sensor and all lights are dimmed together, electrical requirements are reduced significantly. Finally, by adjusting each light individually, lighting energy is reduced to a minimum.

CHAPTER 6

THERMAL MASS

6.1 INTRODUCTION

A primary goal of building simulation is to predict the amount of energy required to maintain a comfortable environment. Usually this amounts to keeping the indoor air temperature in a desired range by the application of heating and cooling loads at appropriate times. Predicting the indoor air temperature response to time-varying thermal gains and losses thus is a necessary part of the simulation process.

If all thermal forces operated directly on the indoor air, then it would be quite straightforward to convert them directly into heating or cooling loads. In reality, however, energy exchanges take place between many components and through different heat transfer processes. Thermal response can and does vary by building component, and this affects the magnitude and duration of air temperature fluctuations.

Energy exchanges can occur by conduction, convection, and radiation and by mass transfer. Indoor air can exchange energy by surface convection and by ventilation mass transfer. As a transparent gas, air is extremely poor at absorbing and emitting radiant energy. Radiant interactions occur primarily with the internal building surfaces. Solar radiation that is transmitted through windows is absorbed by these surfaces, causing them to heat up. When internal surfaces exist at different temperatures, energy is exchanged by emissive radiation between these surfaces. Neither the transmitted solar radiation nor the emissive exchanges directly influence the indoor air temperature. Instead, radiant energy reaches the indoor air by first being absorbed-by and then being convected-from internal building surfaces, including the walls, ceiling, floor, and objects within the building.

Often, the rate that materials can absorb solar radiation is higher than the rate of convection between the absorbing surface and the indoor air. Excess energy is stored in the absorbing material and released gradually with time into the air. Thermal mass is the term given to this ability of matter to store and release energy with time. The heat capacity, conductivity, and dimensions of solid components, and

the surface convection coefficient ultimately determine how much energy is stored or released by a given absorbing material.

Buildings with high thermal mass have a greater ability to store energy than those with low thermal mass. High thermal mass is especially desirable in climates that have a great difference in daytime and nighttime outdoor air temperature. In these cases, solar gains during the daytime result in cooling loads. If the massive parts of the building can absorb and retain much of the solar gains during the daytime and release them at night when the air is cooler, the cooling loads can be modestly reduced. If the air temperature at night is cool enough to warrant heating loads, then these too can be reduced as heat is provided by the discharging of the thermal mass.

While all objects inside a building contribute to its thermal mass, their contributions are not all the same. Thin, lightweight elements like the glass in a window pane have little capacity to store heat. When a thermal force is applied to such elements, response is fast and steady-state heat transfer is reached quickly. Contributing most to the thermal mass effect are the materials that have the largest mass and the highest heat capacity. Thicker and heavier elements, like the floor of a room, have a significant capacity to store heat and release it over a longer duration. Direct-solar radiation that is transmitted through a window typically strikes the lower portion of a room – the floor and lower walls. Accordingly the ability of the floor to store heat is of particular importance.

This chapter describes a method for quickly estimating the influence of thermal mass on the energy balance of a room. An analysis of the thermal mass effects of various internal building components is presented first. A simplified model is then developed and validated against examples of known solution. Agreement is shown to be quite good.

6.2 A SIMPLE THERMAL MASS MODEL

In this section the assumptions of the thermal mass are explained and justified. First, a comparison of the heat capacity of various building components is explored. Next, the convection and radiation heat transfer coefficients are computed

for typical indoor conditions. It is shown that the thermal mass effects in a room are dominated by the building construction – specifically the construction of the floor. Finally, a rapid and accurate technique for computing the thermal mass effect of the floor is described.

Heat Capacity of Typical Building Components

The analysis begins by determining which building components have the greatest ability to store heat. Building components can be classified into three groups:

1. Building construction elements, or ‘dead-load’ (floors, ceilings, and walls);
2. Indoor objects, or ‘live-load ‘ (equipment, furniture, books, etc.); and
3. Indoor air.

Normalized by floor area, the building construction elements are the heaviest of the three and have the highest heat capacity; objects within the room have a secondary impact; and the air has the lowest heat capacity of all. An estimated summary of the heat capacity of these elements for a typical building is given in Table 6-1. The estimations have been made with the following assumptions about a typical room

1. Room dimensions are 5m x 5m x 3m (width x depth x height);
2. The floor is constructed of concrete, 0.10m deep;
3. The interior walls and ceiling are 0.10m-thick, consisting of 75% air and 25% wood/gypsum;
4. The exterior wall is a vertical, 0.10m-thick slab of fiberglass; and
5. The objects inside the room have a combined mass of 60kg/m² of floor area¹⁵, their mass is divided equally between wood, plastic, and metal; and are they are dispersed evenly throughout the room¹⁶.

¹⁵The 60 kg/m² mass of objects in a typical room is a simple estimation. Normally, building codes require structures be strong enough to support a live-load of 40 pounds per square foot (200kg/m²). A survey of office buildings in India showed that a room’s live load is on the order of about 40-60 kg/m² (Kumar).

¹⁶ These are simplifying assumptions made by the author.

The heat capacity per floor area of building component i is computed simply as

$$\frac{C_i}{A_{\text{floor}}} = \frac{m_i c_i}{A_{\text{floor}}} \quad (6-1)$$

where m_i is the total mass of component i in the room, c_i is its specific heat capacity, and A_{floor} is the total floor area. It is clear from Table 6-1 that the building's construction has the largest potential for storing heat – the floor alone has a heat capacity more than twice as large as all other components. A closer look at the heat transfer process will show that the impact of the floor significantly dominates the thermal mass effects in a room.

Table 6-1. Heat capacity of materials in a typical room, estimated (subtotals & totals rounded).

Material	Specific Heat Capacity (J/kg-K)	Mass per Floor Area (kg/m ²)	Heat Capacity per Floor Area (kJ/m ² -K)
<i>Air</i>			
Air in room	1,007	3.5	3.5
Air subtotal	-	3.5	3.5
<i>Objects</i>			
Wood	2,400	20	48
Plastic	900	20	18
Metal	440	20	9
Objects subtotal	-	60	75
<i>Construction</i>			
Concrete floor	2,300	88	200
Interior walls & ceiling (air, wood, gypsum)	1,200	84*	100
Exterior wall (fiberglass)	800	6	5
Construction subtotal	-	180	215
TOTALS	-	240	290

*vertical wall mass is computed, summed, and normalized by floor area

Air in the Room

Due to its low density, indoor air has little capacity to retain heat. When energy is transmitted from a surface to the air via convection, virtually all of that energy causes the air temperature to rise. The well-mixed assumption is made for indoor air, so that all convective gains result in an increased average room

temperature. Local areas of warmer or cooler air are not considered in this model. Thus, convective gains to and from the air are assumed to occur quickly and correspond to instantaneous cooling or heating loads.

Objects in the Room

Compared with the air, the indoor objects or 'live-load' (furniture, equipment, etc.) have a much larger capacity to store heat. Compared with the building construction, however, indoor objects still do not have the largest heat capacity. The limited ability of objects within a room to store heat is partly due to a relatively-low total mass and partly to a greater exposed surface area. Consider a piece of furniture – e.g., a desk, chair, or table. These have complicated geometries, usually with more than one surface exposed to the indoor air. If such objects absorb transmitted-solar radiation, the amount which can be retained is reduced as compared with elements that have only one surface exposed to the room interior.

Walls, Ceilings, and Floors

Comprising an estimated 75% of the typical room's heat capacity, the building's construction or 'dead-load' (walls, ceilings, and floor) generally has the dominant thermal mass effect. While each of the dead-load components has a significant heat capacity, the walls and ceiling of a typical room do not contribute much to its thermal mass as compared with the floor. This is true for two main reasons: 1) the wall and ceiling materials have a modestly low internal conductivity; and 2) a higher amount of solar radiation reaches and is absorbed by the floor as compared with the ceiling and floor.

Walls, and especially exterior walls, are constructed of some combination of insulating materials: usually foam, fiberglass, wood, gypsum, and/or air. The convection and radiation heat transfer coefficients associated with the surfaces of these materials are generally substantially larger than the conductive heat flow into the material. Wood and fiberglass, for example, have conductivities of $k_{\text{wood}}=0.17$ and $k_{\text{fiberglass}}=0.035$ W/m-K. A 0.10 m thick slab of wood or fiberglass has a one-dimensional conduction coefficient of 1.7 or 0.35 W/m²-K. Surface convection

coefficients are usually significantly higher, on the order of 5 to 10 W/m²-K. Consequently, a significant portion of the radiation absorbed by these materials is convected directly into the room. Thus, the thermal mass effect of these surfaces is modestly negligible. This is akin to assuming that most of the internal surfaces (walls and ceilings) exist at or close to the indoor air temperature. Only for concrete¹⁷ is the conduction rate of a similar order of magnitude to that of the combined surface convection and radiation process (~8-15 W/m²-K).

Solar radiation plays a significant role in the heating of buildings. Apart from ground-reflected solar energy, the solar radiation that is transmitted through a window is largely directed towards the lower parts of the room. After passing through the window, the radiation strikes the floor and lower walls where it is absorbed or reflected to other surfaces in the room. Optical surface properties determine how much solar energy is absorbed and how much is reflected. In most buildings the floor has the most potential for absorbing solar radiation. Walls and ceilings are often painted lighter colors to reflect light and make rooms brighter, while floors are darker in color and absorb more solar energy. This can be seen in Table 6-2, which lists properties for some common building surfaces. It is therefore assumed that the exterior wall of the building is constructed of insulating and/or lightweight materials, and its thermal mass contribution is neglected.

Table 6-2. Solar Absorption Properties of Selected Surface Materials (Incropera).

Material	Normal solar-thermal absorptivity
Concrete	0.60
Brick	0.63
Plated metals	0.87-0.93
Paint: White	0.16-0.26
Paint: Black	0.98

¹⁷ In the case of concrete $k_{\text{concrete}}=1.4$. A 0.10 m thick slab has a one dimensional conduction coefficient of 14 W/m²-K.

Modeling Assumptions – Thermal Mass Floor

Because the massive floor has the highest-order thermal mass effects, the simulation neglects the impact of objects in the room. It is assumed that any thermal energy absorbed by objects other than the floor contributes directly and immediately to the heating of the air in the room, Fig. 6-1. While in reality the direct-solar radiation will fall in patterns on the floor, it is assumed that all incoming solar radiation is spread evenly over the floor surface. Since lateral conduction in the floor is not modeled explicitly, the even distribution of incident solar energy over the floor helps to compensate. Temperature is allowed to vary only in the depth-dimension of the floor. Since the magnitude of surface convection is similar to that of conduction through the floor, a lumped-capacitance model is not appropriate. Instead, a numerical technique is used to compute the temperature distribution through the depth of the thermal mass.

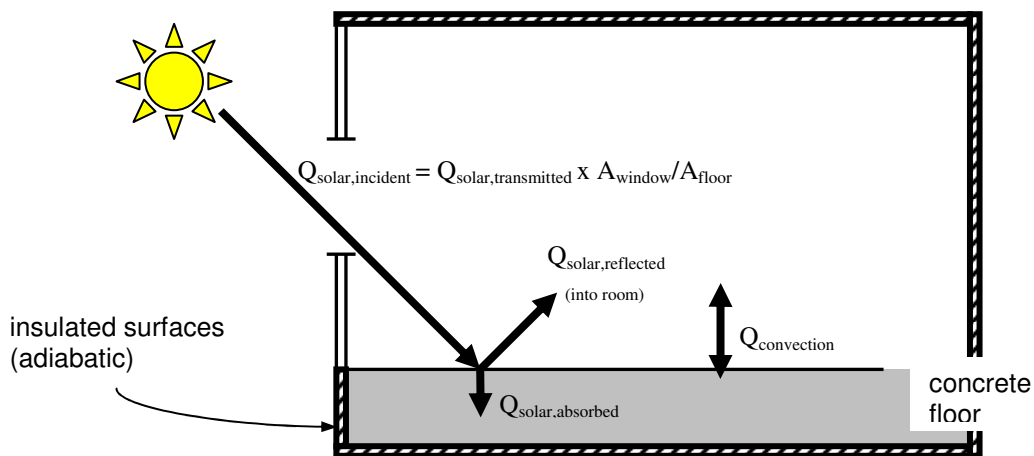


Figure 6-2. Heat exchange between thermal mass and air inside room.

The floor is assumed to be constructed of a concrete slab. Since the amount of thermal mass is a design option, the user must specify between light-, medium-, and heavy-weight building construction. The thickness of the concrete floor is varied according to the user-input as shown in Table 6-3.

Table 6-3. Three levels of thermal mass, specified by the user.

	Quantity of Thermal Mass		
	High	Medium	Low
Thickness, D [m]	0.20	0.10	0.02

Heat Transfer Coefficients

To correctly determine the flow of energy to and from the surface of the floor, it is important to understand the mechanisms by which the energy is transferred. The surface of the floor is in thermal communication with the air in the room via convection and with the surfaces in the room via radiation. While some energy can be transferred via conduction between the floor and the objects resting upon it and to the exterior of the building, these are assumed to be small in comparison to the radiation and convection transfers.

Because air is transparent, the direct radiation exchange between building surfaces and the air in a room is insignificant. Radiation exchanges take place instead between surfaces of differing temperature. The floor typically has a good view of the exposed surfaces of the ceiling, walls, and objects lying within the room. With the exception of poorly-insulated windows and blinds, these surfaces generally exist at or near the indoor air temperature, and they lack significant capacity to store heat. When these surfaces receive radiant energy from a warmed floor surface, much of the received energy is convected into the air. It is therefore assumed that heat transferred by radiation from the floor to these other surfaces ultimately is delivered to the air, despite the fact that it is not absorbed by the air directly. A total heat transfer coefficient consisting of convection and radiation is used to determine the net rate of energy exchange with the floor surface

$$h = h_{total} = h_{cv} + h_r \quad (6-2)$$

The radiation coefficient is computed using a linearization of the Stefan-Boltzmann law

$$h_r = 4\epsilon\sigma T_{avg}^3 \quad (6-3)$$

where σ is the Stefan-Boltzmann constant ($5.67 \times 10^{-8} \text{ W/m}^2\text{-K}^4$), T_{avg} is the mean temperature between the thermal mass surface temperature and the temperature of the body to which it is radiating, and ϵ is the effective emissivity of the radiating bodies in the IR portion of the spectrum given by

$$\epsilon = \frac{1}{\frac{1}{\epsilon_{thermal-mass}} + \frac{1}{\epsilon_{other-surfaces}} - 1} \quad (6-4)$$

Typical values of ϵ are given for painted walls and concrete in Table 6-4 together with the range of radiation and convection heat transfer coefficients.

Table 6-4. Summary of floor surface heat transfer coefficients.

	Typical Values	Units
<i>Radiation</i>		
IR emissivity of Concrete ϵ_1	0.88	none
IR emissivity of painted walls ϵ_2	0.80 to 1.00	none
Average temperature of surfaces T_{avg}	300 to 320	K
Effective IR emissivity ϵ	0.72 to 0.88	none
Average radiation coefficient h_{rad}	5.0	$\text{W/m}^2\text{-K}$
<i>Convection</i>		
Buoyant component	2.0 to 5.0	$\text{W/m}^2\text{-K}$
Stratified component	0.5 to 1.5	$\text{W/m}^2\text{-K}$
Ventilation driven component	2 to 10	$\text{W/m}^2\text{-K}$
Average convection coefficient h_{cv}	3 to 11	$\text{W/m}^2\text{-K}$
Average total heat transfer coefficient h_{total}	10 (approx.)	$\text{W/m}^2\text{-K}$

The radiation coefficient does not vary very significantly with temperature in the normal range of building temperatures & surface emissivity. Fig. 6-2 shows the typical range of variation. A representative value for radiation of about $4 \text{ W/m}^2\text{-K}$ is appropriate.

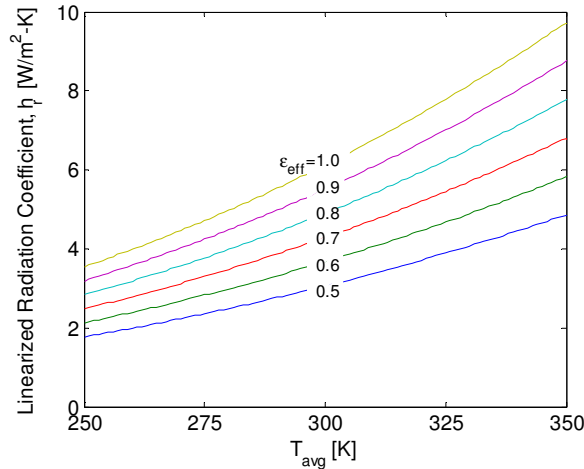


Figure 6-2. Radiation convection coefficient vs. surface temperature & effective emissivity.

Convection coefficients from the floor surface to the air are slightly more complicated. Several convection correlations have been published (Beausoleil) for both the buoyancy-driven and stably-stratified conditions

$$h_{cv,buoyant} = \left(\left\{ \left[1.4 \left(\frac{\Delta T}{D_h} \right)^{1/4} \right]^6 + \left[1.63 \Delta T^{1/3} \right]^6 \right\}^{1/2} + \left\{ \left[\frac{T_s - T_{diffuser}}{\Delta T} \right] \times \left[0.159 + 0.0116 (ac/h)^{0.8} \right] \right\}^3 \right)^{1/3} \quad (6-5)$$

and

$$h_{cv,stratified} = \left(\left\{ 0.6 \left(\frac{\Delta T}{D_h^2} \right)^{1/5} \right\}^3 + \left\{ \left[\frac{T_s - T_{diffuser}}{\Delta T} \right] \times \left[0.159 + 0.0116 (ac/h)^{0.8} \right] \right\}^3 \right)^{1/3} \quad (6-6)$$

where ΔT is the absolute temperature difference between the floor surface and the room; D_h is the hydraulic diameter of the floor ($D_h = 4P_{floor}/A_{floor}$), P_{floor} being the perimeter of the floor; $T_{diffuser}$ is the temperature at which incoming air is introduced to the room; and ac/h is the number of air changes per hour. Eqs. (6-5) and (6-6) are each constructed as blending expressions of component terms. Both of these correlations share a similar term in the RHS, namely

$$h_{common} = \left\{ \left[\frac{T_s - T_{diffuser}}{\Delta T} \right] \times \left[0.159 + .0116(ac/h)^{0.8} \right] \right\} \quad (6-7)$$

This common term is graphed in Fig. 6-3. Typically the hourly air change rate ac/h is less than 5. Only for the unusually high condition of $ac/h=40$ (common of smoking areas) is there a significantly higher-than-normal convection rate. In cases where the ventilation dominates the floor convection rate, the convection rate is typically near 5 and seldom exceeds $10 \text{ W/m}^2\text{-K}$.

When the ventilation rate ac/h approaches zero, the common term {Eq. (6-7)} in Eqs. (6-5) and (6-6) vanishes. Variation of the remaining terms in the correlations is simply a function of ΔT , and D_h as shown in Fig. 6-4. The weak dependence on D_h is evident. For buoyant-driven convection (cool air above a warm floor), the rate is near $4 \text{ W/m}^2\text{-K}$ and for stably-stratified convection (warm air above a cool floor), the rate is roughly $1 \text{ W/m}^2\text{-K}$.

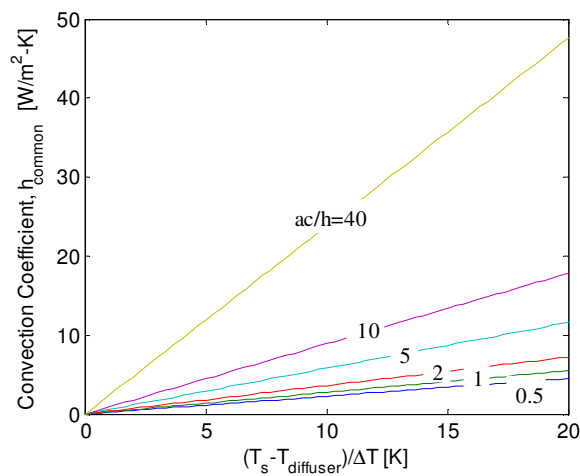


Figure 6-3. Convection driven by ventilation, the common component of Eqs. (6-5) and (6-6).

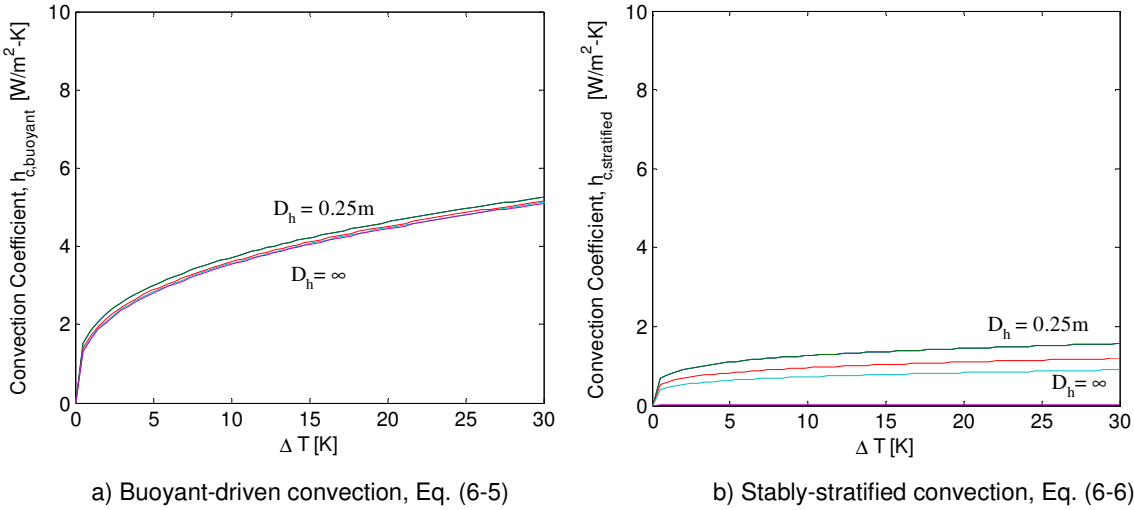


Figure 6-4. Floor-air convection coefficient, ΔT dominated, ac/h term negligible.

The blending expressions used in Eqs. (6-5) and (6-6) take the form

$$h_{blended} = (h_a^3 + h_b^3)^{1/3} \quad (6-8)$$

Substituting typical values of convection from Figs. 6-3 and 6-4 ($h_a=10$; $h_b=4$) into in Eq. (6-8) yields

$$h_{typical} = (10^3 + 4^3)^{1/3} = 10.21 \quad (6-9)$$

This result illustrates that the additive nature of the blending function is small. Since the magnitude of the ventilation-driven component is generally the greater of the two components, it will have the dominant effect on the resultant convection coefficient.

The complexity of these two correlations is excessive for the purposes of an early-stage estimating simulation, especially since the variation with most parameters besides ΔT is quite small. Excluding very special circumstances of high air flow rates in a room, values of the natural convection rate h_c are predicted to lie between 2 and 10 W/m^2-K . Adding the radiation component yields values of h_{total} approximately between 6 and 14 W/m^2-K . Since this range is small, and since actual

airflow conditions within a building are not likely to be known at the conceptual stages of design, a constant representative value $h_{\text{total}} \sim 10 \text{ W/m}^2\text{-K}$ is assumed as a constant.

6.3 ENERGY BALANCE & NUMERICAL TECHNIQUE

Because concrete has a non-negligible thermal resistance, it must be modeled as a series of thin layers, or slices. A one-dimensional energy balance through the depth of the thermal mass is used to capture the thermal mass effects of the floor. A uniform temperature distribution is assumed throughout each of the floor's horizontal layers. Details are given here as to the computation method, and actual values of the concrete material properties are summarized in Table 6-5.

Table 6-5. Thermal mass properties used in the MIT Design Advisor calculations.

Variable Description	Symbol	Value	Units
Floor surface solar radiation absorption factor	α	0.80	(none)
Specific heat capacity	c	880	(kJ/kg-K)
Density	ρ	2300	(kg/m ³)
Conductivity	k	1.4	(W/m-K)
Combined convection + radiation coefficient	h	10	(W/m²-K)

Energy Balance

The thermal mass is first divided into a series of n horizontal slices, each of which is at a uniform temperature, Fig. 6-5. The number of slices required for an accurate simulation will be discussed later. An energy balance is performed on each of the slices, resulting in a system of n equations in n unknowns. The equations for the surface node and the bottom node each take a unique form, while all internal nodes take an identical form. Let i denote the node index numbered from the surface to the bottom, where $i=1$ is the exposed surface node and $i=n$ is the adiabatic bottom node.

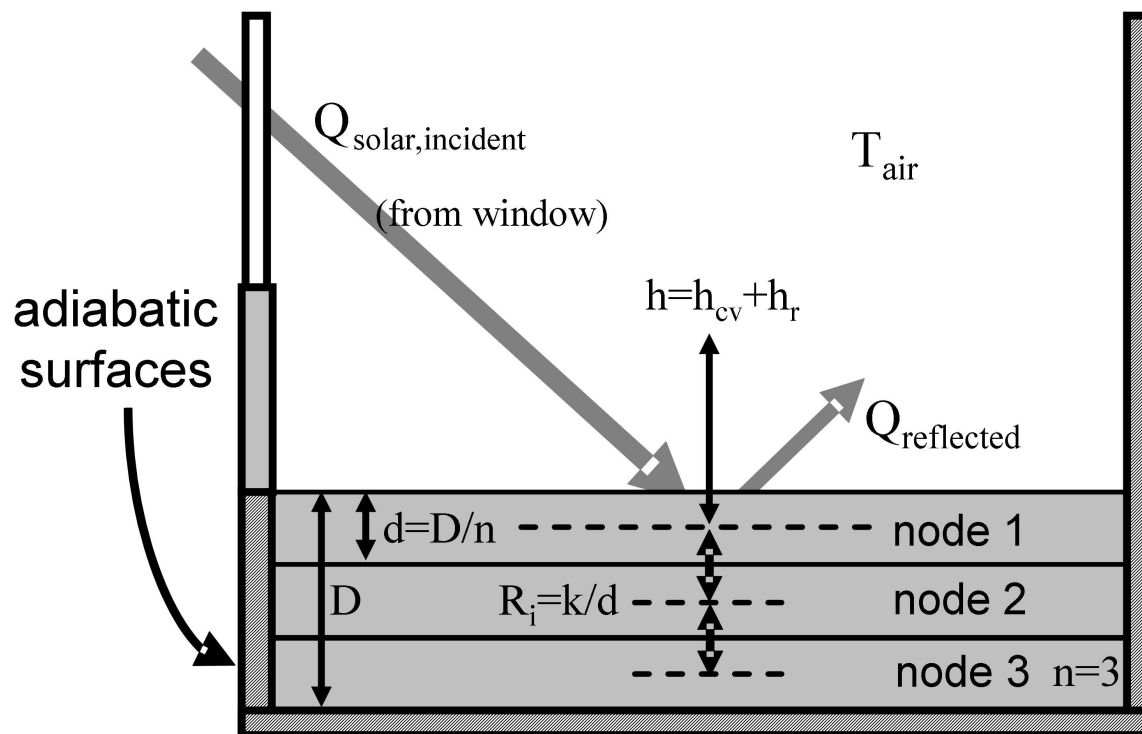


Figure 6-5. Exploded view of thermal mass. Here the depth is divided into 3 slices, each with a temperature node centered vertically in the slice.

The energy balance on each slice is

$$\Delta E_{internal} = (Q_{in} - Q_{out}) \Delta t \quad (6-10)$$

where $E_{internal}$ is the internal energy (J) of a mass slice, Q_{in} and Q_{out} are the rates of energy transfer (W) into/out of the slice, and Δt is the time period over which the energy transfer occurs. The energy balance of Eq. (6-10) yields the following nodal equations

Surface Node, i=1

Solar radiation absorption, convection with room, conduction with node 2

$$mC(T_1^{t+\Delta t} - T_1^t) = \left[\alpha \cdot Q_{solar,incident} + h(T_{room} - \bar{T}_1) + \frac{k}{d}(\bar{T}_2 - \bar{T}_1) \right] \Delta t \quad (6-11)$$

Interior Node, 1 < i < n

Conduction between two adjoining nodes

$$mC(T_i^{t+\Delta t} - T_i^t) = \left[\frac{k}{d}(\bar{T}_{i+1} - \bar{T}_i) + \frac{k}{d}(\bar{T}_{i-1} - \bar{T}_i) \right] \Delta t \quad (6-12)$$

Bottom Node, i=n

Conduction with the only adjoining node, adiabatic surface

$$mC(T_n^{t+\Delta t} - T_n^t) = \left[\frac{k}{d}(\bar{T}_{n-1} - \bar{T}_n) \right] \Delta t \quad (6-13)$$

where m is the slice mass, C is the slice heat capacity, d is the slice thickness, k is the slice thermal conductivity, $T^{t+\Delta t}$ refers to the nodal temperature at the next time step, and \bar{T} indicates the average temperature during the time step Δt

$$\bar{T}_i = \frac{T_i^{t+\Delta t} + T_i^t}{2} \quad (6-14)$$

Numerical Method

Using the average temperature over the duration of the timestep is an average of the forward and backward Euler methods, known as the Crank-Nicolson numerical method. As with implicit methods, this technique requires solving each of the nodal equations simultaneously and is unconditionally stable. If too large a timestep is used, numerically-induced oscillations can occur, which are physically impossible. When a proper timestep and depth-discretization are used, this technique provides higher accuracy than both implicit and explicit methods. Appropriate timestep and slice-thickness selection is discussed later in this chapter.

Substituting Eq. (6-14) into Eqs. (6-11), (6-12), and (6-13), rearranging and collecting the $T^{t+\Delta t}$ on the LHS, and the T^t terms & heat source terms on the RHS, a matrix system of equations takes the form

$$\underline{\underline{B}} \underline{x}^{t+\Delta t} = \underline{\underline{S}} \underline{x}^t + \underline{Q} \quad (6-15)$$

where the \underline{x} vectors represent the temperature distribution within the thermal mass, the $(t+\Delta t)$ superscript indicates the next timestep, and the (t) superscript indicates the current timestep, and \underline{Q} represents the radiation vector. $\underline{\underline{B}}$ and $\underline{\underline{S}}$ are the heat transfer matrices which are built from the temperature-term coefficients of Eqs. (6-11), (6-12), and (6-13). Inverting the $\underline{\underline{B}}$ matrix yields the following solution for the temperature distribution at time $t+\Delta t$

$$\underline{x}^{t+\Delta t} = \underline{\underline{B}}^{-1} \cdot [\underline{\underline{S}} \cdot \underline{x}^t + \underline{Q} \Delta t] \quad (6-16)$$

Only the temperature distribution and heat flux at the present time step are required to arrive at the temperature distribution at the next time step. An example system of equations for a 5-node system is given in Fig. 6-6.

$$\underline{\underline{B}} = \begin{bmatrix} C + \frac{hA\Delta t}{2} + \frac{kA\Delta t}{2d} & \frac{-kA\Delta t}{2d} & 0 & 0 & 0 \\ \frac{-kA\Delta t}{2d} & C + \frac{kA\Delta t}{d} & \frac{-kA\Delta t}{2d} & 0 & 0 \\ 0 & \frac{-kA\Delta t}{2d} & C + \frac{kA\Delta t}{d} & \frac{-kA\Delta t}{2d} & 0 \\ 0 & 0 & \frac{-kA\Delta t}{2d} & C + \frac{kA\Delta t}{d} & \frac{-kA\Delta t}{2d} \\ 0 & 0 & 0 & \frac{-kA\Delta t}{2d} & C + \frac{kA\Delta t}{2d} \end{bmatrix}$$

$$\underline{\underline{S}} = \begin{bmatrix} C - \frac{hA\Delta t}{2} - \frac{kA\Delta t}{2d} & \frac{kA\Delta t}{2d} & 0 & 0 & 0 \\ \frac{kA\Delta t}{2d} & C - \frac{kA\Delta t}{d} & \frac{kA\Delta t}{2d} & 0 & 0 \\ 0 & \frac{kA\Delta t}{2d} & C - \frac{kA\Delta t}{d} & \frac{kA\Delta t}{2d} & 0 \\ 0 & 0 & \frac{kA\Delta t}{2d} & C - \frac{kA\Delta t}{d} & \frac{kA\Delta t}{2d} \\ 0 & 0 & 0 & \frac{kA\Delta t}{2d} & C - \frac{kA\Delta t}{2d} \end{bmatrix}$$

$$\underline{\underline{Q}} = \begin{bmatrix} \alpha \cdot Q_{solar,incident} \\ 0 \\ 0 \\ 0 \\ 0 \end{bmatrix} \quad \underline{\underline{x}} = \begin{bmatrix} T_1^t \\ T_2^t \\ T_3^t \\ T_4^t \\ T_5^t \end{bmatrix} \quad \underline{\underline{x}}' = \begin{bmatrix} T_1^{t+\Delta t} \\ T_2^{t+\Delta t} \\ T_3^{t+\Delta t} \\ T_4^{t+\Delta t} \\ T_5^{t+\Delta t} \end{bmatrix}$$

Figure 6-6. Example of matrix equations for a 5-node (n=5) system.

Because the coefficients of the $\underline{\underline{B}}$ matrix remain approximately constant throughout the simulation it is only necessary to invert the $\underline{\underline{B}}$ matrix a single time for a given building simulation. This is important because matrix inversion, especially for larger matrices, is computationally expensive. Computation time for the inversion of the sparse $\underline{\underline{B}}$ -matrix is order (n^2) , which is much greater than the linear operations required by Eq. (6-16) which are of order (n) . Before computation time can be assessed, it is necessary to determine the appropriate discretization of the numerical dimensions of time and space.

For the energy balance described above, it is assumed that the room air temperature does not change significantly during the timestep. It will be shown in

Chapter 8 that the room air temperature must be computed at least once every five minutes to prevent numerically induced temperature oscillations. As will be shown in the next section, the thermal mass calculations require a time step shorter than five minutes to guarantee accuracy.

Discretization of Time & Space

Selecting appropriate time steps and slice thicknesses is critical to the accuracy and stability of the method. The numerical technique described above is unconditionally stable in time. Since stability does not guarantee accuracy over a single time step, conservative estimates for the step sizes are used. The thickness of the slices is chosen to ensure that each slice is at a relatively uniform temperature, satisfying

$$Bi = \frac{hd}{k} \ll 0.10 \quad (6-17)$$

In this way the lumped capacitance model is applicable for each slice. To be conservative, 0.05 is used (instead of the minimum value of 0.10) as the limiting value of the Biot number in determining the slice thickness. Time steps are also chosen to ensure that no numerical overshooting takes place. The usual relation for stability of a one-dimensional explicit method is given by

$$Fo = \frac{k}{\rho \cdot c} \cdot \frac{\Delta t}{d^2} < \frac{1}{2} \quad (6-20)$$

The maximum time step is found by solving Eq. (6-20) for Δt . Because the method is not an explicit method, this is taking a very conservative approach. The expressions used for the maximum slice thickness and maximum timestep are

$$d_{\max} = 0.05 \frac{k}{h} \quad (6-21)$$

and

$$\Delta t_{\max} = 0.5 \cdot \frac{\rho \cdot c}{k} d_{\max}^2 \quad (6-22)$$

Since Eqs. (6-21) and (6-22) can yield values that are not perfect divisors of the slab depth D and the energy balance timestep (five minutes), these values must be rounded down to the nearest perfect divisor.

Ordinarily it is desirable to minimize the time step size in order to optimize computation time. In this situation since the large ($n \times n$) matrix is only inverted a single time, the remaining calculations are performed rapidly. The benefit of improved accuracy by excessively small timesteps does not adversely affect the computation time. Using the properties of concrete, typical values for slice thickness and time step used by the software are given in Table 6-6.

Table 6-6. Maximum size of slice thickness and time steps used in simulation.

	Units	User-Specified Thermal Mass		
		High	Medium	Low
Thickness, D	meters	0.20	0.10	0.02
<i>Discretization</i>				
Max slice thickness, d_{\max}	meters	0.007	0.007	0.007
Whole number of slices, n	none	29	15	3
Actual slice thickness, d	meters	0.00689	0.00667	0.00667
Maximum time step, Δt_{\max}	sec.	34	32	32
Actual time step, Δt	sec.	30	30	30

6.4 VALIDATING THE MODEL

Semi-Infinite Solid, Closed Form Solutions

A semi-infinite solid, pictured in Fig. 6-7, is a body which extends very far in two dimensions, and finitely in a third dimension. Uniform changes in surface temperature, surface heat-flux, or surface convection result in a one-dimensional response in the temperature distribution within the semi-infinite solid due to conduction heat transfer in the direction normal to the surface. This configuration is quite similar to the one described above for modeling the thermal mass floor.

Conveniently, closed form solutions are available for computing the transient temperature response of a semi-infinite solid undergoing several types of heat transfer (Incropera). For these solutions to remain valid, the temperature of the semi-infinite solid must begin at a uniform initial temperature AND the temperature of the solid far from the surface in the vertical (x) direction must remain at this initial temperature with time.

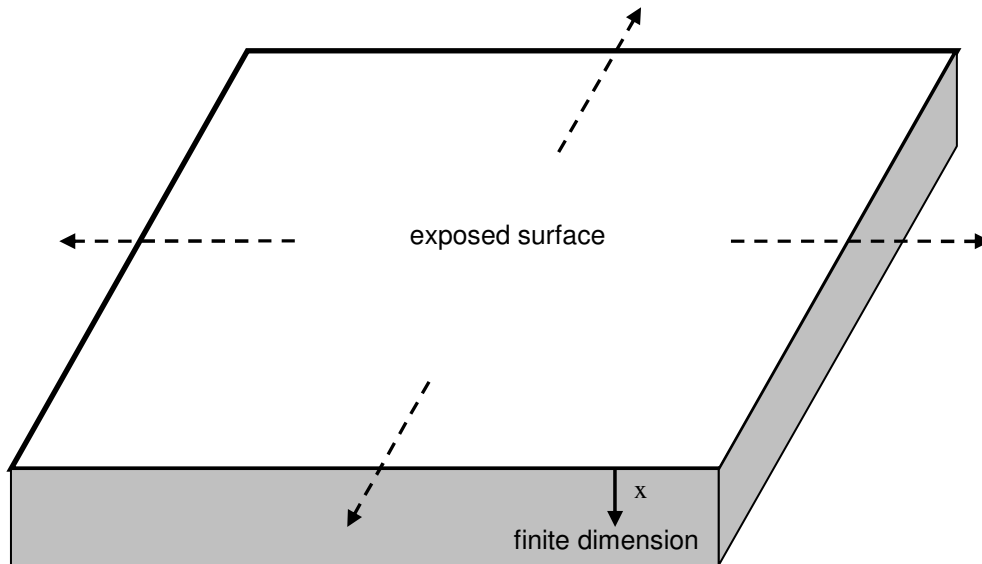


Figure 6-7. The semi-infinite solid extends infinitely in two dimensions and finitely in one dimension.

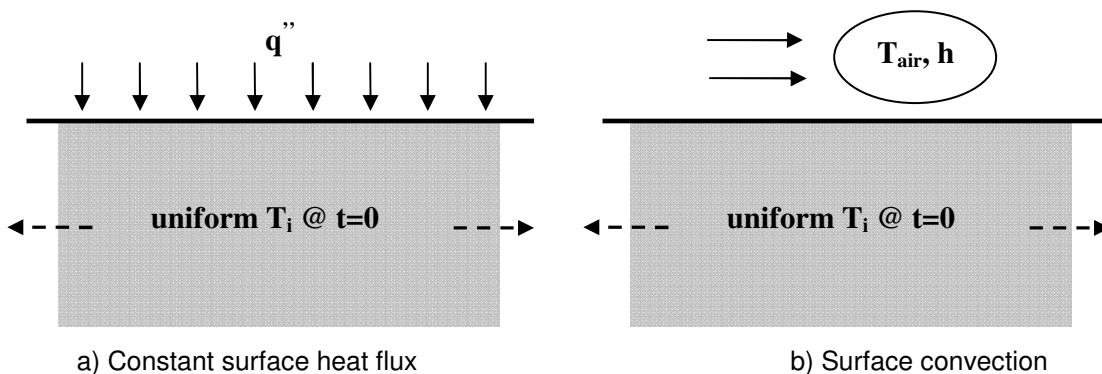


Figure 6-8. A semi-infinite solid with two different surface conditions. Closed-form temperature histories are available for both.

Two such conditions, the constant surface heat flux and the surface convection conditions are shown in Fig. 6-8. Their closed-form solutions (Incropera) are as follows

Case 1 Constant Surface Heat Flux: $q_s'' = q_0''$

$$T(x,t) - T_i = \frac{2q_0'' \left(\frac{k}{\rho c} t \right)^{1/2}}{k} \exp \left[\frac{-x^2}{4 \frac{k}{\rho c} t} \right] - \frac{q_0'' x}{k} \operatorname{erfc} \left(\frac{x}{2 \sqrt{\frac{k}{\rho c} t}} \right) \quad (6-23)$$

Case 2 Surface Convection: $-k \frac{\partial T}{\partial x} \Big|_{x=0} = h[T_{air} - T(0,t)]$

$$\frac{T(x,t) - T_i}{T_\infty - T_i} = \operatorname{erfc} \left(\frac{x}{2 \sqrt{\frac{k}{\rho c} t}} \right) - \left[\exp \left(\frac{hx}{k} + \frac{h^2 \frac{k}{\rho c} t}{k^2} \right) \right] \left[\operatorname{erfc} \left(\frac{x}{2 \sqrt{\frac{k}{\rho c} t}} + \frac{h \sqrt{\frac{k}{\rho c} t}}{k} \right) \right] \quad (6-24)$$

By comparing the results of the numerical simulation with closed-form solutions in cases where the temperature disturbance does not reach the bottom of the slab, a measure of validation can be produced. Four cases have been constructed for this purpose. Cases 1a and 1b indicate a constant surface heat flux condition, and Cases 2a and 2b indicate surface heat transfer. A thick slab of concrete ($D=0.20\text{m}$) was used for this comparison to aid in keeping the bottom node temperature constant during the hour-long time history used in the comparison. The specific parameters for each comparison and the results are summarized in Table 6-7. Time histories of temperature have been plotted in Figs. 6-9 through 6-12. Three temperature nodes have been plotted in each case: the surface-node, the central-node, and the bottom-node. The solid line indicates the closed-form solution

result and the dotted line indicates the numerically-computed solution. Excellent agreement is shown between the model and the semi-infinite solutions. By computing the average temperature within the slab at the end of the hour for both the numerical and the closed-form solutions, a quantitative measure of validation has been produced. Error of less than 3% is observed for all cases investigated.

Table 6-7. Validation cases: assumptions and results

Variable Description	Constant Surface Heat Flux		Convection Heat Transfer	
	Case 1a	Case 1b	Case 2a	Case 2b
<i>Variables</i>				
Concrete depth, D [m]	0.20	0.20	0.20	0.20
Initial temperature [K]	300	320	300	320
Surface radiation flux [W/m ²]	400	-100	-	-
Surface convection, h [W/m ² -K]	-	-	8.0	8.0
Environmental temperature [K]	-	-	320	300
<i>Results at time=1 hr</i>				
Net rate of energy gain, [W/m ²]				
Numerical model	399.96	-99.996	133.81	-133.81
Closed-form solution	400.00	-100.000	131.14	-131.14
% Difference	0.01%	0.004%	2.03%	2.03%

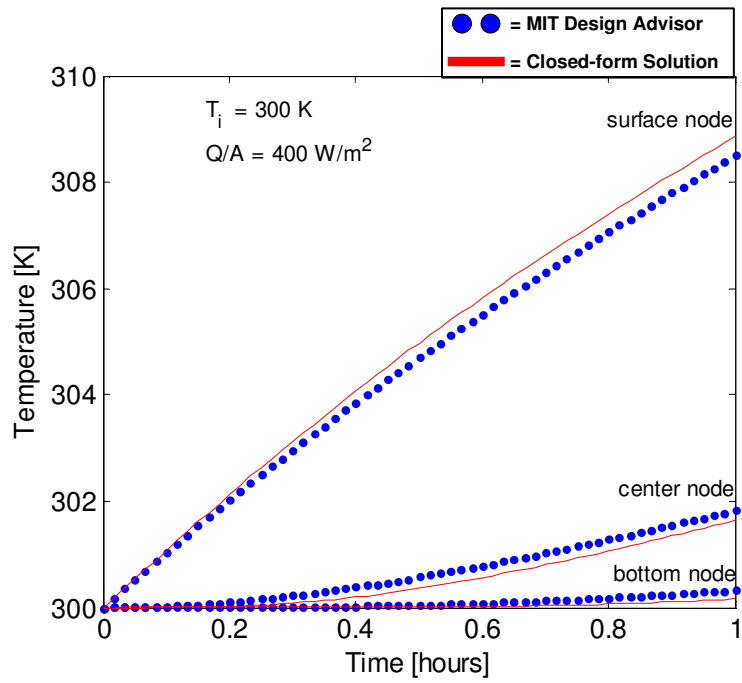


Figure 6-9. Case 1a, constant surface heat flux into thermal mass.

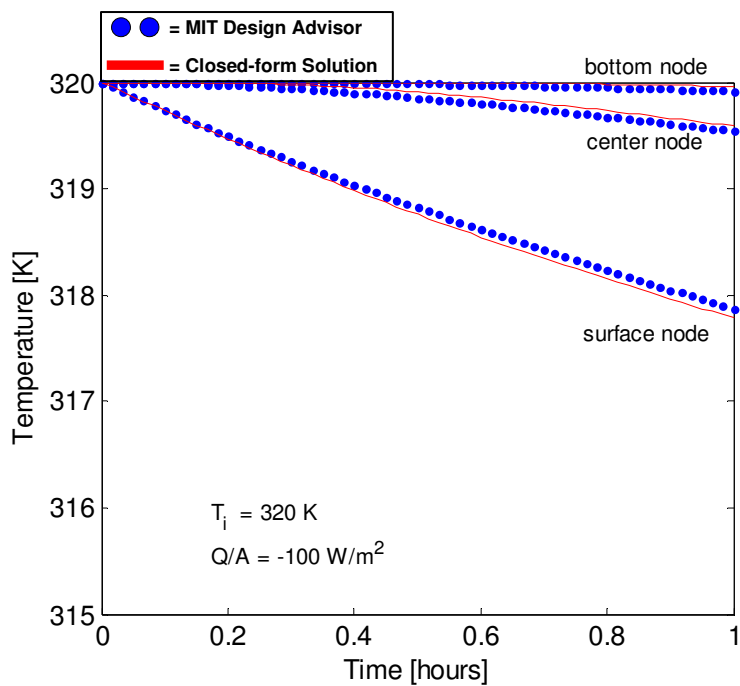


Figure 6-10. Case 1b, constant surface heat flux out of thermal mass.

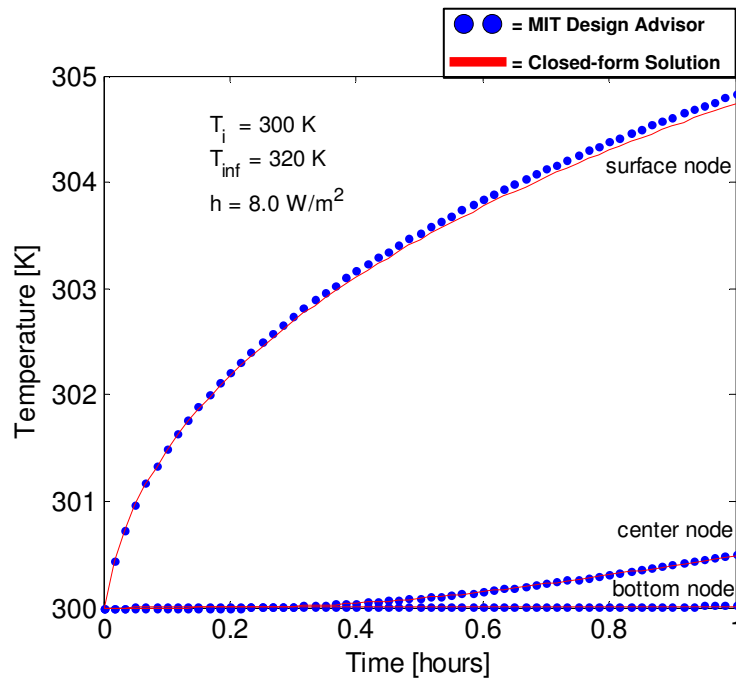


Figure 6-11. Case 2a, surface convection into thermal mass.

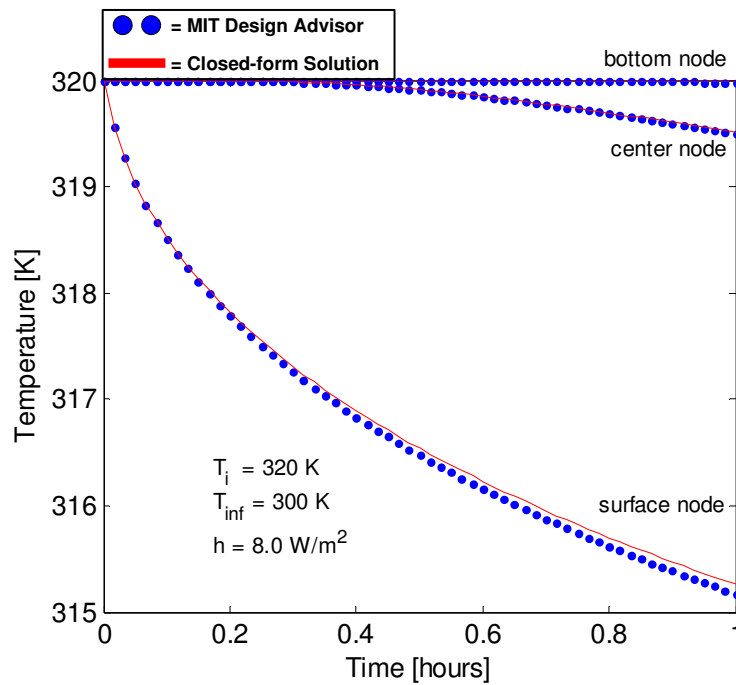


Figure 6-12. Case 2b, surface convection out of thermal mass.

CHAPTER 7

ENVELOPE LOADS

7.1 INTRODUCTION

A building's exterior surfaces permit the exchange of thermal energy between the indoor and outdoor environments. The set of surfaces through which these exchanges occurs – usually walls, windows, and roofing – is termed the building envelope. Thermal exchanges can occur through these components in several ways. Energy is exchanged to and from internal and external surfaces by convection and radiation. Energy is also conducted and radiated through the materials comprising the envelope. The quantity of energy exchanged depends on the indoor and outdoor air temperatures, the incident solar flux, convection conditions, and the ability of the construction materials to resist thermal transmission. In this chapter a method is given for calculating the energy exchange through the building envelope for a set of environmental conditions.

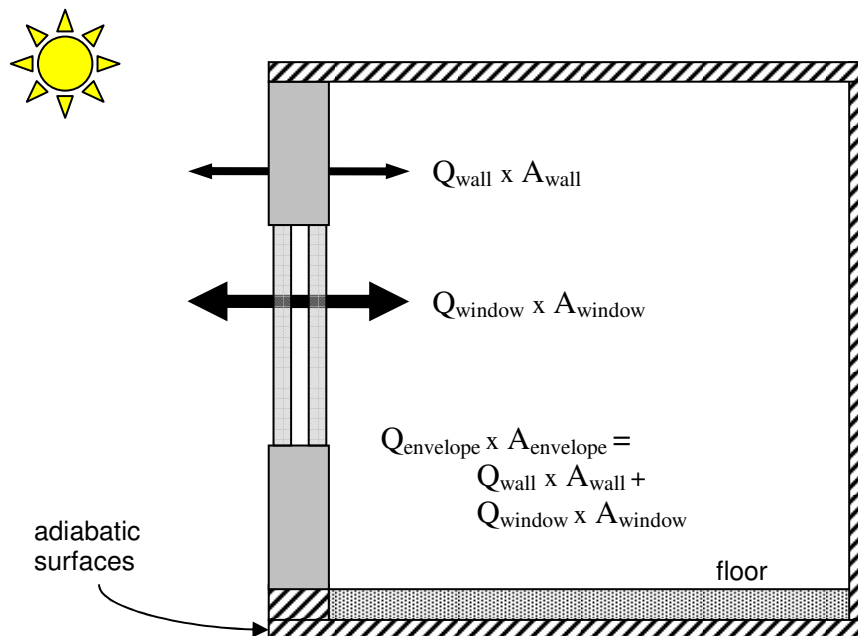


Figure 7-1. Thermal exchange through the building envelope includes the combined heat transfer through the exterior wall and the window.

7.2 THERMAL EXCHANGE THROUGH EXTERIOR WALLS AND WINDOWS

The familiar electrical circuit analogy is used for computing thermal gains through the windows and walls comprising the building envelope. Unless stated otherwise it is assumed that energy is transferred one-dimensionally through the building façade as shown in Fig. 7-1. Energy exchanges are computed independently for thermal transmission through the exterior walls and windows of a building envelope. Simple, one-dimensional relations, given later in this chapter, are used for making most of the energy calculations¹⁸. The net envelope energy exchange (excluding directly transmitted solar radiation, which has already been discussed in Chapters 4 and 6) is computed

$$Q_{envelope} = Q_{wall} + Q_{window} \quad (7-1)$$

in units of power, or watts. Since the gains are computed separately, it is convenient to calculate the gains on a per-area basis

$$q_{wall} = \frac{Q_{wall}}{A_{wall}} \quad (7-2)$$

$$q_{window} = \frac{Q_{window}}{A_{window}} \quad (7-3)$$

$$q_{envelope} = \frac{Q_{wall} + Q_{window}}{A_{wall} + A_{window}} = \frac{q_{wall} A_{wall} + q_{window} A_{window}}{A_{wall} + A_{window}} \quad (7-4)$$

Exterior Walls

Exterior walls are modeled simply as a single conducting element with a thermal resistance, Fig. 7-2. Four temperature nodes are used to model the wall. From the exterior to interior these are: 1.) Outdoor ambient temperature; 2.) Exterior wall surface temperature; 3.) Indoor wall surface temperature; and 4.) Indoor ambient air temperature. These nodes are connected with resistive elements which

¹⁸ An exception is the case of airflow windows, which require a two dimensional method to account for temperature variation in the vertical direction.

are used to model the transport of heat through the surface. Nodes 1 and 2 are connected via convective and radiation resistances in parallel, $R_{cv,ext}$ and $R_{r,ext}$. Nodes 2 and 3 are connected via a conduction resistance $R_{c,wall}$. Nodes 3 and 4 are connected via convective and radiation resistances in parallel, $R_{cv,int}$ and $R_{r,int}$. Equations for computing thermal resistance values are given later in this chapter. The absorbed fraction α_{wall} of the incident solar radiation flux $q_{solar,inc}$ on the exterior wall is introduced as a current source into the exterior surface node. Thermal capacitance effects are ignored in the heat transfer through the walls, as the elements are assumed to reach steady-state temperatures quickly. It is assumed that a building's thermal mass is concentrated primarily in the floor.

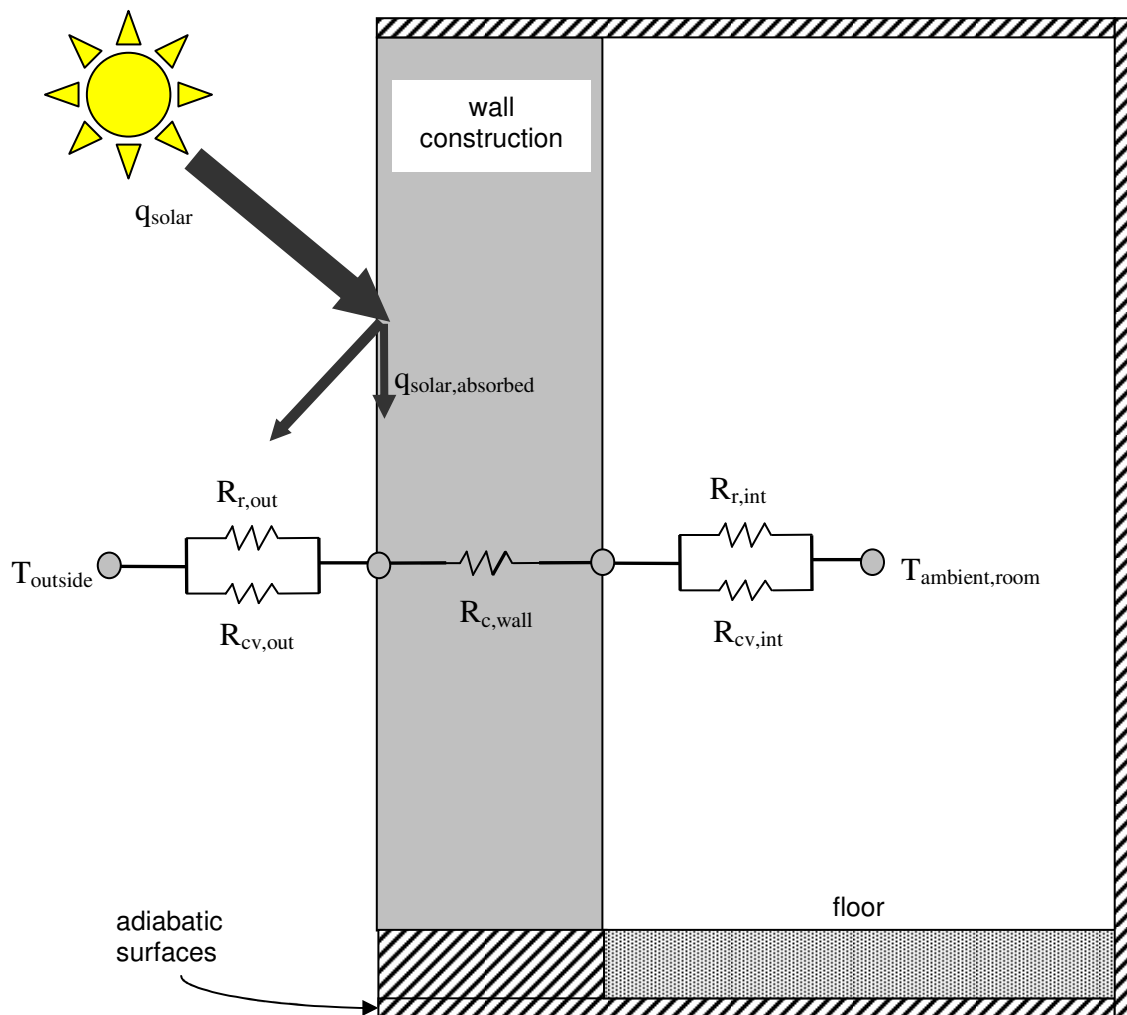


Figure 7-2. Heat transfer through the wall – a simple resistive circuit.

Windows

Windows are modeled similarly to the walls. Each window pane is modeled with two temperature nodes – one at the front and one at the back surface as shown in Fig. 7-3. The inner-most surface and the outer-most surface are connected to their respective ambient temperature nodes with parallel convective and radiation resistances acting in exactly the same way as the wall model described above. In the case of multi-layered glazings, a gas¹⁹ occupies the space between each pane which offers a conductive resistance $R_{c,gap}$ between the surfaces of the facing layers of window pane. Facing window pane surfaces can also exchange energy via radiation across the gap, so a radiation resistance $R_{r,gap}$ must be computed for each pair of facing window panes. The conduction and radiation resistances across the gap act in parallel as shown in the diagram, and the net effective resistance across a gap is given by

$$R_{net,gap} = \frac{1}{\frac{1}{R_{c,gap}} + \frac{1}{R_{r,gap}}} = \frac{R_{c,gap} R_{r,gap}}{R_{c,gap} + R_{r,gap}} \quad (7-5)$$

Conduction across each pane of glass is computed via a conduction resistance $R_{window-conduction}$. This resistance is typically extremely small, making it valid to assume a uniform window temperature. The reason that two nodes are used for each window pane – one for each surface – instead of just one node is to emphasize the fact that optical properties can be different for two sides of the same pane of glass. Reflections, transmissions, and absorptions of solar radiation are computed for each pane surface in a method which has been discussed at length in an earlier chapter.

¹⁹ For this analysis, the fill gas is assumed to be air.

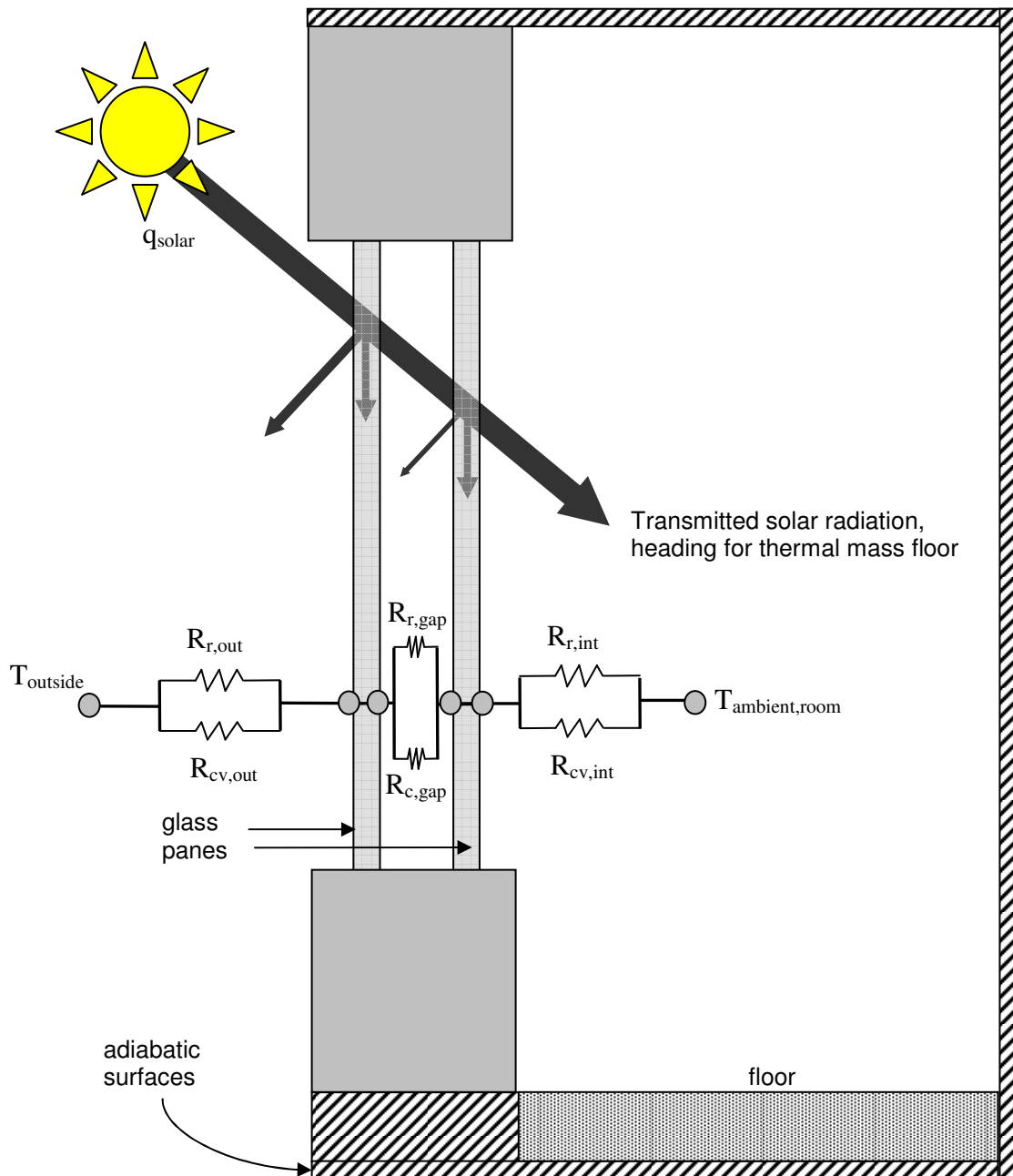


Figure 7-3. Cross section of a room showing the envelope heat exchange and thermal circuit for a double-pane window.

Surface Resistance

At each exposed building surface both a convection and a radiation mechanism can transport energy to the local environment. The combined effect of the two thermal resistances is computed in the same manner as for heat transfer across a gap in a multi-layered glazing

$$R_{net,surface} = \frac{1}{\frac{1}{R_{cv,surface}} + \frac{1}{R_{r,surface}}} = \frac{R_{cv,surface} R_{r,surface}}{R_{cv,surface} + R_{r,surface}} \quad (7-6)$$

For indoor and outdoor surfaces, it is assumed that the mean temperature used to compute the radiation resistance $R_{r,surface}$ is the same as the ambient air temperature. For indoor surface exchanges this is a reasonable assumption as most interior surfaces exist at or near the indoor air temperature. For outdoor surface exchanges this assumption may not always be correct as ground and sky temperatures can differ from the local outdoor air temperatures. Fortunately, except for single-glazed windows, the exterior surface radiation resistance is typically much greater than the convection resistance; and both surface resistances combined are very much smaller than the $R_{net,window}$ or $R_{net,wall}$ values. Thus, even when sky temperatures differ significantly from the outdoor air temperature, little bearing is had on the predicted heat transfer by the assumption.

In the case of multi-layered windows, radiation exchanges between consecutive window panes are often on the same order as the convection or conduction in the air cavity. Because of this, it is important to accurately know the surface temperatures of the window panes for computing thermal interaction within the window cavity. For multi-layered windows, the pane surface temperatures are computed directly and their values are used in determining the pane-to-pane radiation coefficient.

7.3 THERMAL RESISTANCE CALCULATIONS

In this section a method is given for computing each of the thermal resistance values. Conduction across solid components is described first, followed by surface radiation and convection. Finally, thermal exchange within window cavities is discussed. Methods for handling more complicated cases involving blinds and ventilated cavities will be mentioned at the end.

Wall Conduction

In reality walls are comprised of several layers of materials: brick, wood, plaster, gypsum, insulation, etc. Specifying the details of every material layer in the building construction is not necessary for a modestly-accurate early-stage simulation. In practical cases most of the resistance to conduction occurs within the insulation, and so the amount and type of insulation will dominate the predicted exchange through the building envelope²⁰. The user input determines how much conduction resistance is provided by the wall. Users can specify the amount of insulation by selecting the type of insulation and its thickness d , or by specifying a total wall R-Value. When specifying the type of insulation, the user can select from either foam or fiberglass insulation, having thermal conductivity $k_{\text{insulation}}$ of 0.023 and 0.038 W/m-K respectively. An approximate R-Value is computed using

$$R_{\text{wall-construction}} = \sum_i \frac{k_i}{d_i} \approx \frac{k_{\text{insulation}}}{d_{\text{insulation}}} \quad (7-7)$$

where i denotes each layer of the wall's construction.

Window Pane Conduction

Conduction resistances for glazings that contain only one semi-transparent pane are computed in the same manner. Window panes are assumed to have a thickness of 6mm and a glass construction with a corresponding conductivity of 1.38 W/m-K. The conduction resistance is then simply

²⁰ See note at end of chapter for supporting analysis.

$$R_{c,pane} = \frac{d_{insulation}}{k_{insulation}} = \frac{0.006 \text{ m}}{1.38 \frac{\text{W}}{\text{m-K}}} = 0.0044 \frac{\text{m}^2\text{-K}}{\text{W}} \quad (7-8)$$

The resistance across a thin window-pane is quite small and can be neglected.

Window Cavity Gas Fill Heat Transfer

Heat transfer across the gap between panes of multi-layered glazings occurs by convection or conduction through the gas, and also by radiation exchange between the window pane surfaces. Radiation will be covered in the next section. Here we discuss the conduction resistance across the gap.

The type of gas and the cavity width d_{gap} are used to determine the conductive resistance across the gap

$$R_{c,gap} = \frac{d_{gap}}{k_{gas}} \quad (7-9)$$

The conductivities of the common fill gasses air, argon, and krypton are 0.0253, 0.016, and 0.01 W/m-K, respectively. While argon and krypton gasses can improve thermal performance of windows, for simplicity it is assumed the gas fill is comprised of air. When the cavity width is very small, there is little room for convection currents to be established, and the resistance due to conduction as given by Eq. 7-9 holds fairly well. Thermal resistance increases with cavity width, however, convection also begins to assist the heat transfer. When the width reaches 13 mm, the increased conductive resistance is offset by increased convection effects. Further increases in cavity width beyond 13 mm have little effect on the center-of-glass window performance, as shown in Fig. 7-4 (ASHRAE). For modeling simplicity, in all cases the gap thickness d_{gap} is assumed to be 12.7mm and Eq. 7-9 is used to approximate the conduction resistance across the gap.

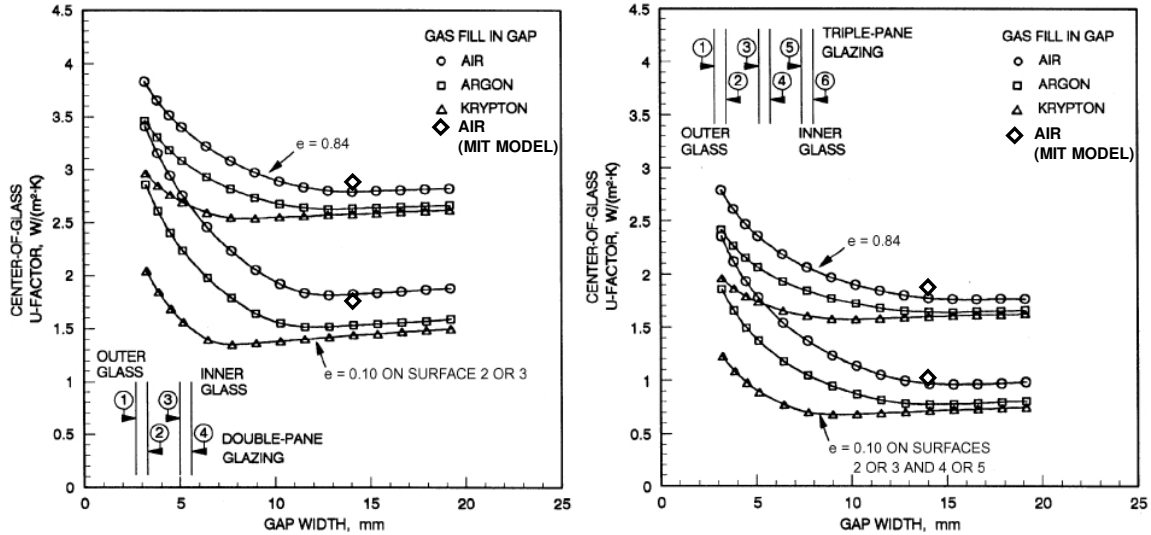


Figure 7-4. Center of glass U-Values for 3 types of gas vs. cavity width (ASHRAE).

Radiation Heat Transfer

Surface temperature differences give rise to radiation heat exchanges. Radiant energy can be transferred from a surface to an environment or from a surface to another surface. Radiant energy is exchanged between 1.) exterior surfaces of walls and windows with the outdoor environment; 2.) interior surfaces of walls and windows with the surfaces inside the room; and for multi-layered glazings 3.) glazing-element surface to surface exchange. A method is described for computing the radiation heat transfer coefficient $h_{r,surface-surface}$ based on the surface and environment properties and temperatures. The radiation resistance $R_{r,surface}$ is simply the inverse of $h_{r,surface-surface}$.

The typical diffuse-grey body assumptions are appropriate for this analysis. For each surface or area used in the radiation calculations, the following assumptions (Siegel 2002) are made:

1. The temperatures of various surfaces do not differ so greatly that their emissions occur in different portions of the spectrum;
2. The temperature of an individual surface is uniform;
3. Surface properties are uniform;
4. Surface emissivity and absorptivity are identical and independent of wavelength and direction;

5. All energy is emitted and reflected diffusely; and
6. Incident and reflected energy flux is uniform over each individual area used in calculations.

Radiant surface emissive power is given by the familiar Stefan-Boltzmann Law

$$j_s = \frac{J_s}{A_s} = \epsilon_s \sigma T_s^4 \quad (7-10)$$

where ϵ_s is the surface emissivity, σ is Stephan-Boltzmann constant (5.67×10^{-8} W/m²-K⁴) the and T_s is the surface temperature in Kelvins. The goal is to use this relation and the assumptions to compute the net radiant exchange between two surfaces.

Radiation exchanges occur between exterior building surfaces and the outdoor environment, which is comprised of the ground, the sky, and any surrounding objects. For estimation purposes, the outdoor air temperature is used to approximate the mean outdoor radiation temperature. It is assumed that exterior building surfaces have a view factor of 1 to the outdoor environment. Similarly, radiation exchange occurs between the inner-most surface of the exterior wall and the room's interior, with the mean surface temperature of the room approximated as the indoor air temperature. Again, a view factor of 1 is assumed. Finally, facing window panes of multi-layered glazings each have a configuration factor of approximately 1, because the gap is typically small compared with the window height and width dimensions.

In the case of windows with blinds, a radiosity method is used to compute the exchange between all window surfaces which interact with the blinds. Hottel's crossed-strings approach is used to compute view factors between elements of the blinds, depending on the blind geometry. See the Master's Thesis of J. Smith for a more detailed description of this approach.

For two surfaces a and b where the configuration factor $F_{a-b}=1$ the net radiation exchange is given by

$$q_{net} = \frac{Q_{a-b}}{A_a} = \varepsilon_{eff} \sigma (T_a^4 - T_b^4) \quad (7-11)$$

where

$$\varepsilon_{eff} = \frac{1}{\frac{1}{\varepsilon_a} + \frac{1}{\varepsilon_b} - 1} \quad (7-12)$$

To simplify the analysis the radiation heat transfer can be linearized so that a radiation heat transfer coefficient can be used in place of the cumbersome T^4 dependence. This can be done by first twice factoring Eq. 14 to arrive at

$$q_{net} = \varepsilon_{eff} \sigma (T_a - T_b)(T_a + T_b)(T_a^2 + T_b^2) \quad (7-13)$$

Expanding the RHS, except for the linear temperature difference term yields

$$q_{net} = \varepsilon_{eff} \sigma (T_a - T_b)(T_a^3 + T_b^3 + T_a^2 T_b + T_b^2 T_a) \quad (7-14)$$

Next an average surface temperature is defined

$$T_{avg} = \frac{T_a + T_b}{2} \quad (7-15)$$

By defining $T_a \geq T_b$ the average temperature can be written as

$$T_{avg} = T_a - \Delta = T_b + \Delta \quad (7-16)$$

where Δ signifies half the difference between T_a and T_b . Next Eq. 19 is substituted into Eq. 17, yielding

$$q_{net} = \varepsilon_{eff} \sigma (T_a - T_b) \left[(T_{avg} + \Delta)^3 + (T_{avg} - \Delta)^3 + (T_{avg} + \Delta)^2 (T_{avg} - \Delta) + (T_{avg} - \Delta)^2 (T_{avg} + \Delta) \right] \quad (7-17)$$

Expanding once again and collecting terms yields

$$q_{net} = \varepsilon_{eff} \sigma (T_a - T_b) (4T_{avg}^3 + 4T_{avg} \Delta^2) \quad (7-18)$$

Grouping terms together, a heat transfer coefficient for radiation is obtained

$$q_{rad} = h_{rad} (T_a - T_b) \quad (7-19)$$

$$h_{rad} = \varepsilon_{eff} \sigma (4T_{avg}^3 + 4T_{avg} \Delta^2) \quad (7-20)$$

$$h_{rad} = \varepsilon_{eff} \sigma \left[4T_{avg}^3 + T_{avg} (T_a - T_b)^2 \right] \quad (7-21)$$

In many cases the Δ^2 term is small according to

$$T_{avg}^2 \gg \Delta^2 \quad (7-22)$$

so the heat transfer coefficient h_{rad} can be approximated as

$$h_{rad} \approx \varepsilon_{eff} \sigma 4T_{avg}^3 \quad (7-23)$$

Over the range of temperatures observed in buildings, the approximation holds accurate to better than 2% of the exact radiation solution.

Combined Surface Heat Transfer Coefficients – Radiation and Convection

Heat exchanges from surfaces to ambient surroundings are computed using a combined radiation and convection heat transfer coefficient according to

$$q_s = h_{net} (T_s - T_{ambient}) \quad (7-24)$$

with

$$h_{net} = h_{cv} + h_{rad} \quad (7-25)$$

and where T_s is the surface temperature. The ambient temperature $T_{ambient}$ can refer to the outdoor air temperature in the case of external building surfaces, or the internal air temperature in the case of interior building surfaces. Although radiation does not occur directly between surfaces and the air in the room, the air temperature is a reasonable approximation of the most interior surface temperatures with the exception of the floor and the inner-most surface of the exterior wall. The following methods are used to compute the values of the heat transfer coefficients.

Convection Surface Heat Transfer

Many correlations exist for predicting the convection heat transfer coefficients for building surfaces. For exterior film coefficients wind velocity is the primary determinant. The ISO15099 standard gives a correlation for the exterior forced convection coefficient

$$h_{cv,forced} = 4 + 4v_{air} \quad (\text{W/m}^2\text{-K}) \quad (7-26)$$

where v_{air} is the air speed in m/s. This correlation is good only for forced convection. A separate correlation for naturally-driven convection is given by Hammond

$$h_{cv,natural} = \left(\left[1.5 \left(\frac{\Delta T}{H} \right)^{1/4} \right]^6 + \left[1.23 (\Delta T)^{1/3} \right]^6 \right)^{1/6} \quad (\text{W/m}^2\text{-K}) \quad (7-27)$$

where ΔT is the temperature difference between the inner-most envelope surface and the indoor air temperature, and H is the height of the vertical surface in meters.

Reference values of surface convection coefficients from the ISO 15099 standard are given in Table 7-1 for summer and winter as an alternative to the

complex correlations. Assumed values for the MIT Design Advisor model are listed as well. These coefficients are employed for both window and wall surfaces.

Table 7-1. Reference Convection Coefficients (W/m²-K).

	ISO 15099		MIT Design Advisor
	Winter	Summer	Yearly Value
$h_{cv,int}$	3.6	2.5	4.0 (3.0)*
$h_{cv,ext}$	20	8.0	14

*The less accurate 4.0 value has been used for all calculations in this manuscript; the more appropriate (3.0) value has been substituted in the actual simulation software.

At the time of this writing, 4.0 W/m²-K has been used as a default convection coefficient for internal surface convection in the MIT Design Advisor model. This figure was arrived at from the forced convection correlation Eq. 7-12 with zero air speed. From Table 7-1 it can be seen that this may be an overestimation of actual conditions. Using a natural convection correlation or a better average value of $h_{cv,int}=3.0$ W/m²-K would yield a more accurate result. This change has since been made in the MIT Design Advisor model, however, the 4.0 W/m²-K value has been used for all calculations in this document.

Heat Transfer with Blinds

Blinds and other shading devices are often included in windows to moderate the amount of incoming light. Three main types of heat transfer are associated with blinds. First, blinds can reflect and absorb (and sometimes transmit) incident solar energy. Secondly, convection occurs between blind surfaces and the surrounding air. And finally, radiation exchanges occur between the blinds and the adjacent surfaces (window panes, interior surfaces, and the outdoor environment). The interaction of blinds with incoming solar radiation has already been considered in Chapter 4. The remainder of this subsection will focus on the convection and radiation exchanges between blinds and their surroundings.

When adjustable blinds are closed they nearly approximate a very thin window pane. Surface convection can be modeled using the Hammond correlation

described by Eq. 7-13, or by using a representative value of about 3 W/m²-K. In the case of airflow windows (described and depicted in the next section), air is forced to flow in a cavity on each side of the blinds, Fig. 7-5. In such cases, the convection coefficient must be computed from a correlation. Several exist which produce somewhat different results. One possibility is the ISO 15099 correlation given in Eq. 7-26. Another option is to use fits to experimental data as by Hens and Saelens (1999)

$$h_{cv,Hens} = \frac{(5.8 + 4v_{air})}{2} \text{ (W/m}^2\text{-K)} \quad (7-26)$$

This correlation is for vertical shades and not for blind slats.

When blinds are opened, convection interactions are not as clear. Thermally driven convection currents can cause air to travel in the spaces between blind slats. If mass transfer of air occurs from one side of the blinds to the other, some error will be introduced in the simulation process. For simplicity, however, it is assumed that air on each side of the blinds is isolated.

Radiation interactions between blinds and other building surfaces can be more complicated. When blinds are adjusted at angles other than vertical, the view factor between upper and lower blind surfaces and other building surfaces (window panes, room interior, etc.) must be computed. In such cases, a radiosity method is used to determine the temperature of the blind slats and nearby surfaces, and the energy flow between the blinds and subsequent building surfaces.

Airflow Windows & Forced Convection

In an airflow window, Fig. 7-5, a stream of air is introduced into the glazing system between two panes of glass. This air flows upward through the space which separates the two panes and is exhausted either 1.) into the room or 2.) out to the exterior environment. When air is exhausted back into the room, its temperature must be known accurately.

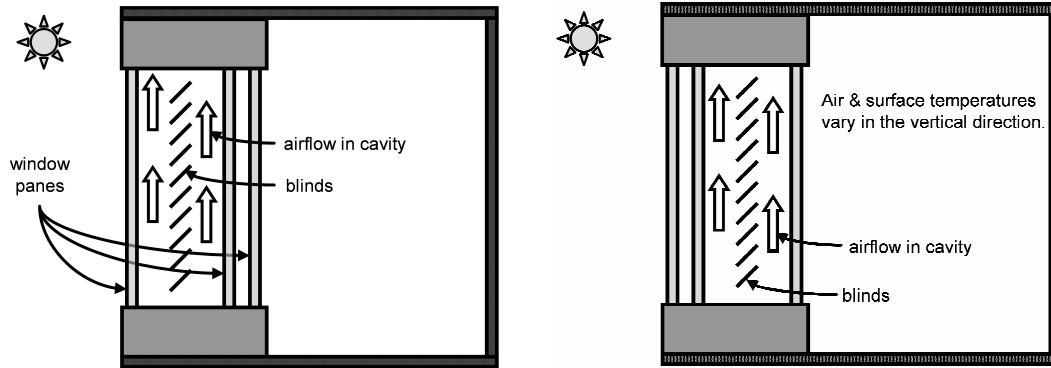


Figure 7-5. Two types of airflow windows. Air enters the cavity bottom & exits at the top. Intake & exhaust vents can connect to either the room interior or the outdoors.

Temperature variation of window elements in the vertical direction is significant for airflow windows, and a one-dimensional model is not sufficient for obtaining accurate estimates of energy transfer. Instead, the cavity is split into a series of slices, and a mass and energy balance is performed on each of the slices, Fig. 7-6.

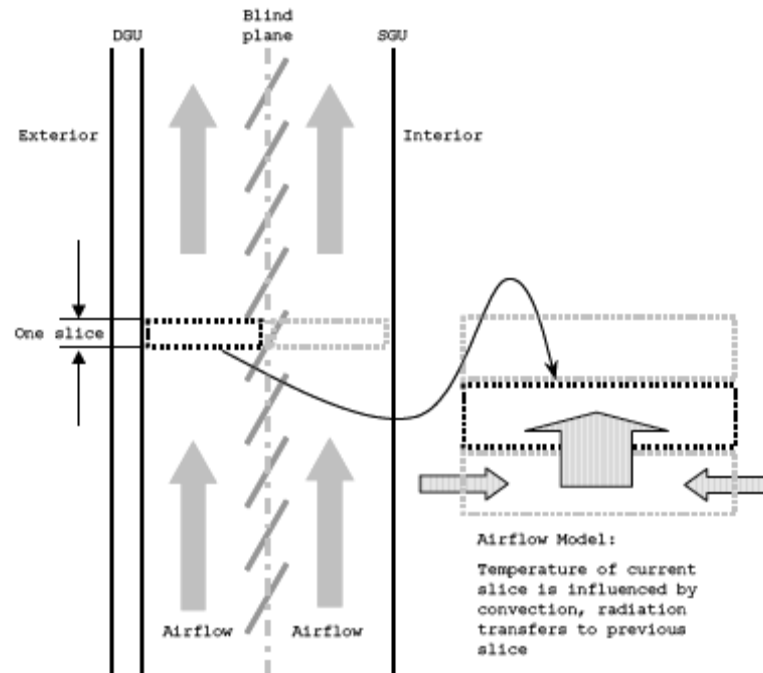


Figure 7-6. A representation of the energy balance in one slice of an airflow window. Five or more slices may be used to model a window system. (Illus. Lehar).

Window Frame

Each window is assumed to have an opaque frame comprising 16% of its area. The frame is assumed to have a construction that will approximate a U-Value of $8.0 \text{ W/m}^2\text{-K}$. Heat transfer through the frame is computed in exactly the same manner as for the opaque insulating wall.

Infiltration

A significant amount of thermal exchange can occur due to leaky construction. Air can leak into or out of a building around the frame of a window or door. Correlations have been developed for estimating the amount of leakage, and values on the order of 0.25 to 0.50 air changes per hour are typical. Mass exchanges due to infiltration are not explicitly modeled; however the effects can be simulated by increasing the fresh air intake rate appropriately.

7.4 ENVELOPE MODEL VALIDATION

To validate the above calculation procedure is to ensure that heat transfer through the envelope is computed properly. One way to do this is to use the solver to predict heat transfer results for known window and wall configurations. The U-Value and the Solar Heat Gain Coefficient (SHGC-Value or g-Value) are two metrics often used in describing the thermal performance of building components. Since to some extent these performance values depend on the environmental temperatures and the amount of incident solar radiation, the National Fenestration Research Council (NFRC) has established standards for how these values are to be calculated or measured. The NFRC standards are used to set the conditions by which the simulations are carried out, Table 7-2. Comparisons are made with the WINDOW5 software developed at the Lawrence Berkeley National Laboratory (LBNL), which uses methodology approved by NFRC for simulating window performance.

Table 7-2. Parameters for Window Thermal Performance Comparisons.

Symbol	Description	Units	U-Value	SHGC
<i>Specified Values</i>				
T_{inside}	Indoor temperature	°C	21.0	24.0
T_{outside}	Outdoor temperature	°C	-18.0	32.0
v_{wind}	Wind velocity	m/s	5.5	2.8
Q_{solar}	Solar flux incident	W/m ²	0.0	783.0
<i>Computed Values</i>				
$h_{\text{cv,int}}$	Inside convection coefficient	W/m ² -K	4.0	4.0
$h_{\text{cv,out}}$	Outside convection coefficient	W/m ² -K	26.0	15.0
$h_{\text{r,in/out}}$	Radiation coefficients	W/m ² -K	Calculated dynamically	Calculated dynamically

U-Values

The U-Value, U-Factor, or thermal transmittance of a building component is defined in the ASHRAE 90.1-2001 Standard as

“Heat transmission in unit time through unit area of a material or construction and the boundary air films, induced by unit temperature difference between the environments on each side. Units of U are W/m²-K.”

The U-Value then is the overall heat transfer coefficient of an insulating element including the surface radiation and convection effects, computed in the absence of solar radiation, Fig. 7-7. The U-Value depends slightly on temperature and on wind conditions as the radiation and convection coefficients of the surfaces can vary. This dependence is most evident in single-pane glazings, since in most cases the surface resistances make up a modest proportion of the total thermal resistance. The surface convection variation has much less impact on multi-layered glazings because most of the resistance occurs within the air gaps between panes. Standard conditions have been established to avoid confusion when making comparisons of U-Values.

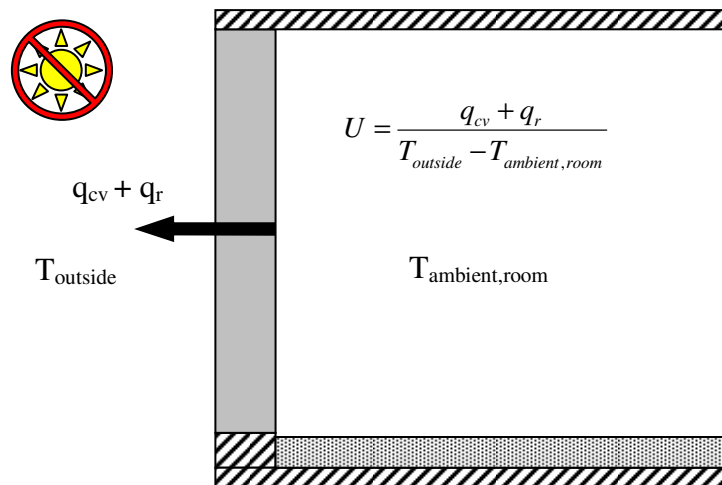


Figure 7-7. U-Value illustration.

The NFRC Standard 100-2001 describes a procedure for determining fenestration product U-Values. The environmental conditions for computing U-Values are summarized in Table 7-2. The NFRC documentation references the ISO15099 document for a standard way of computing the interior and exterior film coefficients. For rating fenestration products, the ISO Standard allows the wind correlation in Eq. 12 to be used. Using the 5.5m/s prescribed by the NFRC, we obtain an external convection coefficient of 26 W/m²-K to be used in the U-Value calculation. As mentioned earlier in this chapter, the internal surface convection coefficient has been specified as 4.0 W/m²-K.

Infrared radiation is computed with linearized radiation coefficient described earlier in this chapter. As before the internal room surfaces are assumed to be at the internal air temperature – a claim that is substantiated by the ISO standard:

“It is often assumed that internal fenestration surfaces are irradiated only by the internal room surfaces, which are treated as a large enclosure existing at the internal air temperature.”

The interior and exterior environmental emissivity values are assumed to be unity for the radiation calculations.

Using the thermal resistance circuit described earlier, the U-Value can be computed directly by taking the inverse of the summed resistances. Since the radiation resistance coefficients depend on the emitting surface temperature, iteration is required to determine the steady-state surface temperatures and radiation coefficients. Very good convergence typically occurs in fewer than four iterations.

Solar Heat Gain Coefficients

The ASHRAE Standard 90.1-2001 defines the Solar Heat Gain Coefficient as

“The ratio of the solar heat gain entering the space through the fenestration area to the incident solar radiation. Solar heat gain includes directly transmitted solar heat and absorbed solar radiation, which is then reradiated, conducted, or convected into the space.”

The SHGC is intended to represent the fraction of incident solar radiant energy $q_{solar,i}$ that ends up inside the building for a given window configuration

$$SHGC = \frac{q_{transmitted,window} + q_{cv,window} + q_{r,window}}{q_{solar,i}} \quad (7-27)$$

The $q_{transmitted,window}$ term represents the radiation directly transmitted through the window, and the $q_{cv,window}$ and $q_{r,window}$ terms represent the radiation that is absorbed by the window elements and is subsequently convected or radiated into the space,

Fig. 7-8. The NFRC standard conditions for calculating the SHGC are based on a normal-incident solar flux of $783 \text{ W/m}^2\text{-K}$ and steady-state indoor and outdoor temperatures of 32 and 24°C . Conditions are summarized in Table 7-2. The amount of incident solar radiation is large enough that the indoor/outdoor temperature difference does not contribute significantly to the SHGC value.

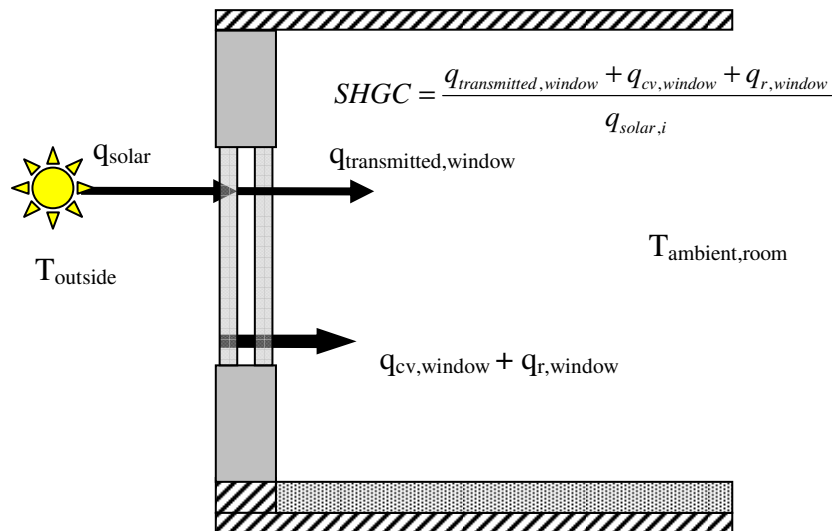


Figure 7-8. Solar Heat Gain Coefficient illustration.

Agreement for both U-Values and SHGC's is quite good as demonstrated by the comparisons shown in Figs. 7-9 and 7-10. Slight discrepancies occur when the air resistance dominates the thermal resistance as in the low-emissivity double- and triple- glazed windows. It is likely that this difference is due to our assumption of zero convection within the gaps. This explains why the U-values are very slightly lower for the MIT Design Advisor prediction.

The MIT Design Advisor U-values for double and triple glazings have been added to the ASHRAE plots in Fig. 7-4. Agreement with the ASHRAE data is good despite the fact that convection parameters are not perfectly matched, as with the LBL comparison. Variation between the MIT model and the ASRHAE is small compared with the magnitude of variation that would, for example, be generated by using a fill gas other than air. Thus, we conclude that the proposed modeling technique is adequate at predicting envelope heat exchange with reasonable accuracy.

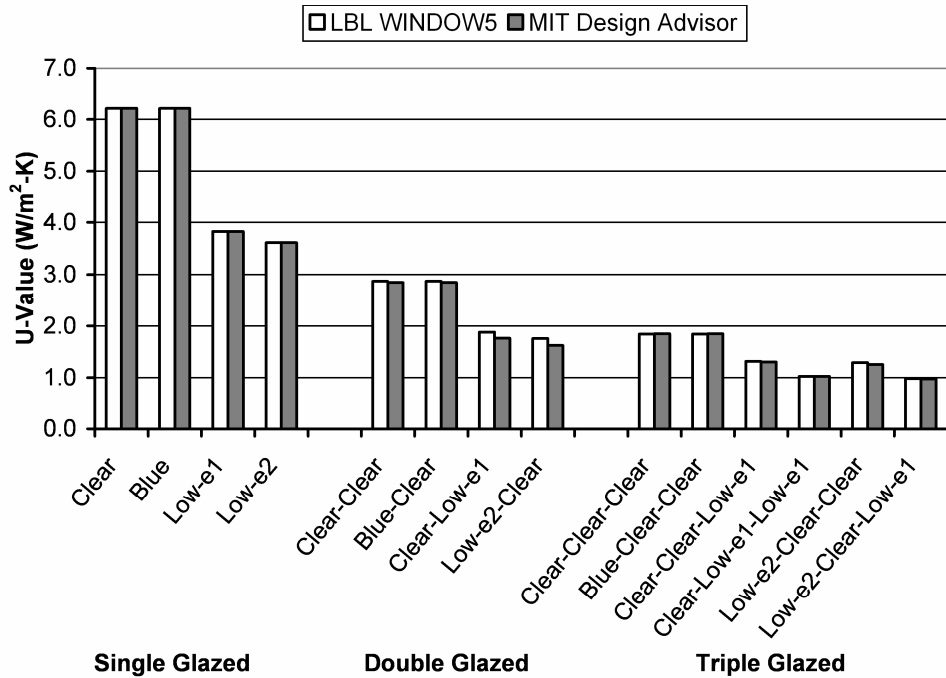


Figure 7-9. Center-of-glass U-Value comparison with LBNL WINDOW5 Software.

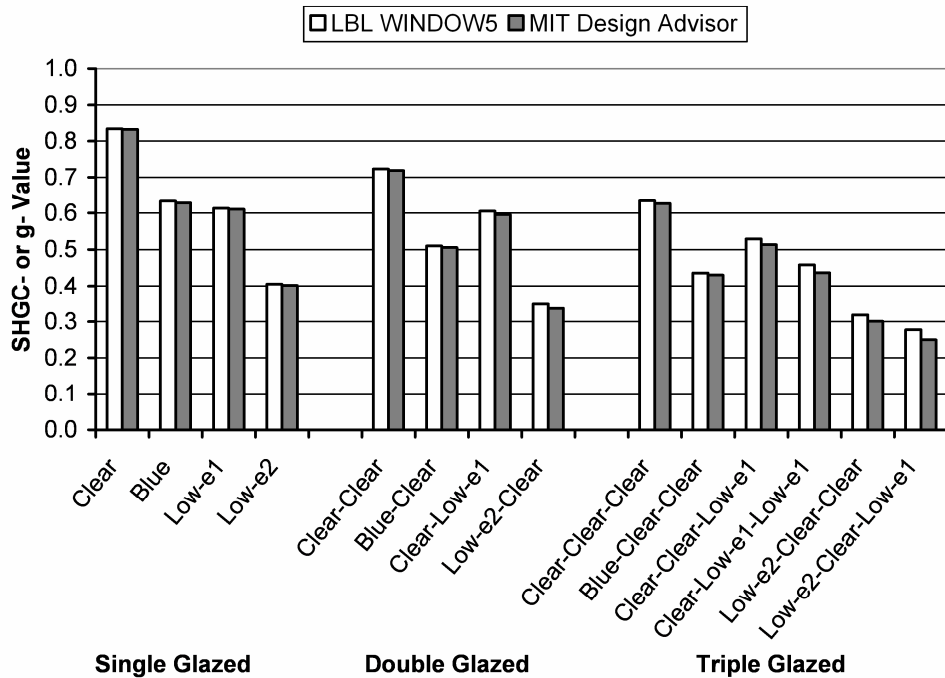


Figure 7-10. SHGC comparison with LBNL WINDOW5 Software.

Table 7-3. U-Value comparison. Values in W/m^2-K

		LBNL Window5	MIT Design Advisor	% Difference
<i>Single</i>	Clear	6.213	6.214	-0.02%
	Blue	6.213	6.214	-0.02%
	Low-e1	3.825	3.826	-0.01%
	Low-e2	3.611	3.611	0.00%
<i>Double</i>	Clear-Clear	2.871	2.848	0.80%
	Blue-Clear	2.871	2.848	0.80%
	Clear-Low-e1	1.880	1.762	6.28%
	Low-e2-Clear	1.756	1.619	7.80%
<i>Triple</i>	Clear-Clear-Clear	1.842	1.850	-0.43%
	Blue-Clear-Clear	1.842	1.850	-0.43%
	Clear-Clear-Low-e1	1.312	1.302	0.76%
	Clear-Low-e1-Low-e1	1.024	1.022	0.20%
	Low-e2-Clear-Clear	1.289	1.255	2.64%
	Low-e2-Clear-Low-e1	0.980	0.976	0.42%

Table 7-4. SHGC comparison.

		LBNL Window5	MIT Design Advisor	% Difference
<i>Single</i>	Clear	0.834	0.8325	0.18%
	Blue	0.633	0.6279	0.81%
	Low-e1	0.613	0.6105	0.41%
	Low-e2	0.405	0.4019	0.77%
<i>Double</i>	Clear-Clear	0.723	0.7188	0.58%
	Blue-Clear	0.510	0.5053	0.92%
	Clear-Low-e1	0.605	0.5956	1.55%
	Low-e2-Clear	0.349	0.337	3.44%
<i>Triple</i>	Clear-Clear-Clear	0.634	0.6266	1.17%
	Blue-Clear-Clear	0.436	0.4297	1.44%
	Clear-Clear-Low-e1	0.529	0.5132	2.99%
	Clear-Low-e1-Low-e1	0.458	0.4365	4.69%
	Low-e2-Clear-Clear	0.319	0.3012	5.58%
	Low-e2-Clear-Low-e1	0.278	0.2497	10.18%

Notes:

Window pane properties are given in Chapter 4.

Spacing between panes of glass in double and triple glazings is 12.7mm.

The gas in the spacing is assumed to be air.

7.5 A NOTE ON THE WALL CONSTRUCTION APPROXIMATION

The intent of this note is to show that including material elements other than the primary insulating material does not significantly affect the computed heat gains for most cases. Looking at two typical cases of wall construction – lightweight and heavyweight – taken from the ASHRAE Standard 140-2004, we compute the overall thermal resistance of the wall (including indoor and outdoor skin coefficients) for the full-wall construction and the insulation-only construction. Differences between the two cases are 7% and 13% as shown. Error is more significant in the heavyweight case because concrete has a modest thermal resistance. When the insulation resistance is higher, as is the case with many residential buildings, the error will be even less.

Table 7-5. Lightweight Case (Plaster Construction)

	R- full construction	R- insulation only	
Interior convection+radiation	0.121	0.121	
Plaster	0.075	-	
Fiberglass	1.650	1.650	
Wood siding	0.064	-	
Exterior convection+radiation	0.034	0.034	
Total:	1.944	1.805	7% difference

Table 7-6. Heavyweight Case (Concrete Construction)

	R- full construction	R- insulation only	
Interior convection+radiation	0.121	0.121	
Concrete block	0.196	-	
Foam insulation	1.537	1.537	
Wood siding	0.064	-	
Exterior convection+radiation	0.034	0.034	
Total:	1.952	1.692	13% difference

CHAPTER 8

ENERGY BALANCE

8.1 INTRODUCTION

Having already outlined methods for finding the component heating loads in the room, it is time to discuss how to incorporate the results to determine the actual heating and cooling loads on a building. In this chapter a method is described to predict the heating and cooling loads required to keep the indoor air temperature within a user-specified temperature band.

A building's energy requirements are computed independently for each façade and the building's central area or core. To predict energy consumption for an entire building, these loads must be averaged appropriately. Methods for performing this averaging will be discussed.

Validation of simulation components has been carried out in prior chapters. In this chapter the accuracy of the entire model is evaluated by testing the integrated model against progressively more complex cases and comparing results with hand calculations and with the industry-accepted Energy Plus software. Results show good agreement in most cases, and discrepancies are discussed and explained.

8.2 MODELING OVERVIEW

The goal of the simulation tool is to compute a building's heating and cooling needs and to provide information about the building's thermal comfort. The computations involved must be performed quickly and with a reasonable degree of accuracy. Here the logic of the model is described.

Heating, cooling, and lighting loads are computed for a representative room on each of the four building faces and for the building's central core space. Each of these load calculations is made independently, and results can be displayed for a representative room on a single façade or for the entire building. When full-building energy analysis is desired, the results for the core space and for each façade must be combined in a meaningful way – usually by a floor-area weight average. .

First a high-level description of the representative rooms and building footprint is given. Next the details of the heating and cooling loads are explained and

calculation methods are described. Finally a method for aggregating the room-results to compute the entire-building energy consumption is provided.

8.3 ROOM & BUILDING DIMENSIONS

Building Configuration

When a building is to be simulated with the Design Advisor software, it is assumed to have simple rectangular dimensions. Real buildings can have complicated shapes, however, most shapes can be approximated modestly well by rectangles. Instead of requiring CAD input, which is time consuming to enter, a simple geometry assumed to provide faster setup time. All that is required to define a building shape is for the user to specify the North-South and East-West rectangular dimensions of the building. Figure 8-1 shows a typical building configuration.

The building is assumed to have enough stories so that the roof, floor, and ground heat exchanges are unimportant when considering the entire building's thermal loads. In this way, energy needs must only be computed for a single, central floor of a building. It is then assumed that the energy needs for all floors are identical. The assumptions are generally appropriate for designing multi-storied commercial buildings, but may cause underestimates of energy needs for residential buildings where roof and floor exchanges can be substantial. Future editions of the software may address such cases.

Four Exterior Zones and the Inner Core

Much of the energy needs of a building are related to thermal exchanges with the exterior environment through the building's envelope (solar gains, conduction through windows and walls). Accordingly, a distinction is made between indoor zones that are and are not in direct thermal communication with the outdoor environment.

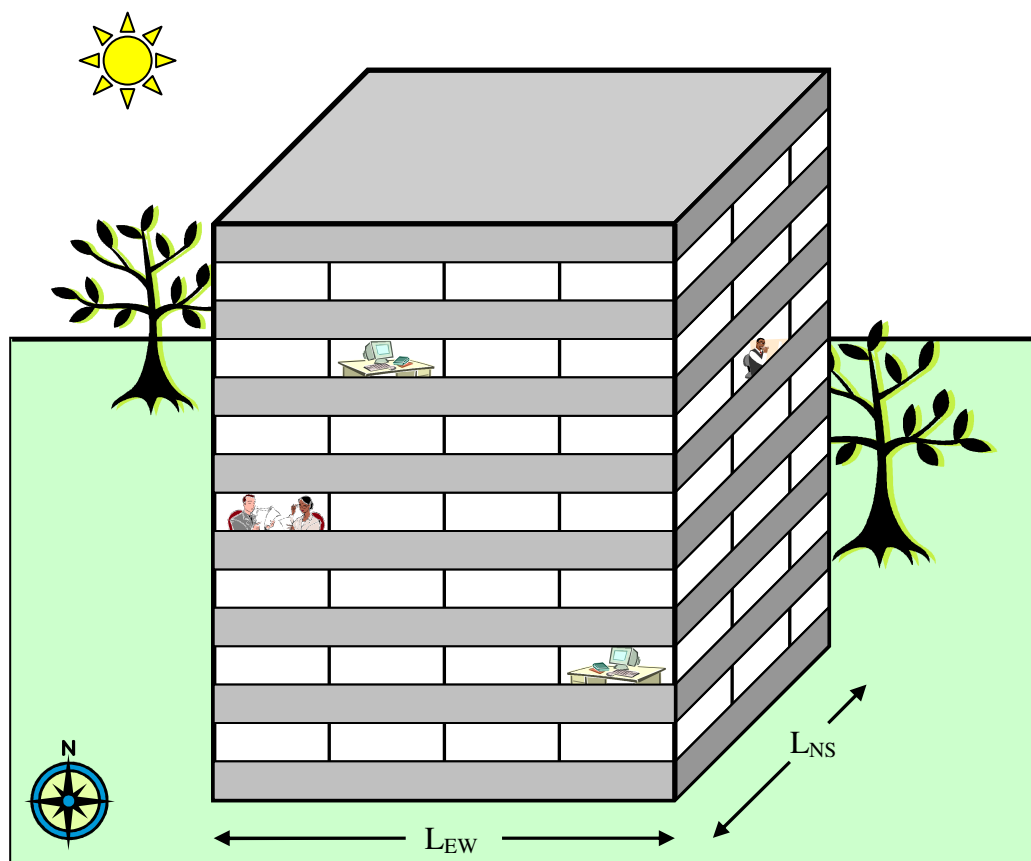


Figure 8-1. Multi-storied rectangular building, 50% glazed façade.

Five separate zones are used, one for each of the exterior façades and one for the interior building core, as shown in Fig. 8-2. Making this distinction allows the energy balance to be performed independently for each of these zones, as solar gains depend largely on the orientation of a façade. The inner core is assumed to receive no direct solar radiation or transmitted sunlight, since these are blocked by the inner-most walls of the exterior zones. The depth of each exterior zone is determined by the distance from the window to the rear of a typical room, Fig. 8-3.

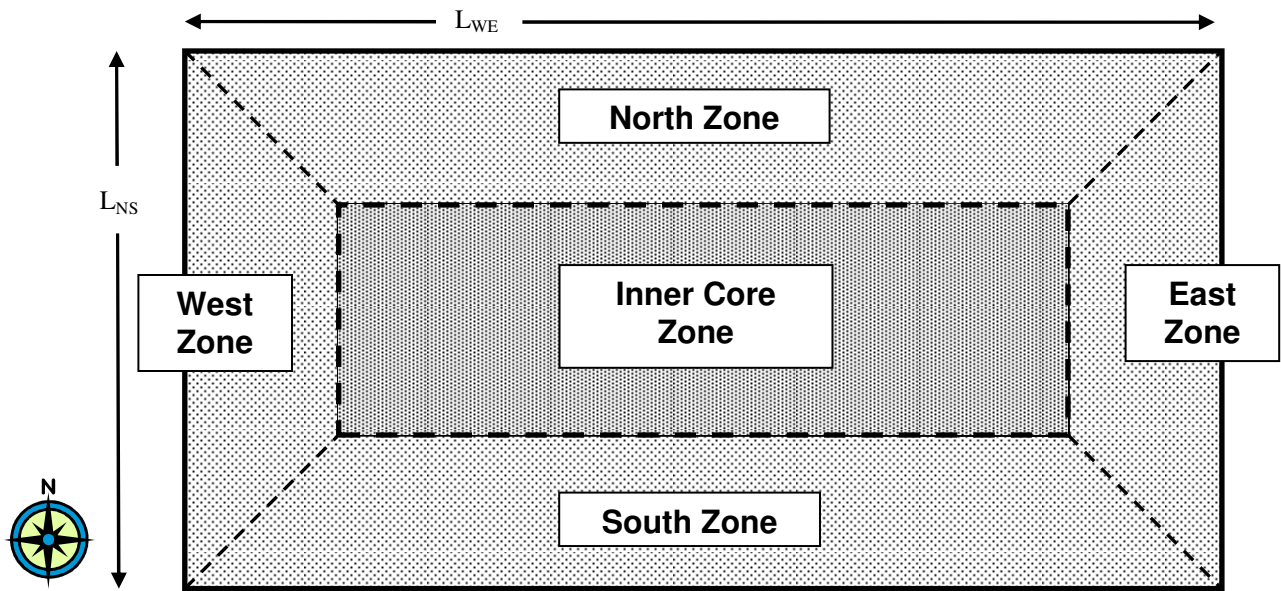


Figure 8-2. Plan view of building divided into 5 subsections: four directional façades and an interior core.

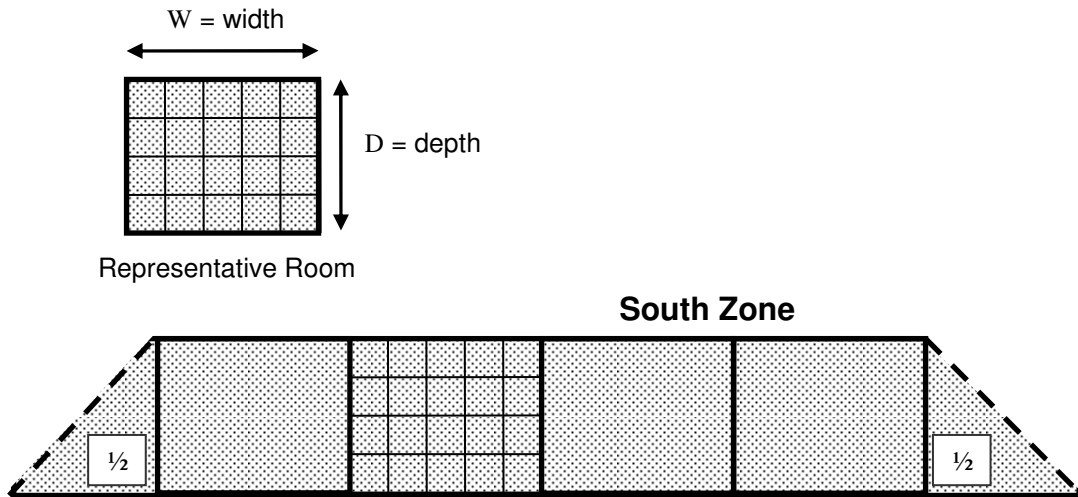


Figure 8-3. An example south-facing zone divided into 6 representative rooms: four full-sized rooms and two half-sized rooms.

The Representative Room

The dimensions of rooms – and especially exterior rooms – prove important in the energy balance of a building. In real buildings each room is somewhat different: some rooms are larger than others, some may have more equipment, and some may have different ventilation requirements. At the early stages of design these possibilities are vast and largely unknown. Describing the specifics of many different rooms would be a time consuming process and computation time would increase substantially. Instead, the notion of a representative room is introduced. A representative room is simply a room that has properties that offer a reasonable depiction of most of the rooms in a building's façade.

To define this representative room, users must specify its depth D , width W , and height H dimensions. The representative rooms are situated on the exterior of a building in the configuration shown in Figs. 8-3 and 8-4. Each room's floor area is given by

$$A_{\text{floor}} = W \cdot D \quad (8-1)$$

and this is used for normalizing thermal loads on a per-area basis. The glazing is specified as a percentage P (%) of the wall area, and the window is assumed to span the entire width of the wall, centered vertically.

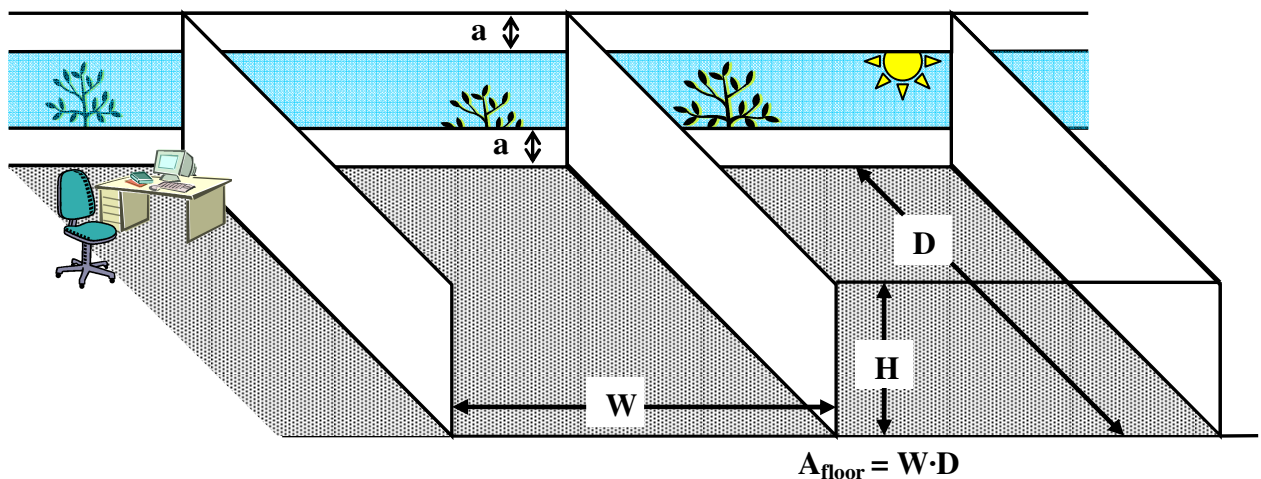


Figure 8-4. Representative exterior room dimensions.
Each façade is comprised of many such rooms.

Specific room details, such as the depth of the floor, characteristics of the window systems, glazing percentages, etc., have been described in detail in previous chapters. Having described the high-level building and room dimensions, it is now time to discuss the method of computing thermal loads for each of the zones.

8.4 DETAILS OF LOAD CALCULATIONS

Since a building's thermal loads vary in time – sometimes erratically – a numerical model must be constructed to capture these effects in detail. Because numerical simulations take longer to run with smaller timesteps, it is useful to look at how frequently each of the thermal loads does vary, and with what accuracy and precision the data are known. The sections below will show how the loads are calculated and a summary of required timesteps are shown in Table 8-1. After the loads calculations are explained a model will be built to integrate the thermal loads and predict the building's hourly heating and cooling needs.

Table 8-4. Summary of variables used for the energy balance.

Component	Symbol	Units	Computational-Frequency
<i>Weather Data</i>			
Outdoor Air Temperature	T_{ext}	K	hourly
Thermal Solar Flux	q_{dir} & q_{dif}	W/m^2	hourly
Visible Solar Illuminance	E_{dir} & E_{dif}	lux	hourly
<i>Internal Loads</i>			
Equipment	q_{equip}	W/m^2	hourly
People	q_{people}	W/m^2	hourly
Lighting	q_{lights}	W/m^2	hourly
<i>Temperature-dependent loads</i>			
Envelope gains	$q_{envelope}$	W/m^2	5 min.
Ventilation	q_{vent}	W/m^2	1 min.
Thermal mass (including reflected solar thermal)	q_{mass}	W/m^2	~30 sec.
<i>Resultant Values</i>			
Room Air Temperature	T_{room}	K	1 min.
Heating / Cooling Load	q_{HVAC}	W/m^2	1 min.

Occupancy Schedule

Before getting into the load calculation procedure, we must briefly introduce the idea of an occupancy schedule. The occupancy schedule is used to define the range of hours that people are in a building. Users specify this range by selecting the

hour that occupancy starts and the hour that the building is vacated. In addition, users must specify the occupant density as the number of people per floor area. These values are used to compute minimum ventilation requirements and the heat loads generated by people.

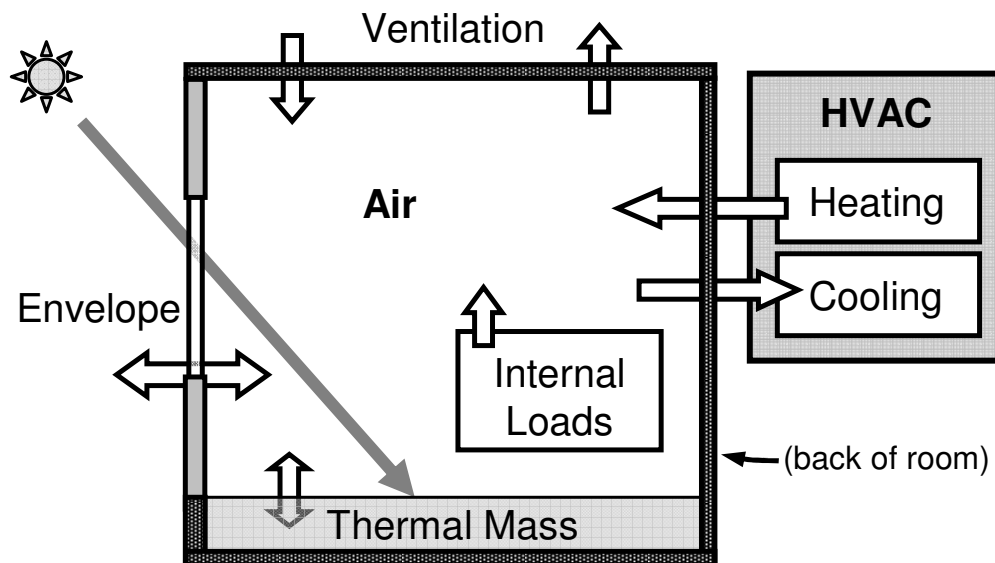


Figure 8-5. Heat exchange with the air in a room. Arrows indicate possible directions of heat flow.

Thermal Loads

Energy can be exchanged with the room's air via several channels as shown in Fig. 8-5. Thermal exchanges are denoted with the symbol Q and have units of power (W), or with sometimes by the symbol q indicating a normalized power per area (W/m^2). Unless otherwise noted, the area with which q is normalized is the floor area of a room or zone. Several types of loads are considered: internal loads, ventilation, envelope, thermal mass, and HVAC. Each load varies in time. Internal loads depend primarily on the occupancy conditions in the building. Ventilation and envelope loads are proportional to the indoor-outdoor temperature difference, and their magnitude can vary modestly within a single hour as the room's air temperature floats between the upper and lower thermostat bounds. Thermal mass loads are more complicated since variation depends on the instantaneous indoor temperature,

the incident heat flux, and the temperature distribution within the mass itself. Weather data for a typical year is available on an hourly basis. While it is suitable to use hourly time increments for computing some of the parameters, substantial accuracy is compromised by using such a large timestep for all thermal load computations. This should become clear in later parts of this section.

Internal Loads

Internal loads are defined as the sum of heat generated by equipment, lights, and people. The internal loads are computed simply as

$$Q_{\text{internal}} = Q_{\text{equip}} + Q_{\text{people}} + Q_{\text{lights}} \quad (8-2)$$

The model assumes that internal loads are constant during any given hour, and so Eq. 8-2 is evaluated only once at the beginning of each hour.

Equipment loads Q_{equip} consist primarily of the electrically-powered devices in a building: computers, printers, audio equipment, televisions, etc. Such devices are typically either on or off during a given time period. Since it is impossible to know exactly when an occupant might switch a device on or off, all internal loads are modeled as constant loads per floor area. The occupancy schedule has the greatest influence on equipment status. When people are in a building, there is a greater chance for equipment to be in use. Similarly, when buildings are unoccupied, the internal loads tend to decrease²¹ as equipment is switched off. Thus, two values of equipment loads are used – one for occupied hours and one for unoccupied hours. If only one value is specified, it is assumed that there are no equipment loads when the building is unoccupied. The logic for equipment loads is expressed as

²¹ Though this is not always the case – sometimes equipment is left on all day long regardless of the occupancy period.

$$\begin{aligned}
 & \text{if (building == occupied)} \\
 & \quad Q_{\text{equip}} = q_{\text{equip,occupied}} \times A_{\text{floor}} \\
 & \text{else (building == unoccupied)} \\
 & \quad Q_{\text{equip}} = q_{\text{equip,unoccupied}} \times A_{\text{floor}}
 \end{aligned} \tag{8-3}$$

Lighting energy can vary substantially during the day depending on how much sunlight is available. The daylight chapter has already discussed in depth how the lighting energy is computed each hour. Briefly – the amount of transmitted daylight is computed for each part of the room, and the deficit between this transmitted light and the user-specified minimum lighting requirement is computed. The lighting deficits are then converted into an energy requirement based on the efficiency of the lights in the room and the dimming capabilities of the lights. Because environmental luminance values are available on an hourly-basis, this is the best accuracy that can be expected.

Occupants provide a continuous source of heat; 60 W of sensible heat is typical for an average person sitting in an office. The thermal load due to occupants is given by

$$Q_{\text{people}} = \frac{60 \text{ W}}{\text{Person}} \cdot \Phi_{\text{person}} \cdot A_{\text{floor}} \tag{8-4}$$

where Φ_{person} is the person-density, or number of people per floor area. In reality the person-density varies throughout the day as people come and go from the building. For simulation purposes, the person-density during occupied hours is a constant that is specified by the user. During unoccupied hours, the building is assumed empty and Φ_{person} is set to zero. Latent heat from the evaporation of moisture (perspiration in the case of humans), is presently neglected. Future editions of this program will incorporate estimates of energy required for dehumidification.

Ventilation

Ventilation exchanges consist of a mass exchange with the outside environment. Fresh air is introduced to the room at the outdoor temperature and mixed with the indoor air, while indoor air is exhausted to the outside environment at the same mass flowrate. The energy exchange from ventilation normalized per unit floor area is given simply as

$$Q_{\text{vent}} = \dot{m} c_{p,\text{air}} (T_{\text{ext}} - T_{\text{room}}) \quad (8-5)$$

where \dot{m} is the mass flow rate of air into/out-of the room; $c_{p,\text{air}}$ is the specific heat capacity of air; T_{ext} is the external or outdoor air temperature; and T_{room} is the instantaneous average indoor air temperature. The specific heat of air varies only very slightly with temperature, and so a constant value of 1,007 J/kg-K is used. The mass flow rate of air is determined by

$$\dot{m} = \rho \dot{V} \quad (8-6)$$

where ρ is the density of air and \dot{V} is the volumetric flow rate of the air intake. The volumetric flow rate is determined by the user and is held constant during any given hour. The air density, however, may vary modestly according to temperature and this variation is captured by the ideal gas relation

$$\rho_a = \frac{P}{R_a T_a} \quad (8-7)$$

where P is the atmospheric pressure (assumed to be 101 kPa), R_a is the gas constant of dry air (287.05 J/kg-K), and T_a is the temperature of the air in Kelvins. As shown in Fig. 8-6, the density ranges between 1.1 and 1.3 over a typical range of outdoor temperatures.

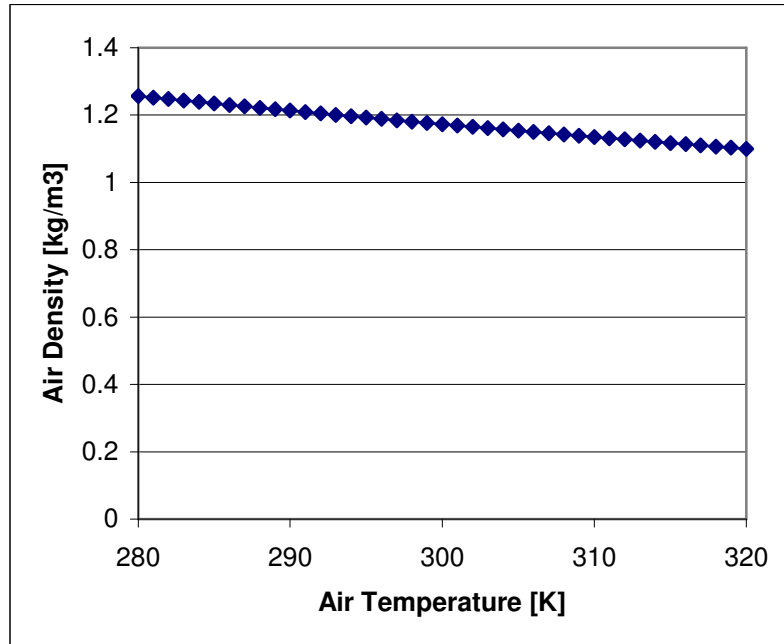


Figure 8-6. Air density variation with temperature, according to the ideal gas law.

To ensure safe levels of fresh air exist in a building, the rate of air intake is made to be proportional to the number of people in a given space. The per-person flow rate $\dot{V}_{\text{per-person}}$ is specified by the user, and the total volumetric flow rate is then computed using

$$\dot{V} = \dot{V}_{\text{per-person}} \cdot P_{\text{density}} \cdot A_{\text{floor}} \quad (8-8)$$

Typical per-person ventilation rates range from about 2.5 to 10 L/s-person for non-smoking areas and about 40 L/s-person for smoking areas (ASHRAE 62.1-2004). When natural ventilation is allowed by the user, windows are opened and closed during the day to allow favorable outdoor conditions to help temper the indoor air. When windows are opened, a crossflow natural ventilation model²² is used to compute the ventilation rate \dot{V} based on the aspect ratio of the room, dimensions of the window orifice, surrounding building height, and wind speed and direction taken from the weather data. In cases where the minimum ventilation rate is not achieved

²² Developed by Grosso (1992) and implemented by MIT Ph.D. Candidate Jin Chau Yuan.

by natural ventilation alone, mechanical ventilation is used to provide the deficit. Windows are opened or closed in a logical manner based on the outdoor and indoor temperature to help improve occupant comfort and reduce HVAC loads. More information on the logic of window operation will be given later in this chapter.

The outdoor air temperature is assumed constant over the duration of a given hour according to the resolution of the weather data files; while the indoor air temperature can vary during an hour in response to all of the time-varying thermal loads. Since Q_{vent} is proportional to the time-varying room air temperature, it must be computed at many instances during the hour to ensure accuracy.

Envelope & Solar Gains

Energy exchanges through the building envelope include directly transmitted radiative gains through window elements, and convective-conductive gains through windows, walls, and other insulating members. Instead of using tables of U-Values and Solar Heat Gain Coefficients (SHGCs), which are typically only appropriate for harsh design conditions, a dynamic calculation of the thermal gains is made several times each hour based on environmental conditions. This is important because radiation coefficients vary with material temperature, and spectral properties of glazing elements vary with angle of incidence. Variation in radiation coefficients are computed using a linearized radiation heat transfer coefficient, as discussed in Chapters 6 and 7. Angular-spectral variation is determined via the Fresnel equations as explained in Chapter 4.

Transmitted solar gains include the portion of sunlight reaching the room interior. TMY2 weather data files supply direct-normal and diffuse-horizontal radiation flux values for solar-thermal radiation. These values are converted to incident values on a vertical surface using the solar geometry calculations outlined in ASHRAE (Fundamentals 2005-31.16). Each hour the transmitted fraction of incident radiation is computed, and a one-bounce method is used to compute interactions within a multi-layered façade. Spectrally-selective materials are modeled with a tri-band radiation model: IR radiation, visible light, and Solar-thermal radiation are each considered separately. Since windows are made of lightweight materials, their heat

capacity effects are insignificant. The thermal circuits for window and wall systems have been described in detail in Chapter 7. These circuits are used to compute the amount of heat convected from the inner-most envelope surface to/from the room. This is normalized by the indoor/outdoor temperature difference to compute an instantaneous U-Value for the both the wall and the window.

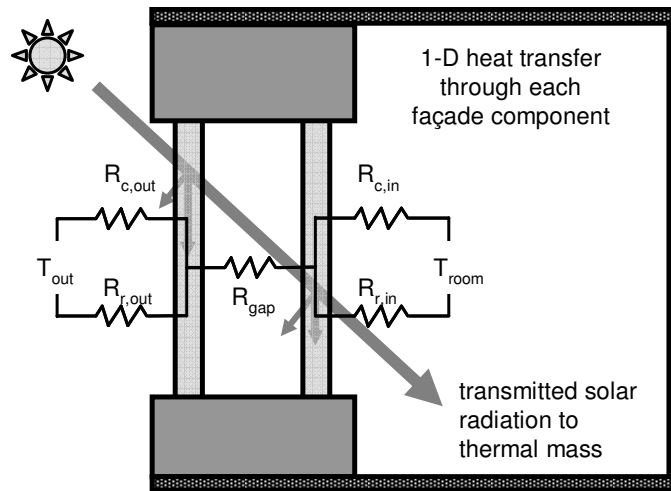


Figure 8-7. Thermal circuit for heat exchange through a window.

Thermal Mass

A slab of concrete covering the entire floor area is used to model thermal mass. Transmitted solar energy is assumed to be evenly distributed over the surface of the thermal mass. The amount of energy that is delivered to the room from the surface of the thermal mass is

$$Q_{\text{thermal-mass}} = Q_{\text{transmitted}} (1 - \alpha) + Q_{\text{surface-convection}} \quad (8-9)$$

where $Q_{\text{transmitted}}$ is the solar radiation transmitted through the window, α is the solar absorption fraction of the thermal mass floor (assumed 80%), and $Q_{\text{surface-convection}}$ is the amount of energy convected between the floor surface and the air. Rooms that are located in the building's core do not receive solar gains, and thermal mass loads in these areas depend only on the room's air temperature fluctuations. Because of

this, there is little opportunity for significant heat storage in the core zone, and the effect of thermal mass on core zone building loads is small²³.

For a typical thickness of thermal mass (0.1 to 0.2 meters), the maximum time step size for an explicit numerical method is on the order of 30 seconds to 1 minute; however, for the implicit technique that is employed, this is extremely conservative. Details have been given in Chapter 6.

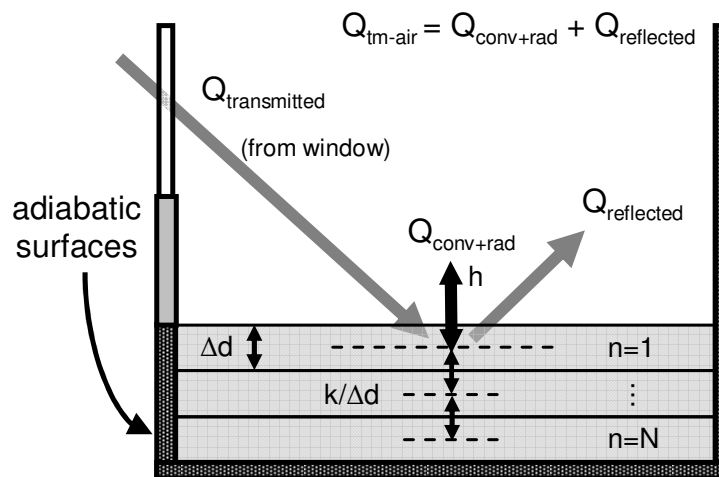


Figure 8-8. Thermal mass: solar radiation is absorbed and reflected from the surface, heat is convected from the surface to the room, and heat is conducted vertically through the mass.

8.5 ENERGY BALANCE

An accurate and common approach to solving a complicated thermal system is to label each surface (walls, floors, ceilings, window panes, etc.) with a temperature node n and perform an energy balance, yielding a system of at least n -equations in n -unknowns (more in the case of radiation exchanges). Such a system can be solved via matrix inversion, and the results used to find the room temperature and required loads at each successive timestep for the entire year. This approach fails in the present application as the heat transfer coefficients are temperature dependent, and the heat-transfer matrix changes along with nodal temperatures. If the matrix approach were used, new matrices would need to be inverted frequently, and the computation time would become unreasonably long.

²³ This is true except for cases where there is a wide allowable temperature band.

Instead a combination of explicit and implicit techniques is used to generate accurate results in a reasonably short time. Hourly timesteps are inadequate at providing accurate predictions of thermal mass behavior. Here we outline how each of the four types of loads is computed and show how these loads can be used to predict the required HVAC heating or cooling energy.

Energy Equation and Solution

Here we explore the procedure for computing the required heating and cooling loads on a representative room. Assuming air is well-mixed in the zone, a room energy balance can be written as

$$m_{\text{air,room}} c_p \frac{\partial T_{\text{room}}}{\partial t} = (T_{\text{ext}} - T_{\text{room}}) \left[(UA)_{\text{window}} + (UA)_{\text{wall}} + \dot{m} c_p \right] + Q_{\text{internal}} + Q_{\text{thermal-mass}} \quad (8-10)$$

where T_{room} is the room temperature, T_{ext} is the outdoor temperature, UA is the product of the dynamically-computed U-value and the associated exposed area, \dot{m} is the mass flow rate of air from ventilation, c_p is the specific heat capacity of air, and $m_{\text{air,room}}$ is the mass of one roomful of air. Discretizing the above equation in time for room temperature, and solving for room temperature at the next timestep yields

$$T_{\text{room}}^{t+\Delta t} = \frac{m_{\text{air,room}} c_p T_{\text{room}}^t + \Delta t \left[Q_{\text{internal}} + Q_{\text{thermal-mass}} + T_{\text{ext}} (UA_{\text{window}} + UA_{\text{wall}} + \dot{m} c_p) \right]}{m_{\text{air,room}} c_p + \Delta t (UA_{\text{window}} + UA_{\text{wall}} + \dot{m} c_p)} \quad (8-11)$$

A Look Time Step Sizes

Since the coefficients associated with the t timestep are always positive, this method is unconditionally stable regardless of the timestep size Δt that is used. Accuracy, however, is not guaranteed with large timesteps. The appropriate timestep size depends on the degree at which the parameters of Eq. 8-11 vary during a given hour. The behavior of the ventilation and the thermal mass loads are

very closely linked with the indoor air temperature. Time steps on the order of minutes are required to ensure accurate thermal mass calculations.

A spreadsheet program has been developed to examine the effect of two time-dependent parameters on the stability of solutions. By changing thermal mass and ventilation parameters, it is possible to explore the behavior of the temperature prediction and observe the occurrence of numerically induced oscillations. These assumptions are summarized in Table 8-2.

Table 8-2. Parameters for Stability Analysis.

Simulation Parameters	Value
Room Dimensions	Width = 5m Depth = 5m Height = 3m
Interior Surface Properties	Adiabatic Walls (interior and exterior) and ceiling
Thermal Mass Floor	Surface temperature at 27°C or 300K, decaying ²⁴ linearly by 0.05°C/min. or 3°C/hr. Combined convection and radiation coefficient $h_{tm}=10 \text{ W/m}^2\text{-K}$
Ventilation Rate	5 air changes per hour
Outdoor Temp	0 °C
Internal load	None
Envelope gains	None
Initial indoor air temperature	27°C or 300K.

From the results shown in Fig. 8-9, accurate results can be obtained with timesteps of about five minutes or less. When Δt is set at 10 minutes or 20 minutes, numerical oscillations are clearly observed. Such oscillations are physically impossible and can lead to predictions of heating and/or cooling loads when none are actually required.

²⁴ The temperature decay of thermal mass has a significant effect on the final predicted indoor air temperature, but does not strongly influence the oscillation-induced error.

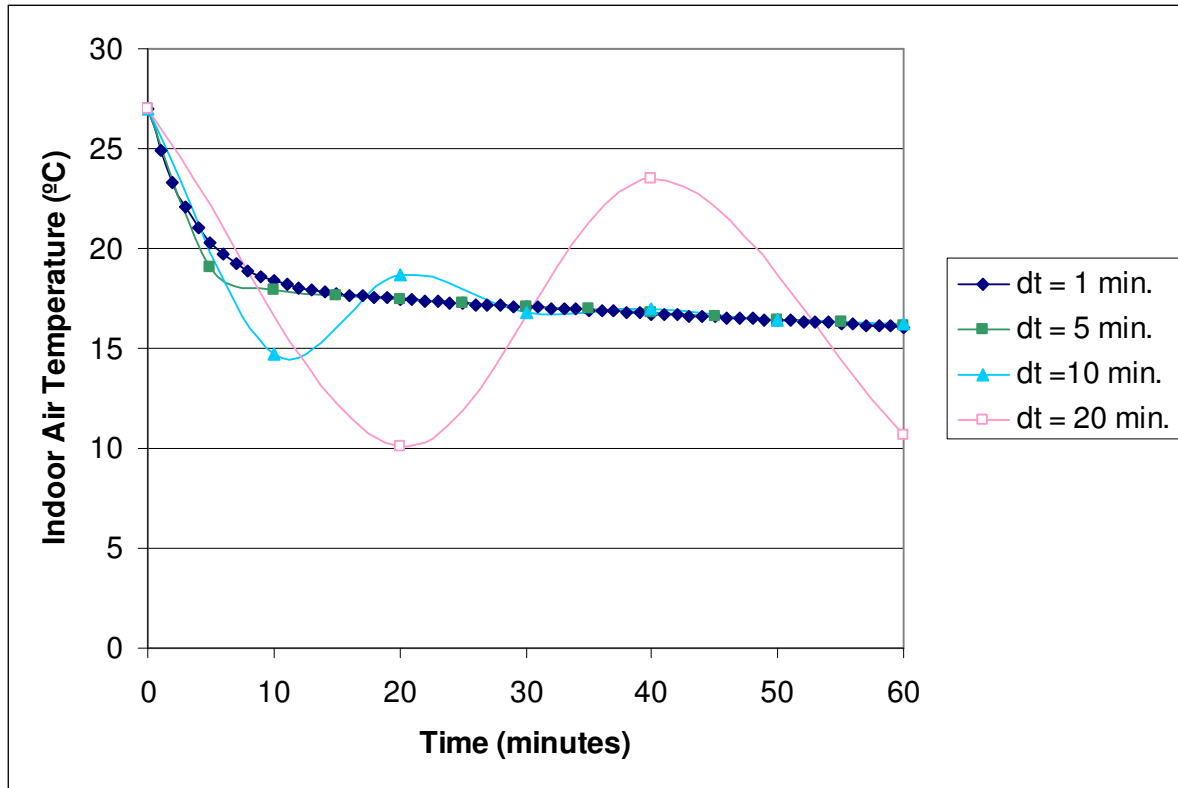


Figure 8-9. Air temperature predictions with varying timestep size.

Fortunately, Eq. 8-11 can be computed quickly and directly from the RHS parameters. Using a small timestep does not increase the computation time significantly, especially since each component of the heating load can be computed only as frequently as necessary. Each variable in Eq. 8-11 behaves differently during an hour. Q_{internal} , for example, is a fixed constant. Rather than re-computing it at each Δt , its value is determined once at the start of the hour and used repeatedly. The dynamically computed U-Values change slightly with temperature, but the dependence is not strong. This is also fortunate, since inverting the envelope-matrix is the slowest part of the modeling process. It is sufficient to re-compute these values only several times per hour, perhaps once every 15 or 20 minutes. Since the thermal mass heat transfer is computed using a timestep on the order of one minute, this may serve as an appropriate Δt , even if it is a highly conservative value.

A logic diagram of the hourly calculation procedure is shown in Fig. 8-10.

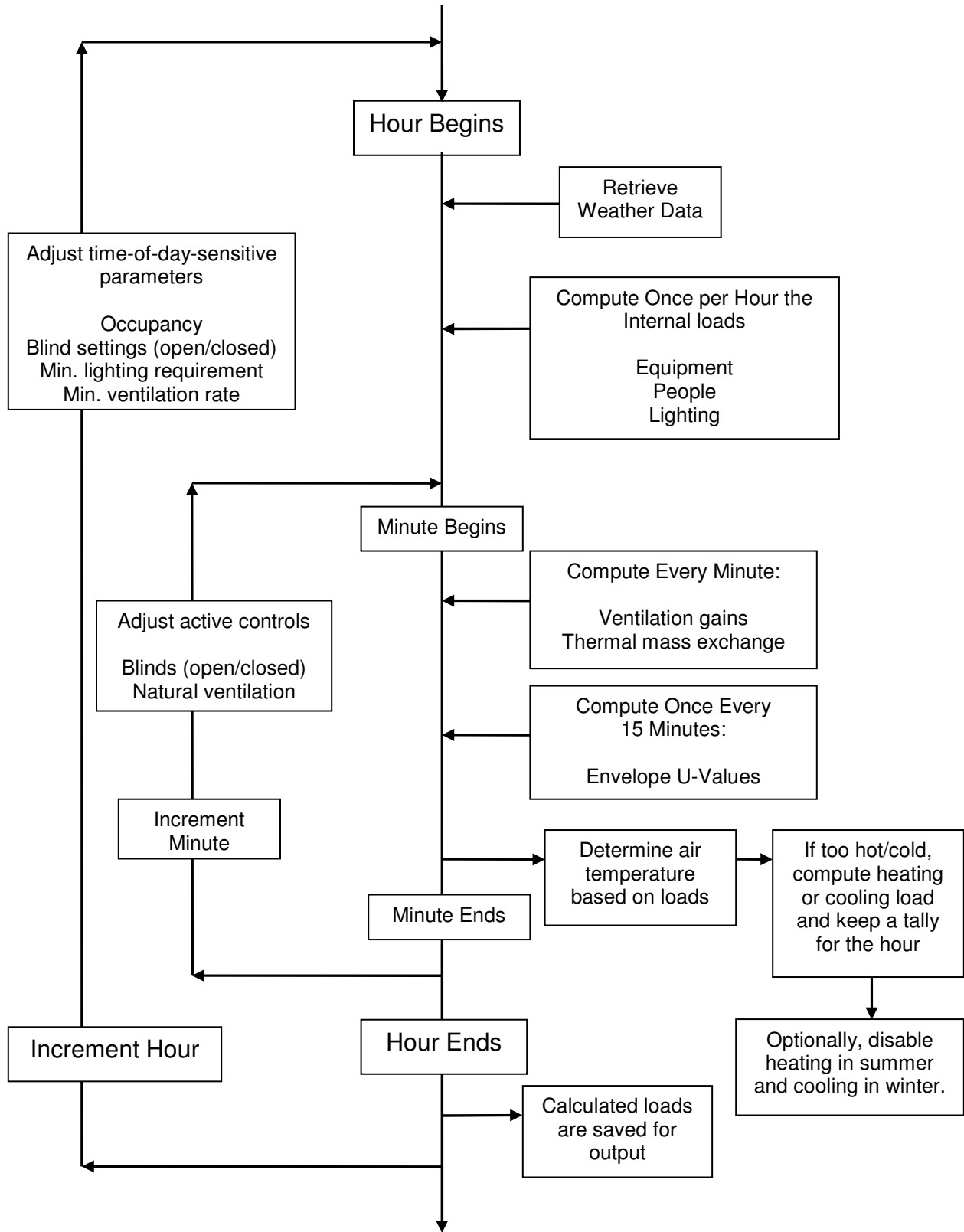


Figure 8-10. Hourly software logic for room load calculations.

Each minute of the year Eq. 8-11 is solved to predict the room temperature at the next time step. If a temperature bound is exceeded, then heating or cooling loads are applied to return the zone-air to a comfortable temperature. The magnitude of the heating/cooling load is

$$Q_{\text{HVAC}} = mC_{\text{air}} \left(T_{\text{max (or min)}} - T_{\text{room}}^{t+\Delta t} \right) \quad (8-12)$$

The room temperature then takes the value of the boundary (max or min) that it crossed. If natural ventilation is permitted, the windows are adjusted (opened or closed) to assist with heating or cooling. This will adjust the mass flow rate of air from the mechanical rate to that which arises from environmental conditions. Heating and cooling loads are tallied and monthly and annual loads are reported.

For rooms in the core of the building, the calculation procedure is the same, except that there are no solar gains or conductive gains through walls or windows.

8.6 WEIGHTED AVERAGE OF ENERGY USE IN BUILDING SPACE

Hourly heating and cooling requirements for each façade and the central core are computed independently and normalized to a per-area value according to

$$q_{\text{cooling},i} = \frac{Q_{\text{room,cooling},i}}{A_{\text{floor},i}} \quad (8-13)$$

and

$$q_{\text{heating},i} = \frac{Q_{\text{room,heating},i}}{A_{\text{floor},i}} \quad (8-14)$$

where the subscript i denotes the façade index (North, South, East, West, or Core), Q_i is the hourly heating or cooling load on a room, and $A_{\text{room},i}$ is the floor area of the representative room on façade i given by

$$A_{\text{floor}} = L_{\text{NS}} \cdot L_{\text{WE}} \quad (8-15)$$

Thus, five such q_i values are produced. These values must be averaged together in an area-weighted manner to produce appropriate heating and cooling loads for the full building. Two configurations are considered in this model: air is well mixed between zones and air is unmixed between zones.

When there is no mixing between air in zones, then the building energy use is simply a direct area-weight average. So the full building heating & cooling loads are computed as:

$$q_{\text{cooling,building}} = \frac{\sum_i q_{\text{cooling},i} \cdot A_i}{\sum_i A_i} = \frac{\sum_i q_{\text{heating},i} \cdot A_i}{A_{\text{total}}} \quad (8-16)$$

and

$$q_{\text{heating,building}} = \frac{\sum_i q_{\text{heating},i} \cdot A_i}{\sum_i A_i} = \frac{\sum_i q_{\text{heating},i} \cdot A_i}{A_{\text{total}}} \quad (8-17)$$

where A_{total} is the total floor area of the building, or just the sum of the floor areas of the façades and central core. The area of the core is computed as

$$A_{\text{core}} = (L_{\text{NS}} - 2D)(L_{\text{WE}} - 2D) \quad (8-18)$$

and the area of the façades are computed as the area of the trapezoids shown in Figs. 8-2 and 8-3. The area of the north and south-facing façades is then

$$A_{\text{south}} = A_{\text{north}} = (L_{\text{EW}} - D)D \quad (8-19)$$

and similarly for the east and west facing façades

$$A_{\text{east}} = A_{\text{west}} = (L_{\text{NS}} - D)D \quad (8-20)$$

In the case of mixed air between zones, it is assumed that a cooling load on one side of a building can be offset by a heating load from another zone, and vice-

versa. As implemented, the heating and cooling loads are computed independently for each zone and are tallied and stored as hourly loads. This means that when air between zones is mixed, the simulation will only permit a cooling load or a heating load during a given hour (and not both). When air is unmixed between zones, it is possible for a building to require both cooling and heating energy.

Corner Rooms

Rooms situated on the corners of buildings experience different conditions than the remaining rooms do. In real buildings the corner rooms can have more than one exterior walls, which would alter the solar gains and envelope exchanges. Since there are only four such rooms in a rectangular building, the atypical nature of such rooms should not normally dominate the results of a full-building simulation. For simulation purposes, the corner rooms are split diagonally in half and each half is assumed to have the same energy requirements per floor area as the non-corner rooms of the adjacent façade, see Fig. 8-3.

8.7 VALIDATION

Energy Plus Comparison

A series of calibrated comparisons have been made against the Energy Plus software with good agreement. All parameters have been matched where possible. The climate data for each simulation is that of Boston, MA taken from the METEONORM library and used in both programs. As the MIT Design Advisor software does not yet model latent loads, humidity has been completely removed from the weather data files for these comparisons. The runs are each built from an identical base simulation, with one or more parameters varied. The base parameters and specific case runs are described in Tables 8-3 and 8-4.

Table 8-3. Common Parameters for Detailed Simulation Comparison.

Base Case Parameters	Value
<i>Fixed Parameters*</i>	
Building Location / Climate Data	METEONORM TMY2 Data for Boston, MA Humidity manually removed from weather data file
Façade Orientation	East-facing
Room Dimensions	Width = 5m Depth = 5m Height = 3m
Interior Wall Properties	Adiabatic side walls and rear wall, no thermal mass in walls
Ceiling Properties	Adiabatic ceiling, no thermal mass in ceiling
Thermal Mass Floor	Floor is concrete $k=1.4 \text{ W/m-K}$; $\rho=2300 \text{ kg/m}^3$ $\alpha=0.80$ low mass=0.02m thick; high mass=0.20m thick adiabatic lower surface
Convection Coefficients	Indoor surface to air: $4 \text{ W/m}^2\text{-K}$ Outdoor surface to air: $14 \text{ W/m}^2\text{-K}$
Radiation Coefficients	Computed dynamically
<i>Variable Parameters**</i>	
Exterior Wall Properties	Adiabatic exterior wall, no thermal mass in walls
External Windows	No windows in base case
Internal load	Zero
Ventilation rate	Zero

*Fixed parameters are in common for all comparison cases

**Variable parameters are as listed, unless stated otherwise in case description.

Table 8-4. Specific Details of Case Comparisons.

Case Number	Description
Case 1	Base Case + 6 W/m^2 internal load from 7am to 8pm
Case 2	Case 1 + 1.8 air changes per hour from 7am to 8pm.
Case 3	Case 1 + East facing wall has R-value of $4.6 \text{ m}^2\text{-K/W}$.
Case 4	Case 3 + 1.8 air changes per hour from 7am to 8pm.
Case 5	Case 3 + Triple-glazed clear-pane window*, comprising 84% of East wall area, the remainder of wall is adiabatic.
Case 6	Case 5 + 3.6 air changes per hour from 7am to 8pm.
Case 7	Case 5 + Internal loads & ventilation schedule is 24 hours per day.

*Glass properties in Chapter 4, glass thickness is 6mm. Spacing between panes is 12.7mm, air.

Case 1 represents an internal load inside an adiabatic box, so for this case, the sensible cooling load is computed to maintain a maximum zone temperature of 26°C. The cooling load for case 1 should be – and is for both models – exactly equal to the internal load. All other cases (2-7) have been run to compute heating loads based on a minimum zone temperature of 20°C. Room temperatures in cases (2-7) were allowed to float freely above 20°C. Results of the annual load comparisons are shown in Fig. 8-11, and an example monthly plot is shown in Fig. 8-12. The data for the simulation comparisons are given for all cases in Tables 8-5 and 8-6.

The greatest differences occurred in cases with high thermal mass, and with large amounts of window area. Differences due to glazing systems appear to stem from differently-computed U-Values. By simulating windows in both models, the calculated Energy Plus U-Values were found to be as much as 10% higher than predicted by the MIT Design Advisor. In the MIT model, the air between window panes is assumed stagnant, while in Energy Plus some amount of natural convection may be allowed, which could cause the observed deviations.

Differences related to the quantity of thermal mass are likely due to dissimilar modeling techniques. The MIT model assumes uniform distribution of solar radiation on the floor, while it is possible that the Energy Plus model traces the path of transmitted radiation. Also, it was attempted to make the four walls and ceiling adiabatic in the Energy Plus model, however, upon inspection of the output data, it appears that some energy was by conducted out of the space through the highly-insulating interior walls.

Finally due to stability constraints in the Energy Plus methodology, the minimum timestep is 1/6 hour, which could have an adverse impact on accuracy, especially with heavily-massive buildings.

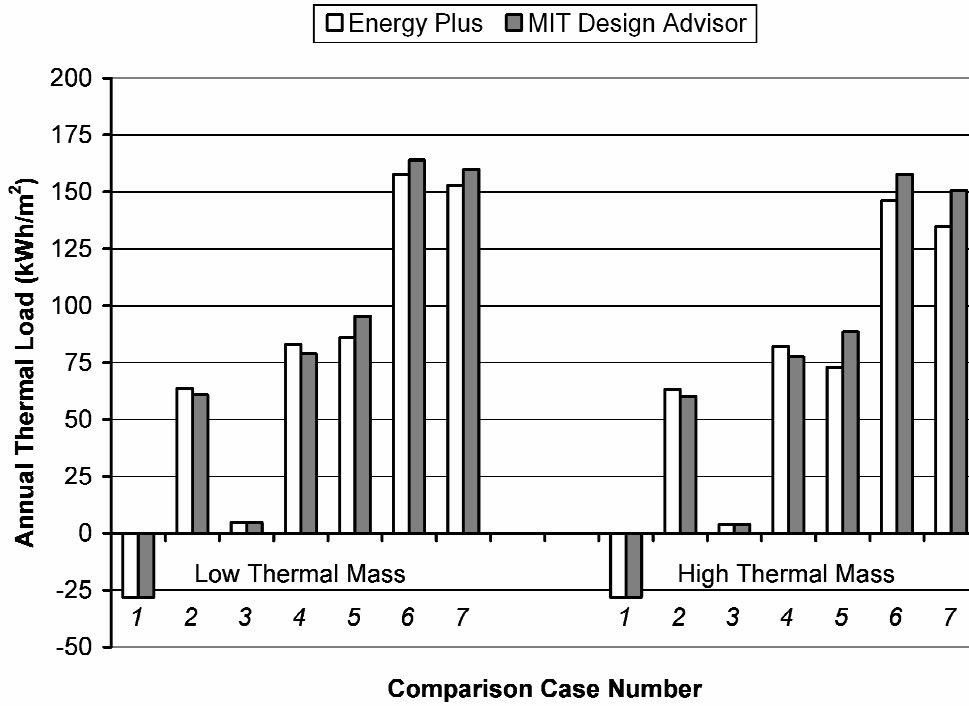


Figure 8-11. Annual load comparison, low and high thermal mass.

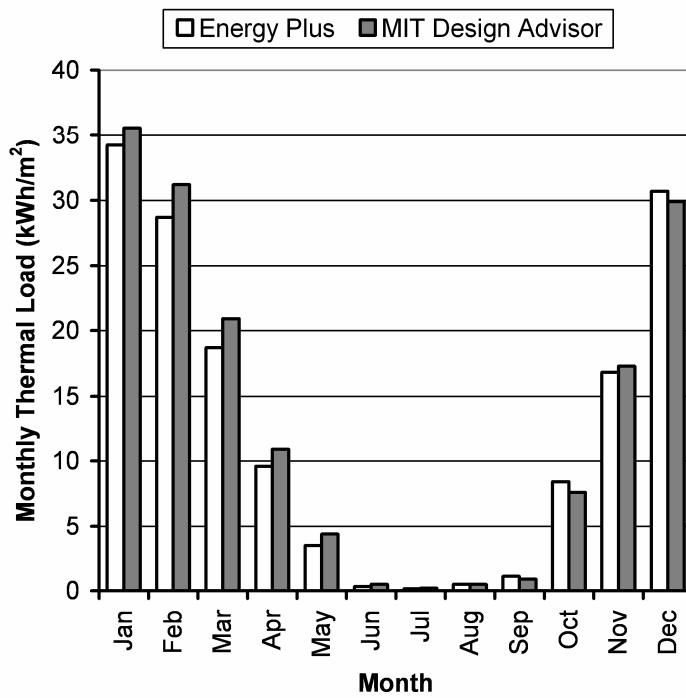


Figure 8-12. Case 6 monthly comparison, low thermal mass.

Table 8-5. Data for Low Thermal Mass Case Comparisons.

<i>Month</i>	<i>Case Number</i>													
	1		2		3		4		5		6		7	
	MIT	EP	MIT	EP	MIT	EP	MIT	EP	MIT	EP	MIT	EP	MIT	EP
January	-2.3	-2.3	13.6	14.0	1.5	1.6	17.3	17.9	23.2	21.3	38.0	37.2	35.6	34.3
February	-2.3	-2.3	12.3	12.8	1.3	1.3	15.7	16.4	19.2	16.2	32.9	30.4	31.2	28.7
March	-2.3	-2.3	8.3	8.5	0.5	0.5	10.7	11.1	11.3	9.0	20.3	17.6	20.9	18.7
April	-2.3	-2.3	4.6	4.7	0.1	0.0	6.0	6.2	5.1	3.7	9.9	8.3	10.9	9.6
May	-2.3	-2.3	1.6	1.5	0.0	0.0	2.1	2.1	1.7	1.1	3.5	2.7	4.4	3.5
June	-2.3	-2.3	0.0	0.0	0.0	0.0	0.1	0.0	0.0	0.0	0.3	0.1	0.5	0.3
July	-2.3	-2.3	0.0	0.0	0.0	0.0	0.0	0.0	0.0	0.0	0.1	0.1	0.2	0.2
August	-2.3	-2.3	0.1	0.0	0.0	0.0	0.2	0.1	0.2	0.2	0.5	0.5	0.5	0.5
September	-2.3	-2.3	0.1	0.0	0.0	0.0	0.3	0.2	0.2	0.3	0.7	0.8	0.9	1.1
October	-2.3	-2.3	2.7	3.4	0.0	0.0	3.6	4.6	4.1	4.3	7.3	8.2	7.6	8.4
November	-2.3	-2.3	6.4	6.6	0.3	0.1	8.4	8.7	10.7	10.1	18.2	18.0	17.3	16.8
December	-2.3	-2.3	11.2	12.1	1.0	1.2	14.4	15.6	19.7	19.7	32.3	33.9	29.9	30.7
Annual	-28.1	-28.1	60.9	63.6	4.7	4.7	78.8	82.9	95.4	85.9	164.0	157.8	159.9	152.8

Table 8-6. Data for High Thermal Mass Case Comparisons.

<i>Month</i>	<i>Case Number</i>													
	1		2		3		4		5		6		7	
	MIT	EP	MIT	EP	MIT	EP	MIT	EP	MIT	EP	MIT	EP	MIT	EP
January	-2.3	-2.3	13.6	14.0	1.5	1.3	17.3	17.9	23.1	20.8	38.0	37.1	35.6	33.7
February	-2.3	-2.3	12.3	12.8	1.1	1.3	15.7	16.4	19.1	15.2	32.9	30.3	31.1	27.8
March	-2.3	-2.3	8.3	8.5	0.4	0.5	10.7	11.1	10.3	6.3	19.8	15.8	20.0	15.6
April	-2.3	-2.3	4.5	4.6	0.0	0.0	5.9	6.2	3.0	0.8	8.4	4.9	8.8	5.0
May	-2.3	-2.3	1.5	1.5	0.0	0.0	1.9	2.0	0.5	0.0	2.2	0.9	2.6	1.1
June	-2.3	-2.3	0.0	0.0	0.0	0.0	0.0	0.0	0.0	0.0	0.0	0.0	0.0	0.0
July	-2.3	-2.3	0.0	0.0	0.0	0.0	0.0	0.0	0.0	0.0	0.0	0.0	0.0	0.0
August	-2.3	-2.3	0.0	0.0	0.0	0.0	0.0	0.0	0.0	0.0	0.0	0.0	0.0	0.0
September	-2.3	-2.3	0.0	0.0	0.0	0.0	0.0	0.0	0.0	0.0	0.0	0.0	0.0	0.0
October	-2.3	-2.3	2.3	3.0	0.0	0.0	3.2	4.3	2.8	2.0	6.3	6.3	6.1	5.9
November	-2.3	-2.3	6.4	6.6	0.0	0.0	8.4	8.7	10.1	8.6	17.9	17.1	16.7	15.3
December	-2.3	-2.3	11.2	12.1	0.8	0.7	14.4	15.6	19.6	19.4	32.2	33.8	29.8	30.4
Annual	-28.1	-28.1	60.1	63.1	3.8	3.7	77.5	82.2	88.5	73.0	157.7	146.2	150.7	134.8

8.8 CONCLUSION

This concludes this discussion of the MIT Design Advisor energy modeling technique and validation. Improvements, modifications, and additions are to be expected. A few of the planned additions include a humidity model, roof and ground thermal model, improved convection relations for systems with blinds, and additional flexibility in the user-controlled building operation decisions. Detailed building load comparisons will be made against the ASHRAE 140-2004 standard. Future work and analysis will be published on the Internet at <http://designadvisor.mit.edu/>.

CHAPTER 9

NOMENCLATURE

CHAPTER 1 INTRODUCTION: BUILDINGS, ENERGY, AND SIMULATION

none

CHAPTER 2 THE MIT DESIGN ADVISOR INTERFACE

none

CHAPTER 3 RADIANT SOLAR FLUX

Symbols

AST	hour	apparent solar time
B	deg	angle parameter for ET calculation
C	none	astronomical coefficient
D	day	day of the year
$E_{\text{dif,h}}$	W/m^2	diffuse-horizontal radiation, terrestrial
$E_{\text{dif,i}}$	W/m^2	diffuse radiation, incident
$E_{\text{dir,i}}$	W/m^2	direct radiation, incident
$E_{\text{dir,n}}$	W/m^2	direct-normal radiation, terrestrial
ET	min	equation of time
H	deg	hour angle
$I_{\text{dif,h}}$	lux	diffuse-horizontal illuminance, terrestrial
$I_{\text{dif,i}}$	lux	diffuse-illuminance, incident
$I_{\text{dir,i}}$	lux	direct illuminance, incident
$I_{\text{dir,n}}$	lux	direct-normal illuminance, terrestrial
L	deg	local latitude
LON	deg	local longitude
LSM	deg	local standard time meridian
LST	hour	local standard time of day in hours
\hat{n}	deg	surface normal vector
Y	none	ratio of diffuse-normal to diffuse-horizontal radiation
β	deg	solar altitude
γ	deg	surface solar azimuth
δ	deg	solar declination
θ	deg	angle of incidence
ρ	none	reflectivity of a surface
Σ	deg	surface tilt
φ	deg	solar azimuth
ψ	deg	surface azimuth

Subscripts & Superscripts

dif	diffuse
dir	direct
g	ground
i	incident
ref	reflected
vis	visible

CHAPTER 4 WINDOW OPTICS

Symbols

A	none	absorptance on by glazing layer
n	none	index of refraction of air
n'	none	index of refraction of glazing layer
R	none	reflectance from a glazing layer

t	m	thickness of material
T	none	transmittance through a glazing layer
α	m^{-1}	absorption coefficient
α	none	solar absorptivity of a blind slat material
ε	none	infrared emissivity
θ	deg	angle of incidence
θ'	deg	angle of refraction
κ	none	extinction coefficient
λ	m	wavelength of radiation
ρ	none	reflectivity of a surface
τ	none	transmissivity of a surface

Subscripts & Superscripts

b	back surface
D	diffuse
f	front surface
i	glazing layer index
ir	infrared
p	p- polarization of radiation
s	s- polarization of radiation
sol	solar
λ	wavelength band

CHAPTER 5 ARTIFICIAL LIGHTING*Symbols*

A	m^2	area
E	lm/m^2	luminous intensity
F	lm	luminous output
h	m	height of workplane surface
Q_e	W	electrical power input
ε	lm/W	luminous efficacy
η	none	overall lighting efficiency

Subscripts & Superscripts

(i,j)	grid indices
e	electric
ideal	ideal light source
min	minimum
source	real light source
v	visible

CHAPTER 6 THERMAL MASS*Symbols*

A	m^2	area
ac/h	hr^{-1}	air changes per hour
\underline{B}	J/K	heat transfer matrix, current timestep
Bi	none	Biot number
C	J/K	heat capacity
c	J/kg-K	specific heat capacity
d	m	depth of slice
D	m	depth of thermal-mass slab
D_h	m	hydraulic diameter
E	W/m^2	internal energy per area
F_o	none	Fourier number
h	W/m^2-K	heat transfer coefficient
k	W/m-K	conductivity

m	kg	mass
n	none	number of slices
P	m	perimeter
Q	W	power
\underline{q}	W	power source vector
R	$m^2\text{-K/W}$	thermal resistance
\underline{S}	J/K	heat transfer matrix, future timestep
\overline{T}_i	K	average temperature between current and next timesteps
ΔT	K	temperature difference
\underline{x}^t	K	nodal temperature matrix, current timestep
$\underline{x}^{t+\Delta t}$	K	nodal temperature matrix, future timestep
α	none	solar absorptivity of a solid material
ε	none	effective surface-surface infrared emissivity
ρ	kg/m^3	density
σ	$\text{W/m}^2\text{-K}^4$	Stefan-Boltzmann constant

Subscripts & Superscripts

avg	average
cv	convection
i	initial
i	material index
inf	infinity, surroundings
max	maximum
r	radiation
t	current timestep
t+ Δt	next timestep

CHAPTER 7 ENVELOPE LOADS*Symbols*

A	m^2	area
d	m	material thickness
Δ	K	half the difference between the surface and environmental temperatures
F	none	configuration factor or view factor
H	m	height of room, floor to ceiling
J	W	emissive power
j	W/m^2	emissive power per area
k	W/m-K	conductivity
Q	W	power
q	W/m^2	power per area
R	$m^2\text{-K/W}$	thermal resistance
v	m/s	air speed
ε	none	effective surface-surface infrared emissivity
σ	$\text{W/m}^2\text{-K}^4$	Stefan-Boltzmann constant

Subscripts & Superscripts

a,b	arbitrary surface indices
c	conduction
cv	convection
eff	effective
r	radiation
s	surface

CHAPTER 8 ENERGY BALANCE*Symbols*

A	m^2	area
c	J/kg-K	specific heat capacity

D	m	depth
E	lux	illuminance
L	m	length
m	kg	mass
\dot{m}	kg/s	mass flow rate
P	none	percentage
q	W/m ²	power per area
R	m ² -K/W	thermal resistance
T	K	temperature
U	W/m ² -K	U-Value
W	m	width
α	none	solar absorptivity of a solid material
Φ	persons/m ²	person-density, per floor area

Subscripts & Superscripts

dif	diffuse
dir	direct
equip	equipment
EW	east-west
ext	exterior, outdoor
HVAC	heating, ventilation, and air conditioning
mass	thermal mass
NS	north-south
out	outdoor
vent	ventilation

CHAPTER 10

REFERENCES

CHAPTER 1 INTRODUCTION: BUILDINGS, ENERGY, AND SIMULATION

- BOMA. 1999. Building Owners and Managers Association.
- DOE. 2004. Buildings energy database. U.S. Department of Energy. <<http://buildingsdatabook.eren.doe.gov>>.
- DOE. 2004. Building energy efficiency, building envelope. U.S. Department of Energy. <http://www.eere.energy.gov/EE/buildings_envelope.html>.
- DOE. 2006. Design and analysis tools for building simulation. U.S. Department of Energy. <<http://www.eere.energy.gov/buildings/info/design/integratedbuilding/design.html>>.
- DOE-2. 2007. eQUEST Software v.3.6, The Quick Energy Simulation Tool. U.S. Department of Energy. March 2007. <<http://doe2.com/equest>>.
- Energy Plus. 2006. Energy Plus Software v.1.4. U.S. Department of Energy. January 2007. <<http://www.eere.energy.gov/buildings/energyplus/>>.
- EIA. 2006. How energy is used in commercial buildings. *Energy Kid's Page*. Energy Information Administration. 2006. <<http://www.eia.doe.gov/kids/energyfacts/uses/commercial.html>>
- Hong, T., Chou, S.K., and Bong, TY. 1999. Building simulation: an overview of developments and information sources. *Building and Environment*. 35 (2000), pp. 347-61.
- Hui S.C.M. 2001. Low energy building design in high density urban cities. *Renewable Energy* 24. pp. 627-640.
- Hui, S.C.M. 2002. Using performance-based approach in building energy standards and codes. *Proceedings of the Chongqing-Hong Kong Joint Symposium 2002*. pp. A52-61. <<http://web.hku.hk/~cmhui/chongqing-pbbec01.pdf>>.
- Kosonen R., and Shemeikka J. 1997. The use of a simple simulation tool for energy analysis. *IBPSA Proceedings of Building Simulation '97*, 1, pp. 369-376. <<http://www.ibpsa.org/proceedings/bs97/papers/P103.PDF>>.
- Lehar M.A., and Glicksman L.R. 2004. A simulation tool for the optimization of advanced facades. *SimBuild Conference Proceedings 2004*. IBPSA-USA National Conference. Boulder, CO.
- MIT Design Advisor. 2007. *The MIT Design Advisor*. Massachusetts Institute of Technology. May 2007. <<http://designadvisor.mit.edu>>.
- NREL. 2004. High performance buildings research. National Renewable Energy Laboratory. <http://www.nrel.gov/buildings/highperformance/building_envelope.html>
- Pedersen, I. et al. 2001. Sustainable energy building and construction taskforce report. *The Institution of Engineers, Australia*.
- Price L, Worrel E, Khurshch M. 1999. Sector trends and driving forces of global energy use and greenhouse gas emissions: focus in industry and buildings. *LBNL-43746*. Lawrence Berkeley National Labs. <<http://eetd.lbl.gov/EAP/IES/iespubs/43746.pdf>>.

- Urban, B and Glicksman, L. 2006. A simplified rapid energy model and interface for non-technical users. Intended for publication in Oak Ridge National Laboratory, Buildings Conference X, 2007 Proceedings.
- Weil, S., et al. 1998. The role of building energy efficiency in managing atmospheric carbon dioxide. *Environmental Science & Policy*. 1 (1998), pp. 27-38.

CHAPTER 2 THE MIT DESIGN ADVISOR INTERFACE

- ASHRAE. 2001. *ANSI/ASHRAE Standard 62.1-2001, Ventilation for Acceptable Indoor Air Quality*. Atlanta: American Society of Heating, Refrigeration, and Air-Conditioning Engineers, Inc.
- ASHRAE. 2001. *ASHRAE/IESNA Standard 90.1-2001, Energy Standard for Buildings except Low-Rise Residential Buildings*. Atlanta: American Society of Heating, Refrigeration, and Air-Conditioning Engineers, Inc.
- Lehar, M. 2003. A simulation tool for the estimation and optimization of electrical lighting energy. Masters Thesis, Massachusetts Institute of Technology.
- Lehar, M. 2005. A branching fuzzy-logic classifier for building optimization. Ph.D. Thesis, Massachusetts Institute of Technology.
- MIT Design Advisor. 2007. *The MIT Design Advisor*. Massachusetts Institute of Technology. May 2007. <<http://designadvisor.mit.edu>>.

CHAPTER 3 RADIANT SOLAR FLUX

- ASHRAE. 2005. Solar heat gain and visible transmittance. *ASHRAE Handbook – Fundamentals*. p. 31.13-17. Atlanta: American Society of Heating, Refrigeration, and Air-Conditioning Engineers.
- Energy Plus. 2006. Energy Plus Software v.1.4. U.S. Department of Energy. January 2007. <<http://www.eere.energy.gov/buildings/energyplus/>>.
- METEONORM. 2000. Global Meteorological Database for Solar Energy and Applied Climatology. CD-ROM by MeteoTest, Bern.
- Marion, W., and Urban, K. 1995. User's Manual for TMY2s. National Renewable Energy Laboratory. May 2007. <<http://rredc.nrel.gov/solar/pubs/tmy2/tab3-2.html>>.

CHAPTER 4 WINDOW OPTICS

- Arons, D. 2000. Properties and applications of double-skin façades. Section 4.2.8.a, pp. 105-10. Masters Thesis, Massachusetts Institute of Technology.
- ASHRAE. 2005. Solar optical properties of glazing. *ASHRAE Handbook – Fundamentals*. pp. 31.18-24. Atlanta: American Society of Heating, Refrigeration, and Air-Conditioning Engineers.
- Energy Plus. 2006. Energy Plus Engineering Reference. U.S. Department of Energy. May 2007. <<http://www.eere.energy.gov/buildings/energyplus/pdfs/engineeringreference.pdf>>.
- LBNL. 2007. Windows and Daylighting Software WINDOW 5.2. Lawrence Berkeley National Labs. <<http://windows.lbl.gov/software/window/window.html>>.
- WIS. 2005. WinDat Window Information System Software v.3.0.1. August 2005. <<http://www.windat.org>>.

CHAPTER 5 ARTIFICIAL LIGHTING

- 1000 Bulbs. 2007. Light bulbs, rope lights, halogens, & fluorescent light bulbs. May 2007. <<http://www.1000bulbs.com>>.
- ASHRAE. 2005. Daylighting. *ASHRAE Handbook – Fundamentals*. pp. 31.56-59. Atlanta: American Society of Heating, Refrigeration, and Air-Conditioning Engineers.
- DOE. 2006. Building technologies program: lighting research and development. U.S. Department of Energy. April 2007. <<http://www.eere.energy.gov/buildings/tech/lighting>>.
- EIA. 1999. Commercial Building Electricity Consumption by End Use. Energy Information Administration. April 2007. <http://www.eia.doe.gov/emeu/aer/pdf/pages/sec2_29.pdf>.
- EIA. 2001. End-Use Consumption of Electricity by End Use Appliance. *Residential Energy Consumption Survey*. Energy Information Administration. April 2007. <<http://www.eia.doe.gov/emeu/recs/recs2001/nduse2001/enduse2001.html>>.
- Energy Plus. 2006. Energy Plus Engineering Reference. U.S. Department of Energy. May 2007. <<http://www.eere.energy.gov/buildings/energyplus/pdfs/engineeringreference.pdf>>.
- LBNL. 2007. Windows and Daylighting Software WINDOW 5.2. Lawrence Berkeley National Labs. <<http://windows.lbl.gov/software/window/window.html>>.
- Lehar, M. 2003. A simulation tool for the estimation and optimization of electrical lighting energy. Masters Thesis, Massachusetts Institute of Technology.
- Lehar, M.A., and Glicksman, L.R. 2004. Rapid algorithm for modeling daylight distributions in office buildings. *Building and Environment*. 42 (8), pp.2908-19.
- METEONORM. 2000. Global Meteorological Database for Solar Energy and Applied Climatology. CD-ROM by MeteoTest, Bern.
- Mischler, G. 2003. Lighting Design Glossary: Workplane. Lighting Design Knowledgebase. <<http://www.schorsch.com/kbase/glossary/workplane.html>>.
- MIT Design Advisor. 2007. *The MIT Design Advisor*. Massachusetts Institute of Technology. May 2007. <<http://designadvisor.mit.edu>>.
- MSN Encarta. 2007. Light. Microsoft Encarta Online Encyclopedia. <http://encarta.msn.com/encyclopedia_761579230_2/Light.html>.
- Radiance Synthetic Imaging System. 2002. Lawrence Berkeley National Laboratory. University of California, Berkeley.
- WinDat. 2006. Window Information System. WIS Software. <<http://www.windat.org>>.

CHAPTER 6 THERMAL MASS

- ASHRAE. 2005. Calculating cooling load. *ASHRAE Handbook – Fundamentals*. p. 30.23. Atlanta: American Society of Heating, Refrigeration, and Air-Conditioning Engineers.
- Beausoleil-Morrison, I. 2001. An algorithm for calculating convection coefficients for internal building surfaces for the case of mixed flow in rooms. *Energy and Buildings*. 33 (4), pp. 351-61.

- Infrared Services. 2000. Emissivity Values for Common Materials. May 2007. <<http://www.infrared-thermography.com/material-1.htm>>
- Incropera, F.P., and DeWitt, D.P. 2002. Introduction to Heat Transfer. 4th ed. Wiley & Sons. New York.
- Kumar, S. 2001. Live Loads in Office Buildings: point-in-time load intensity. *Building and Environment*. 37 (1), pp. 79-89.
- Smith, J. 2004. Building energy calculator: a design tool for energy analysis of residential buildings in developing countries. Masters Thesis, Massachusetts Institute of Technology.

CHAPTER 7 ENVELOPE LOADS

- Alamdari, F., and Hammond, G.P. 1983. Improved data correlations for buoyancy-driven convection in rooms. *Building Services Engineering Research and Technology*. 4 (3) pp. 106-12.
- Arons, D. 2000. Properties and applications of double-skin façades. Masters Thesis, Massachusetts Institute of Technology.
- ASHRAE. 2005. Solar optical properties of glazing. *ASHRAE Handbook – Fundamentals*. pp. 31.18-24. Atlanta: American Society of Heating, Refrigeration, and Air-Conditioning Engineers, Inc.
- ASHRAE. 2001. *ANSI/ASHRAE Standard 140-2004, Standard Method of Test for the Evaluation of Building Energy Analysis Computer Programs*. Atlanta: American Society of Heating, Refrigeration, and Air-Conditioning Engineers, Inc.
- ASHRAE. 2001. *ASHRAE/IESNA Standard 90.1-2001, Energy Standard for Buildings Except Low-Rise Residential Buildings*. Atlanta: American Society of Heating, Refrigeration, and Air-Conditioning Engineers, Inc.
- Incropera, F.P., and DeWitt, D.P. 2002. Introduction to Heat Transfer. 4th ed. Wiley & Sons. New York.
- ISO. 2003. *Standard ISO 15099 (E)-Thermal performance of windows, doors, and shading devices – Detailed calculations*. Geneva, Switzerland: International Organization for Standardization.
- LBNL. 2007. Windows and Daylighting Software WINDOW 5.2. Lawrence Berkeley National Labs. <<http://windows.lbl.gov/software/window/window.html>>.
- NFRC. 2001. *Standard NFRC 100-2001 Procedure for Determining Fenestration Product U-factors*. Maryland: National Fenestration Research Council, Inc.
- NFRC. 2001. *Standard NFRC 300-2001 Standard Test Method for Determining the Solar Optical Properties of Glazing Materials and Systems*. Maryland: National Fenestration Research Council, Inc.
- Siegel, R., and Howell, J. 2002. *Thermal Radiation Heat Transfer*. New York: Taylor and Francis.
- Smith, J. 2004. Building energy calculator: a design tool for energy analysis of residential buildings in developing countries. Masters Thesis, Massachusetts Institute of Technology.

CHAPTER 8 ENERGY BALANCE

- Grosso, M. 1992. Wind pressure distribution around buildings: a parametrical model. *Energy and Buildings*. 18 (2), pp. 101-131.
- Incropera, F.P., and DeWitt, D.P. 2002. Introduction to Heat Transfer. 4th ed. Wiley & Sons. New York.
- Smith, J. 2004. Building energy calculator: a design tool for energy analysis of residential buildings in developing countries. Masters Thesis, Massachusetts Institute of Technology.
- Urban, B and Glicksman, L. 2006. A simplified rapid energy model and interface for non-technical users. Intended for publication in Oak Ridge National Laboratory, Buildings Conference X, 2007 Proceedings.